

TENSILE CAPACITY OF HIGH-STRENGTH  
ANCHOR BOLT GROUPS EMBEDDED IN  
CIRCULAR CONCRETE PIERS

APPROVED:

---

---

A mis padres

TENSILE CAPACITY OF HIGH-STRENGTH  
ANCHOR BOLT GROUPS EMBEDDED  
IN CIRCULAR CONCRETE PIERS

BY

MARCOS RAFAEL CALZADILLA, B.S.C.E.

T H E S I S

Presented to the Faculty of the Graduate School of  
The University of Texas at Austin  
in Partial Fulfillment  
of the Requirements  
for the Degree of  
MASTER OF SCIENCE IN ENGINEERING

THE UNIVERSITY OF TEXAS AT AUSTIN

December 1982

## A C K N O W L E D G M E N T S

The author is very grateful to Dr. James O. Jirsa for his direction and encouragement throughout the test program, and for his assistance in the writing of this report. He also appreciates suggestions by John E. Breen, who revised a preliminary draft of the text.

The author extends his cheerful appreciation to Neil Cichy and Bill Smart, who shared tasks and sweat with the author during the fabrication and testing stages of the program; to fellow graduate students Julio Ramirez and Roberto Leon for their open advice on laboratory duties; and to Laurie Golding, secretary, and Dan Perez, technician, whose exceptional disposition in performing their jobs at the lab significantly smoothed the advance of this project. The staff of the Ferguson Structural Engineering Laboratory is much thanked for their assistance.

Suggestions on the paste-up work by Isabel de la Torre and her refreshing friendship during the writing of this thesis are most valued by the author.

The author wishes to express his profound gratitude to his family for their constant care and support and dedicate this work to them.

M.R.C.  
November 1982

# T A B L E O F C O N T E N T S

Chapter		Page
1	INTRODUCTION . . . . .	1
	1.1 General . . . . .	1
	1.2 Single Bolt Capacity . . . . .	3
	1.3 Behavior of Bolts in a Group . . . . .	7
	1.4 Objective and Scope . . . . .	9
2	EXPERIMENTAL PROGRAM . . . . .	10
	2.1 Introduction . . . . .	10
	2.1.1 Prototype . . . . .	10
	2.1.2 Test Parameters . . . . .	15
	2.2 Specimen Description . . . . .	17
	2.2.1 Geometry and Details . . . . .	17
	2.2.2 Materials . . . . .	22
	2.2.3 Fabrication . . . . .	25
	2.2.4 Instrumentation . . . . .	31
	2.3 Loading System . . . . .	37
	2.3.1 Test Frame . . . . .	37
	2.4 Test Procedure . . . . .	45
	2.4.1 Loading Sequence . . . . .	45
	2.4.2 Load Stage Measurements . . . . .	46
3	TEST RESULTS . . . . .	49
	3.1 Introduction . . . . .	49
	3.2 Load-Slip Relationships . . . . .	52
	3.3 Crack Patterns . . . . .	60
	3.4 Transverse Reinforcement . . . . .	79

Chapter	Page
4 TEST COMPARISONS . . . . .	87
4.1 Introduction . . . . .	87
4.2 Single Bolt Capacity . . . . .	88
4.3 Effect of Bolt Spacing . . . . .	89
4.4 Effect of Clear Cover . . . . .	93
4.5 Effect of Bolt Staggering . . . . .	97
4.6 Effect of Reduced Bearing Area . . . . .	102
4.7 Summary of Test Results . . . . .	105
4.7.1 Hasselwander's Tests . . . . .	105
4.7.2 Capacity Reduction for Bolt Group . . . . .	106
5 SUMMARY AND CONCLUSIONS . . . . .	111
5.1 Summary of Study . . . . .	111
5.2 Summary of Test Results . . . . .	112
5.3 Conclusions . . . . .	114
APPENDIX A . . . . .	115
A.1 Equilibrium Check . . . . .	116
A.2 Modification to Cichy's Results . . . . .	124
A.3 Reliability in Measured Bolt Forces . . . . .	125
BIBLIOGRAPHY . . . . .	129

L I S T O F T A B L E S

Table		Page
2.1	TDHPT Standard Plans - Cantiliver Overhead Sign Support Structure . . . . .	12
2.2	Summary of Test Parameters . . . . .	16
2.3	Check on Test Parameters . . . . .	30
4.1	Single Bolt Capacity . . . . .	89
4.2	Effect of Bolt Spacing . . . . .	92
4.3	Effect of Clear Cover . . . . .	96
4.4	Effect of Bolt Staggering . . . . .	100
4.5	Effect of Reduced Bearing Area . . . . .	104
4.6	Hasselwander's Two-Bolt Group Tests . . . . .	106
A.1	Error Due to Simplifying Assumptions . . . . .	123
A.2	Methods for Calculating Bolt Force . . . . .	126
A.3	Mid Gage vs. Lead Gage Average Reading at Bolt Capacity . . .	128

## L I S T   O F   F I G U R E S

Figure	Page
1.1    Conditions around the anchorage after formation of the cone of crushed concrete . . . . .	5
1.2    Comparison of lead slip-lead stress curves of bolts in a group . . . . .	8
2.1    TDHPT details-cantilever overhead sign support base . . . . .	11
2.2    Orientation of loading on bolt group . . . . .	14
2.3    Typical specimen geometry and details . . . . .	18
2.4    Bolt group patterns . . . . .	20
2.5    Bolt group nomenclature . . . . .	23
2.6    Bolt template mounted on wood frame . . . . .	26
2.7    Plumbed tube secured to base . . . . .	26
2.8    Anchor bolt template . . . . .	27
2.9    Spiral cage in place . . . . .	27
2.10   Bolts inside formwork - tests STG1 and SC7 . . . . .	28
2.11   Instrumented bolts on template . . . . .	29
2.12   Typical specimen after stripping formwork . . . . .	29
2.13   Location of bolt instrumentation . . . . .	32
2.14   Strain gages mounted on spiral bars at the anchorage end of the top bolts . . . . .	33
2.15   Lead slip wire, tail slip wire and strain gage at the anchorage end . . . . .	35
2.16   Slip measurement device mounted on specimen . . . . .	36
2.17   Free body diagrams of test set-up . . . . .	38
2.18   Test frame - elevation . . . . .	39



Figure	Page
2.19 Test frame - plan view . . . . .	40
2.20 Test set-up prior to testing . . . . .	41
2.21 Rear reaction assembly of test frame . . . . .	43
2.22 Front loading assembly of test frame . . . . .	43
2.23 Anchor bolts fixed to loading beam . . . . .	44
2.24 Specimen - loading beam interface . . . . .	44
2.25 Electric pump, pressure gage, and strain box used to control the load applied on the beam . . . . .	47
3.1 Lead strain gages mounted on threaded length . . . . .	51
3.2 Loading and load-slip curves of anchor bolts in test NOW . . . . .	53
3.3 Loading and load-slip curves of anchor bolts in test SC6 . . . . .	54
3.4 Loading and load-slip curves of anchor bolts in test SC7 . . . . .	55
3.5 Loading and load-slip curves of anchor bolts in test SC8 . . . . .	56
3.6 Loading and load-slip curves of anchor bolts in test STG1 . . . . .	57
3.7 Loading and load-slip curves of anchor bolts in test STG2 . . . . .	58
3.8 Development of crack patterns of top bolts in test NOW . . . . .	61
3.9 Development of crack patterns of top bolts in test SC6 . . . . .	62
3.10 Specimen surface at failure: test SC6 . . . . .	63
3.11 Development of crack patterns of top bolts in test SC7 . . . . .	64
3.12 Specimen surface at failure: test SC7 . . . . .	65

Figure	Page
3.13 Development of crack patterns of top bolts in test SC8 . . . . .	66
3.14 Specimen surface at failure: test SC8 . . . . .	67
3.15 Initial cracks and bolt data near failure in test STG1 . . . . .	68
3.16 Crack patterns of top bolts: test STG1 . . . . .	69
3.17 Initial cracks and bolt data near failure in test STG2 . . . . .	70
3.18 Crack patterns of top bolts: test STG2 . . . . .	71
3.19a Cone of crushed and compacted concrete in front of anchorage device . . . . .	73
3.19b Anchor bolts after removal from test specimen showing cone of compacted concrete . . . . .	74
3.20 Splitting force radiated out of concrete cone . . . . .	76
3.21 Model of wedge-splitting failure of top bolts . . . . .	77
3.22 Position of spiral bars ahead of bearing face . . . . .	80
3.23 Spiral stress vs. percentage of bolt strength and tail slip of top bolts in tests NOW and SC8 . . . . .	81
3.24 Spiral stress vs. percentage of bolt strength and tail slip of top bolts in tests STG2 and SC7 . . . . .	83
3.25 Spiral stress vs. percentage of bolt strength and tail slip of top bolts in tests STG1 and SC6 . . . . .	85
4.1 Effect of bolt spacing: tests SC1 and SC7 . . . . .	90
4.2 Effect of bolt spacing: tests SC2 and SC4 . . . . .	91
4.3 Effect of clear cover: tests SC6 and SC8 . . . . .	94
4.4 Effect of clear cover: tests SC1 and SC4 . . . . .	95
4.5 Effect of bolt staggering: tests SC1 and STG1 . . . . .	98
4.6 Effect of bolt staggering: tests SC2 and STG2 . . . . .	99

Figure	Page
4.7	Effect of reduced bearing area: tests SC6 and NOW . . . . . 103
4.8	Reduction in average capacity for bolts in a group with spacing . . . . . 107
4.9	Effect of circular shape . . . . . 109
A.1	Equilibrium check in tests NOW and SC6 . . . . . 117
A.2	Equilibrium check in tests SC7 and SC8 . . . . . 118
A.3	Equilibrium check in tests STG1 and STG2 . . . . . 119
A.4	Reactions at the specimen-loading beam interface . . . . . 121
A.5	Grooved plate detail . . . . . 122

# C H A P T E R 1

## INTRODUCTION

### 1.1 General

Anchor bolt groups to connect supports for steel members to structural concrete members have many applications in highway structures. Current ASSHTO specifications, however, lack satisfactory guidelines for the design and understanding of high-strength, anchor bolt group installations.

Cichy<sup>1</sup> has recently surveyed typical anchor bolt applications and details from a selected number of state highway departments including Texas. The review of the material indicated that the use of anchor bolt groups for light standard supports, sign structure supports, traffic signal supports, and bridge shoe connections is fairly common in current practice. Several methods of anchoring bolts in the concrete were identified, such as: hooked ends, threaded plates, nuts and washers, solely or in combination with square or ring plates. Low-strength,  $f_y = 36$  ksi, and high-strength,  $f_y = 75$  to 120 ksi, bolts are presently in use.

Three studies<sup>1,3,4</sup> have been conducted at the University of Texas at Austin to identify the factors affecting the strength and the behavior of isolated anchor bolts. These investigations have focused on highway-related installations, which typically use long embedment length and relatively small edge cover. Such installations should be distin-

guished from bolts embedded for short lengths in mass concrete with very large cover. In the latter case, the bolt might exhibit an entirely different failure mechanism, and consequently, the results from the investigations do not apply directly to bolts embedded in mass concrete.

The first study<sup>2</sup> was directed toward determining the required embedment length for A7 ( $f_y = 33$  ksi) anchor bolts. A nut or a nut and a standard washer were used for the anchorage device. For the 1-1/4 in. to 3 in. bolts tested, it was concluded that a length of ten diameters (10D) was needed to develop bolts up to 2-1/2 in., 15D was required for the 3 in. bolts. The end anchorage was identified as the main load-carrying element, while concrete-to-steel bond played a minor role in the development of the strength of the anchor bolt. Concrete cover over the bolt was reported to influence the strength significantly.

A second study by Lee and Breen<sup>3</sup> investigated the effects of clear cover, low-cycle repeated loading, circular shape of the specimen, low concrete strength, 90° bend as anchorage device, and the method of loading. Bolts with a 60 ksi yield stress, 1-1/4 in. and 2 in. diameters, embedded to 10D, and anchored with a standard nut were used.

It was established through this investigation that clear cover was the single most important factor in the development of the strength of an anchor bolt installation. Low concrete strength adversely affected the bolt ultimate strength and behavior. The presence of a compressive force along the length of the bolt, characteristic of the loading method in the first study, did not significantly influence the strength, but it increased the stiffness of the anchor bolt. A limited number of

tests indicated that 90° bends were not as efficient as the standard nut anchorage. Finally, the effects of a circular specimen (as compared to a rectangular one), and of low-cycle repeated loading, were considered negligible.

## 1.2 Single Bolt Capacity

The most recent investigation, reported by Hasselwander et al.<sup>4</sup>, with ASTM A193 alloy steel extended the results of the earlier studies to high-strength anchor bolts (105 ksi yield stress). The major objectives of the study were to evaluate the effects of various factors on the ultimate load capacity and the behavior of high-strength anchor bolts as follows:

- (1) Bolt diameter - 1 in. and 1-3/4 in. bolts were used.
- (2) Embedment length - 10, 15 and 20 bar diameters.
- (3) Clear cover - ranged from 1.0 in. to 4.5 in. for the 1 in. bolts, and from 2.5 in. to 6.0 in. for the 1-3/4 in. bolts.
- (4) Bearing area - various washer sizes were used with variation in clear cover.

In addition, limited exploratory tests were conducted to determine the influence of: cyclic loads, lateral load, bolt groups and transverse reinforcement.

Three distinct failure modes, dependent on the amount of cover and embedment length, were identified from the test results. These were: (1) bolt yielding, generally in the threaded region; (2) cover spalling, a relatively sudden localized spalling of the cover over the

anchorage device for small clear cover; and (3) wedge-splitting, the formation of a cone of crushed and compacted concrete in front of the washer which split the concrete into blocks and forced the spalling of a large portion of the cover in cases with large clear cover.

The mechanism by which an anchor bolt transfers load to the concrete has been described as "a sequence involving steel to concrete bond, bearing against the washer, and wedging action by the cone of concrete ahead of the washer."<sup>4</sup> As bond along the bolt is lost after the early stages of loading, high bearing stresses develop at the anchorage, which compact the concrete forming the cone ahead of the washer (see Fig. 1.1). The cone acts like a wedge to split the cover and cause failure.

The study concluded that clear cover and bearing area were the main variables governing the strength of single anchor bolts. The variables were incorporated into an equation for predicting the strength of isolated anchor bolts, subjected to simple tension and failing in a wedge-splitting mode:

$$T_n \text{ (kips)} = 0.140 A_b \sqrt{f'_c} \left[ 0.7 + \ln\left(\frac{2C}{D_w - D}\right) \right]$$

where  $A_b$  is the net bearing area ( $\text{in.}^2$ ),  $D$  and  $D_w$  are the bolt and washer diameter ( $\text{in.}$ ), and  $C$  is the clear cover to the bolt ( $\text{in.}$ ). The design tensile strength,  $T$ , was determined as:

$$T \leq T_n \text{ but } \leq A_{sm} f_y$$

where

$\phi$  = a capacity reduction factor of 0.75,

$A_{sm}$  = mean tensile area of the anchor bolt,

$f_y$  = yield stress of the bolt material.

The design equation was developed from a regression analysis on test

results of bolts failing in the wedge-splitting mode only. A minimum embedment length of  $12(D_w - D)$  was suggested to allow the wedge-splitting mechanism to form. A restriction which accounted for a reduced bearing efficiency observed for large washers, limited the bearing area to  $4D^2$ . Furthermore, a minimum washer thickness,  $D_w/8$ , was suggested to prevent excessive flexibility of the washer.

The results of the exploratory tests identified specific areas requiring further research. It was shown that the application of a lateral force in the direction of the cover significantly reduced the ultimate tensile strength. For a lateral load roughly equivalent to the shear capacity of the anchor bolt installation, failure occurred at a 30 to 50 percent lower strength than a bolt with similar geometry and no lateral load. The destruction of the top cover at the front of the specimen and the longitudinal splitting along the bolt axis were reported to account for the reduced ability of the cover to resist wedge-splitting. Transverse reinforcement, in the form of two hairpins around the anchor bolt, ahead of the anchorage device, was observed to assist the layer of clear cover in resisting wedge-splitting. It was concluded that the presence of transverse reinforcement can result in a significantly higher ultimate strength (about 20 percent in one test) and ductility than would otherwise be available with relatively shallow cover. Low-cycle repeated loading at service loads (defined at  $0.6f_y$  mean stress level for a 1 in. and 1-3/4 in. bolt tested) did not show a significant effect on the performance of an anchor bolt.



### 1.3 Behavior of Bolts in a Group

Limited test results reported by Hasselwander et al.<sup>4</sup> indicated that the interaction among bolts embedded in close proximity may result in an abrupt, nonductile failure of the bolt group at individual bolt loads significantly less than predicted for an isolated bolt with similar geometry. Three tests were conducted on two-bolt groups with 1 in. bolts on 5 in., 10 in., and 15 in. center-to-center spacing. All three groups had a clear cover of 2.5 in., an embedment length of 15D, and an end anchorage consisting of a 1/2 in. thick nut and standard-diameter (2.5 in.) washers.

In Fig. 1.2, the two-bolt groups and a single bolt with similar geometry are compared in terms of lead slip and average mean stress normalized with respect to  $\sqrt{f'_c}$ . On the average, the capacity of the bolts in a group was 51, 65, and 58 percent that of the single bolt for the 5 in., 10 in. and 15 in. spacing respectively. The reduction in strength for the bolt groups was attributed to the interaction of splitting forces between the two bolts which did not allow the wedge-splitting mechanism to fully develop.

It has been established<sup>4</sup> that the ultimate strength of a bolt group can not be defined on the basis of the strength of a single bolt with similar geometry. Extended investigation on the bolt interaction is needed first. The fact that the critical spacing beyond which the bolts behave as single bolts is apparently much larger than is normally found in highway practice further points to needed research.

#### 1.4 Objective and Scope

In the present study, the behavior and ultimate capacity of high-strength anchor bolt groups embedded in reinforced concrete piers was investigated. The effect of bolt spacing on the group capacity was the main factor examined. In addition, the effect of (1) clear cover, (2) variable anchorage lengths in a bolt group, and (3) transverse reinforcement were evaluated to a more limited extent.

Anchor bolts with 1-3/4 in. diameter and 105 ksi yield stress were arranged in 4-bolt groups and tested to failure in simple tension. The bolts were observed to fail in a wedge-splitting mode. The response of the anchor bolts was measured in terms of bolt force versus slip curves. The group interaction was evaluated by comparing the actual strength of bolts in a group with the predicted capacity for an isolated bolt with similar geometry. The test results indicated that bolts in a group embedded at close spacing (8.9 in. to 13.5 in. were used) will have about a 30 percent reduction in ultimate capacity.

## C H A P T E R 2

### EXPERIMENTAL PROGRAM

#### 2.1 Introduction

This study is part of a broad program to determine the tensile capacity of high-strength anchor bolt groups embedded near edges of reinforced concrete piers. Specifically, the anchor bolt groups are loaded in tension (no transverse shear force) and fail in a wedge-splitting mode.<sup>4,5</sup>

Hasselwander et al.<sup>4</sup> reported an equation for the tensile capacity of an isolated bolt failing in a wedge-splitting mode. A series of exploratory tests on two-bolt groups showed that interaction of the failure surfaces reduce the capacity compared with an individual bolt. The objective of this project is to identify modifications to the single bolt strength for the bolt group interaction in typical anchor bolt applications.

2.1.1 Prototype. Drawings representing various anchor bolt group applications were obtained from the Bridge Division of the Texas Department of Highways and Public Transportation (TDHPT). A cantilever overhead sign support base was chosen as the prototype for the study. The original details used in the development of the specimen are shown in Fig. 2.1. The specimen represents a reinforced concrete drilled shaft footing with cast-in-place anchor bolts. The bolts are used to anchor the overhead sign structure to the footing. Typical details call

for six, equally spaced, high-strength ( $f_y = 105$  ksi) anchor bolts arranged in a circular pattern for the base connection. The prototype bolt pattern was modified to accommodate eight bolts (four in tension) in designing the test specimen (see Fig. 2.2).

The design procedure used by the TDHPT for this connection is governed by the size of tower pipe required. When computing design loads, the neutral axis in bending is assumed at the centroid of the bolt group. Bolts are typically embedded to a length of twenty bolt diameters (20D). The design stress at service (unfactored) load level is limited to 55 ksi for high-strength bolts because of fatigue considerations. No reduction factor for the group capacity is used to account for bolt interaction.

In the test program, the applied moment is oriented to yield the lowest capacity from the eight bolt connection. Such loading pattern calls for two bolt levels; in each level there is a pair of bolts equally spaced from the bending axis as shown in Fig. 2.2.

Horizontal wind pressure on the overhead sign structure induces moment at the base. The moment produces tensile forces in half the bolts, and compression in the other half. On the specimen, such a loading condition is simulated by a loading beam which extends approximately ten feet from the end of the specimen. The beam applies a tensile force to the four-bolt test groups and compression is transmitted to a plate, bearing on the end of the specimen. In this manner, two tests (four bolts each) are obtained from the test specimen without compromising the nature of the loading on the bolts subjected to tension.

2.1.2 Test Parameters. The results of nine tests (summarized in Table 2.2) are reported. Bolt spacing, clear cover and variation in anchorage length are the major variables in the test program.

Clear cover and bolt spacing values represent the typical range for highway applications. "Clear cover" is the clear distance between a bolt and the concrete surface along a radial line. In the test program, values from 2.4 to 7.4 in. were used. "Bolt spacing" is defined as the length of a straight line, center-to-center, between two adjacent bolts and varied between 8.9 and 13.5 inches.

Standard anchorage, as defined in Table 2.2, was used in all tests except NOW, STG1 and STG2. In test NOW (no washers), only a nut was placed at the embedded end of the bolts. The original TDHPT anchorage detail (1977) calls only for the nut, but this is likely to be modified in the future.

Staggered bolts in tests STG1 and STG2 were used to offset the interaction of the failure surfaces. Staggering consisted of moving adjacent bolts five inches above and below the standard 35 in. embedded length. On the average, the group embedment was not changed and those bolts with a short embedment (30 in.) still satisfied the minimum imbedment,  $15D$ , recommended in previous studies<sup>2,4</sup>. The two tests were aimed toward finding a practical method, other than increasing the bolt spacing, to separate the cones of crushed and compacted concrete at front of the anchorage device. The staggered bolts were tested with two significantly different cover conditions.

Not evident from Table 2.2 is the attention given to the role of

Table 2.2 SUMMARY OF TEST PARAMETERS

Test	Drilled Shaft Dia. (in.)	Bolt Circle Dia. (in.)	Date Cast	Date Tested	$f'_c$ Test Date (psi)	(1) Bolt Spacing (in.)	(1) Clear Cover (in.)	(2) Anchorage Type
SC1	36	29 3/8	7-22-81	9-25-81	3500	11.2	2.4	STD
SC2	36	23 3/8	7-22-81	10-22-81	3600	8.9	5.4	STD
SC3 (3)	42	31 3/8	11-11-81	1-20-82	4100	12.0	4.4	STD
SC4	42	29 3/8	11-11-81	2-04-82	4200	11.2	5.4	STD
NOW	36	25 3/8	12-07-81	3-03-82	3900	9.7	4.4	NOW
SC6	36	25 3/8	12-07-81	4-07-82	3900	9.7	4.4	STD
SC7	42	35 3/8	2-22-82	5-12-82	3600	13.5	2.4	STD
SC8	42	25 3/8	2-22-82	5-20-82	3600	9.7	7.4	STD
STG1	36	29 3/8	4-30-82	5-24-82	3800	11.2	2.4	STG
STG2	36	23 3/8	4-30-82	6-11-82	3900	8.9	5.4	STG

(1) See Fig. 2.5 for definition.

(2) STD: 1 3/4 in. bolt dia. Embedment length = 35 in.  
 Nut and 2 washers 3/8 in. total thickness  
 Bearing area = 10.16 in.<sup>2</sup> Except

NOW: No washers. Net bearing area = 4.29 in.<sup>2</sup>

STG: Staggered Bolts (10 in.)  
 Average embedment length = 35 in.

(3) This test has been eliminated from the results due to problems with the data acquisition.

transverse reinforcement in bolt group behavior. The spiral cage in every specimen was instrumented where the spiral bar crosses the most highly stressed bolts. The increase in the tensile force in the spiral with increase in the bolt force provides additional data regarding the failure mechanism.

Tests SC1 to SC4 have been reported previously in detail by Cichy<sup>1</sup>. For this report, the data was reevaluated in calculating the bolt forces from the recorded data. This conversion is discussed in Appendix A.

## 2.2 Specimen Description

2.2.1 Geometry and Details. The geometry and details of the specimens are sketched in Figs. 2.3 and 2.4. For 36 and 42 in. drilled shafts, the TDHPT calls for 8 to 16 longitudinal bars (#10 or #11) and #3 or #4 plain bar spirals at 6 in. pitch. For the test specimens, sixteen #11 bars were used for the first two tests, and eight #11 plus eight #9 bars were used in the fabrication of the last three specimens. The smaller bars were placed in pairs at 45 degrees with the horizontal bolt group axis (defined in Fig. 2.5). The specimens were overreinforced, compared with the prototype, to ensure that the bolt group failed prior to flexural failure of the cylinder or anchorage failure of the rebars.

The bolts in a typical specimen were embedded into the concrete about 37 inches, which includes 2 inches for the nut and washers. Previous research<sup>5</sup> indicates that a single standard-diameter washer may not be fully effective in bearing. To prevent excessive bending in the washers,

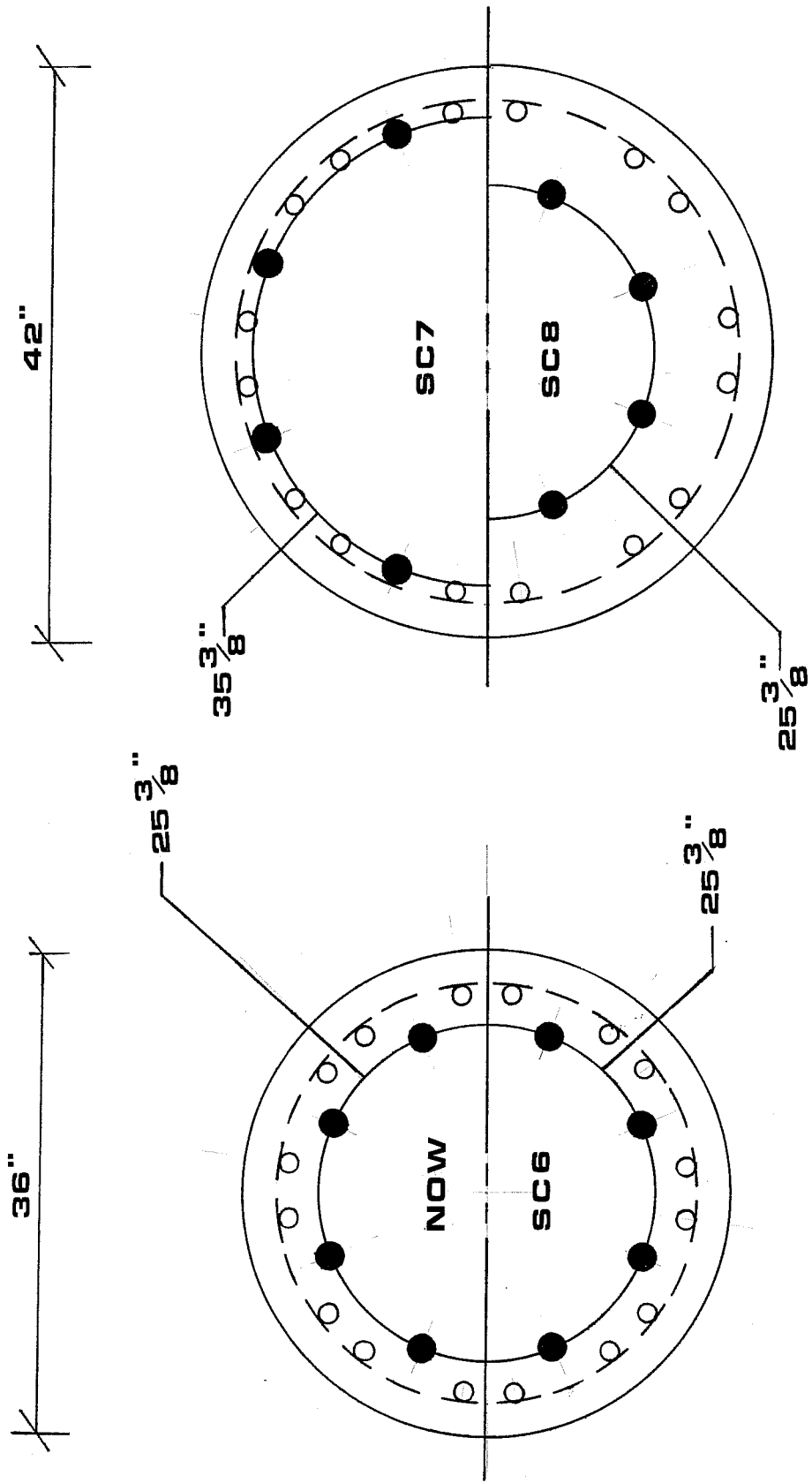


Fig. 2.4 (Cont.)



a minimum thickness  $D_w/8$  ( $D_w$  is washer diameter) has been suggested. To approximate this requirement for the 1-3/4 in. bolts, two 3/16 in. washers ( $D_w = 4.0$  in.) were specified along with a nut as the anchorage device. One bolt group in specimen 3 (test NOW) was cast without washers. Bolts in specimen 5 were staggered as shown in Fig. 2.3b. The group average embedment length (35 in.) is equal to that in all other tests.

The overall concrete specimen length, 6.5 ft., was chosen to eliminate interference from the reaction supports on the anchorage region. In addition, the layout of the test frame and the floor reaction system also dictated certain constraints on the specimen length.

Figure 2.4 shows the bolt patterns for each test, particularly the bolts' proximity to the spirals. The bolt nomenclature followed in the report for a typical specimen cross-section is sketched in Fig. 2.5.

2.2.2 Materials. In general, selection of materials conformed to the standard specifications<sup>6</sup> of the TDHPT. The specifications also served as a reference guide for the construction.

Anchor Bolts, Nuts, Washers. The materials used in the fabrication of the anchor bolts conformed to ASTM A193 Grade B7, with a minimum yield strength of 105 ksi and tensile strength of 125 ksi<sup>7</sup>. No stress-strain curve was obtained for the bolt material. Instead, a modulus of elasticity of 30,000 ksi, as suggested by the bolt supplier, was assumed in the analysis.

The end anchorage for each bolt consisted of an ASTM specification A194 Type 2H (Heavy Hex) nut and two 3/16 in. thick standard-

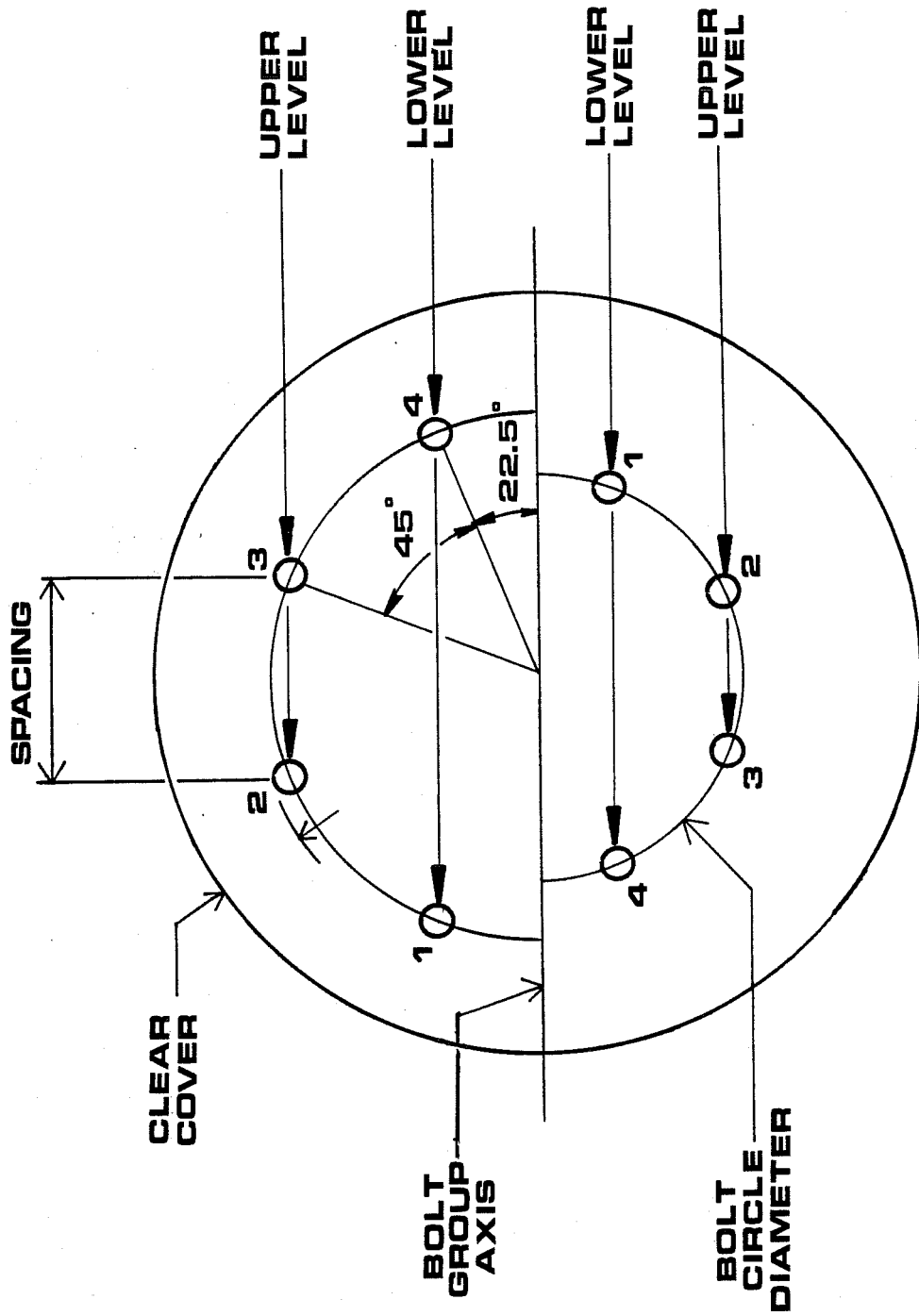


Fig. 2.5 Bolt group nomenclature

diameter (4.0 in.) washers. Thread for the bolts and nuts conformed to ANSI B1.1, 8UN designation.

Concrete. Ready-mixed concrete was obtained from a local supplier. Normal-weight concrete was designed for a nominal strength  $f'_C = 3600$  psi. Type I cement, Colorado River sand and gravel, 1 in. maximum size, were used. An air-entraining agent, Septair, was added to the mix at the plant to provide 6 percent air. The mix design for specimens 1 and 5 (cast in warm weather) is shown below. Only 80 percent of

Concrete Mix Design ( $f'_C = 3600$  psi)

Quantities per cubic yard

Cement (5 sacks/cu.yd.)	470 lb.
Water (5.5 gal./sack)	27.5 gal.
Gravel	1890 lb.
Sand	1375 lb.
Entrained-air (Septair)	6%

the water was added at the plant, the rest was added at the lab to obtain a desired slump of 6 to 8 inches.

Specimens 2, 3 and 4 were cast in colder weather. For the second mix, the cement content was decreased to 4.5 sacks/cyd., but the water-cement ratio was held constant at 5.5 gal./sack.

Concrete compressive strength ( $f'_C$ ) was determined from the average of three 6 x 12 in. standard cylinders. Concrete strength at the test date is listed in Table 2.2.

Steel Reinforcement. The spiral was fabricated from Grade 40, #4 deformed bars. The TDHPT plans call for the spiral to be fabricated from plain bar; however, it was learned that the TDHPT is currently specifying deformed bars for spirals. Grade 60, #9 and #11 longitudinal bars were used inside the spiral cage.

### 2.2.3 Fabrication.

Formwork Assembly. The formwork consisted of a circular tube supported by a wooden frame and base. Commercially available 36 and 42 in. cardboard tubes cut to 6.75 ft. height were used to form the pier. The wooden frame braced the tube at three levels and supported a template in which the bolts were secured for casting (Fig. 2.6). A space between the top of the tube and the template was left for vibrating the concrete and finishing the surface. The tube was seated on a 3 in. thick circular plate, plumbed, and nailed in place (Fig. 2.7). The bolt template (Fig. 2.8) held the bolts in their prescribed pattern while casting. A square hole in the center of the template provided access to the inside of the tube, for working on the specimen prior to casting and for concrete placement.

Once the formwork was in place, the spiral cage was lifted into position with a crane (Fig. 2.9). The bolts, previously cleaned (degreased) and instrumented (Fig. 2.11) were secured to the template and mounted on the frame.

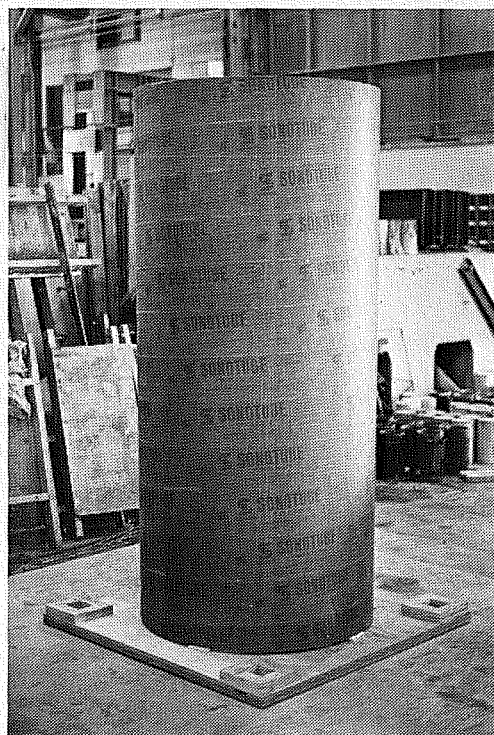
After the cage and bolts were in place, the spiral was instrumented. Inserts were installed to support the slip measurement devices, and holes were drilled in the tube wall for strain gage and slip wires. Lifting inserts were also installed. The inside of the tube prior to casting is shown in Fig. 2.10.

Care was taken to control bolt spacing and edge cover at the anchorage end of the bolts. Inside the tube, the alignment for each bolt was verified and bolts were secured to the spiral cage by means of tie wires and plain #2 bars. In Table 2.3, as-built dimensions measured



Fig. 2.6 Bolt template mounted on wood frame

Fig. 2.7 Plumbed tube secured to base



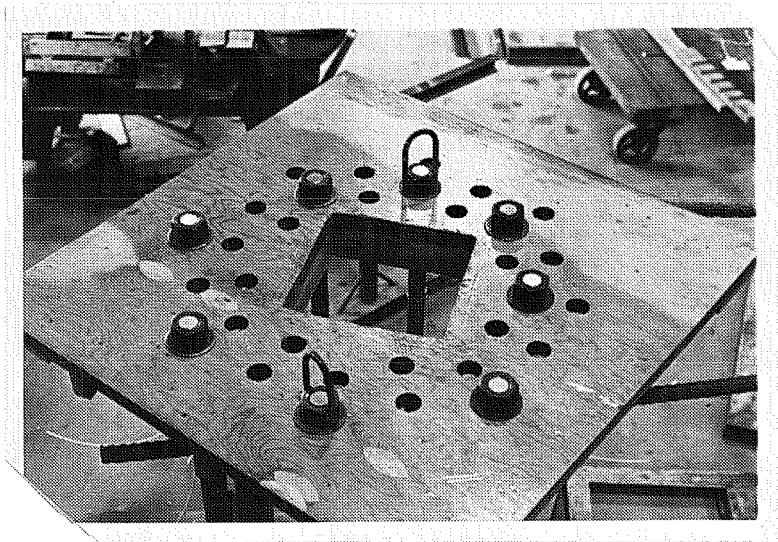


Fig. 2.8 Anchor bolt template

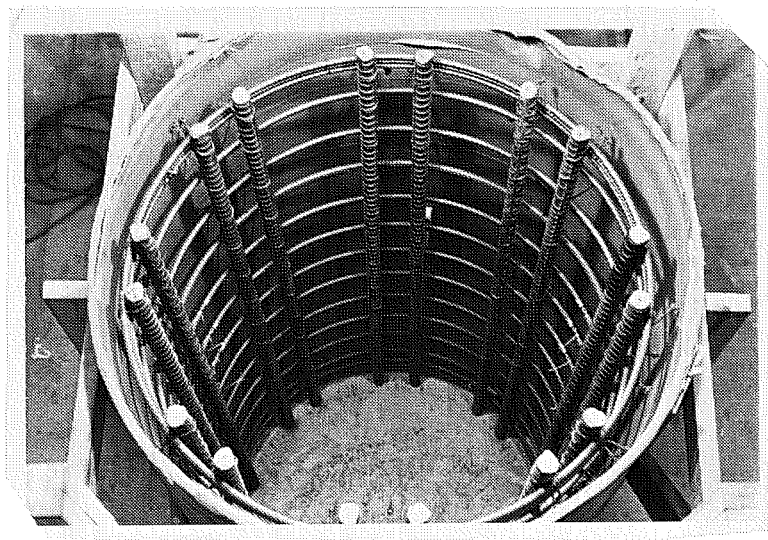


Fig. 2.9 Spiral cage in place

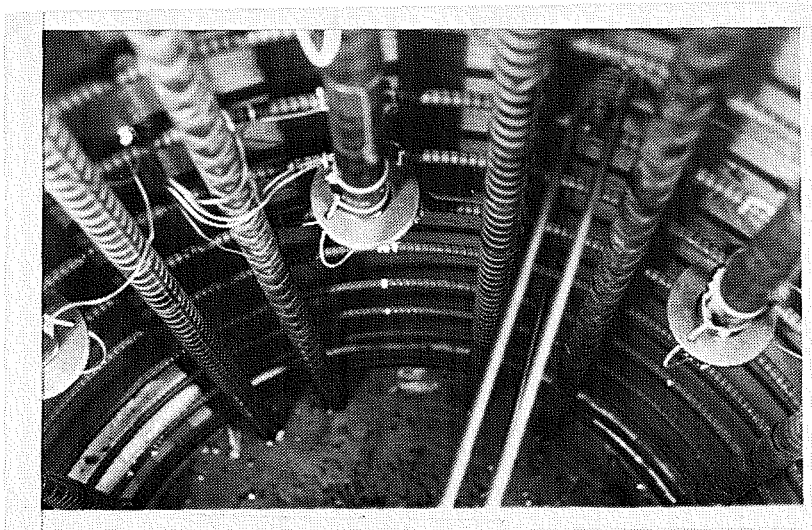
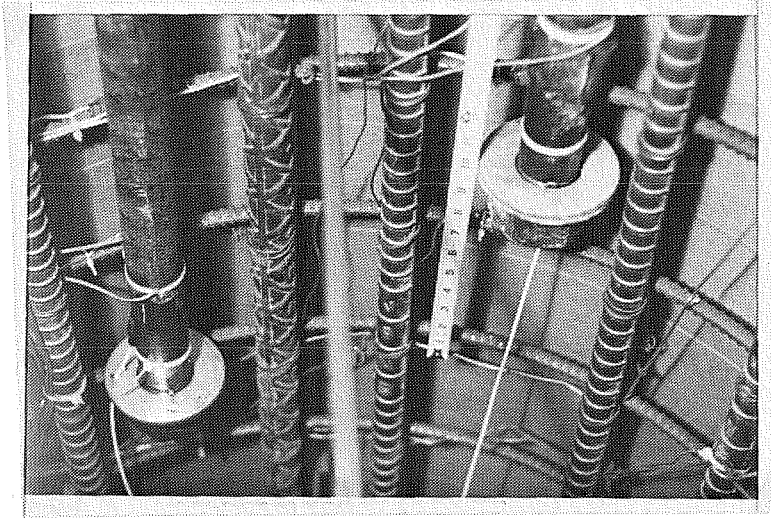


Fig. 2.10 Bolts inside formwork – tests STG1 and SC7

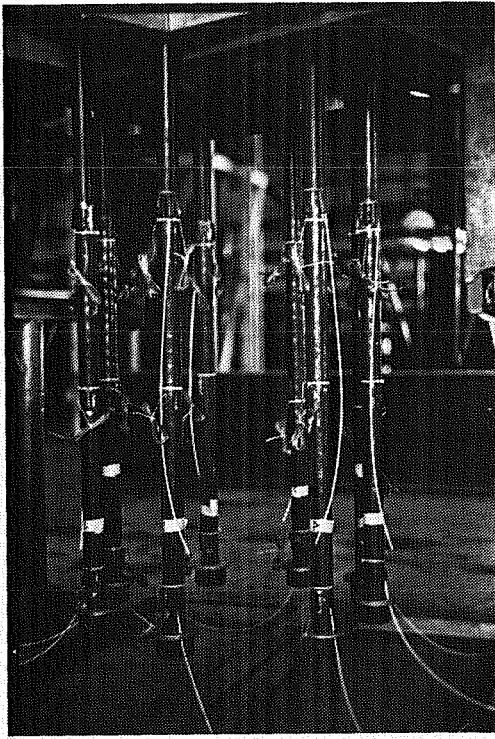


Fig. 2.11 Instrumented bolts  
on template

Fig. 2.12 Typical specimen  
after stripping  
formwork

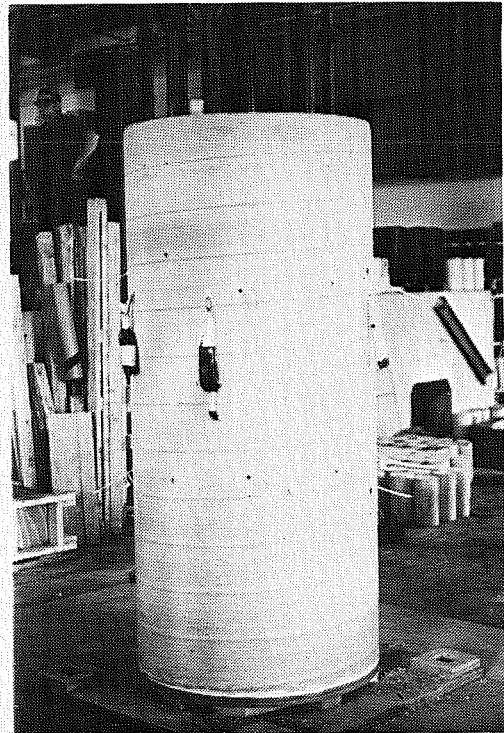




Table 2.3 CHECK ON TEST PARAMETERS

Test	Clear Cover (in.)		Design	Bolt Spacing (in.)	
	As-Built Bolt 2	Bolt 3		As-Built	Design
SC1	2.6	2.8	2.4	11.4	11.2
SC2	5.7	5.8	5.4	9.1	8.9
SC3	4.0	3.9	4.4	12.0	12.0
SC4	5.6	5.6	5.4	11.0	11.2
NOW	4.7	4.7	4.4	10.0	9.7
SC6	4.5	4.5	4.4	10.0	9.7
SC7	2.4	2.4	2.4	13.6	13.5
SC8	7.8	7.8	7.4	9.3	9.7
STG1	-	-	2.4	-	11.2
STG2	-	-	5.4	-	8.9

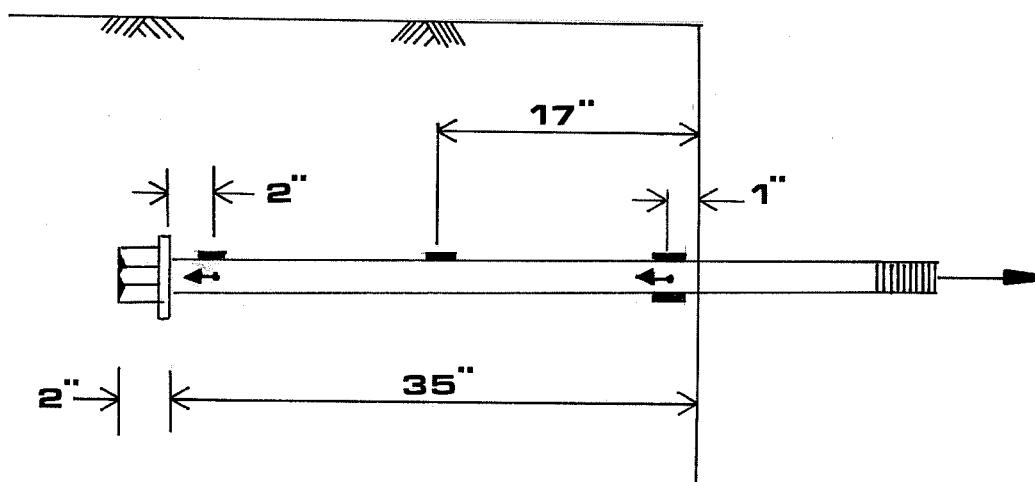
after removal of the destroyed concrete cover are compared with the nominal dimensions for the test groups. Small tolerances justify the use of nominal clear cover and bolt spacing values in the study.

Casting. The specimen was cast in a vertical position. Concrete was placed in several lifts, using a concrete bucket and overhead crane during a 10 to 15 minute operation. Standard 6 x 12 in. cylinders were cast to monitor the strength of the concrete. The top face of the specimen was allowed to bleed for thirty minutes, troweled smooth and covered with plastic sheets. The shaft formwork was usually stripped three days after casting; at that time the cylinders were removed from the molds. Figure 2.12 shows a typical specimen after stripping the form.

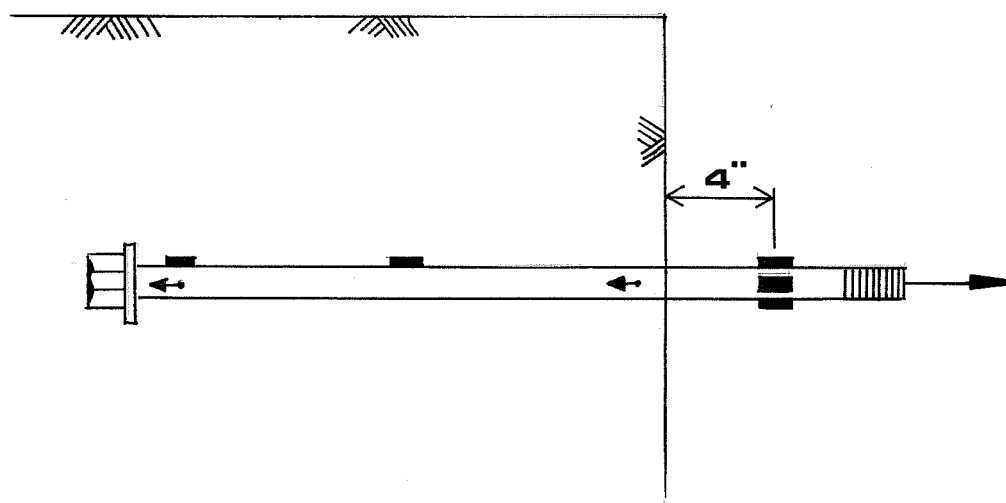
2.2.4 Instrumentation. Strain gages and slip wires attached to the bolts (see Fig. 2.13) were used to measure the response under loading. The spirals at the anchorage end of the upper-level bolts were gaged as shown in Fig. 2.14.

Strain Gages. Electrical resistance strain gages measured bolt strains. The 0.64 in. paper-backed gages were attached to a cleaned surface with an adhesive. Lead wires were soldered to the gage wires and the connection was waterproofed with a coat of silicone sealer and a polymer rubber pad. The rubber pad also served as a protective layer for the gage during concrete placement.

The location of strain gages along the bolt is illustrated in Fig. 2.13. For the first four tests, two gages were placed just below the face of the concrete; one at mid length, and one at the anchorage



(a) Tests SC1 through SC4



(b) Tests NOW through STG2

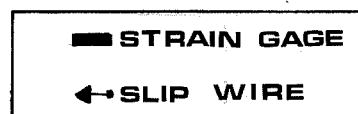


Fig. 2.13 Location of bolt instrumentation

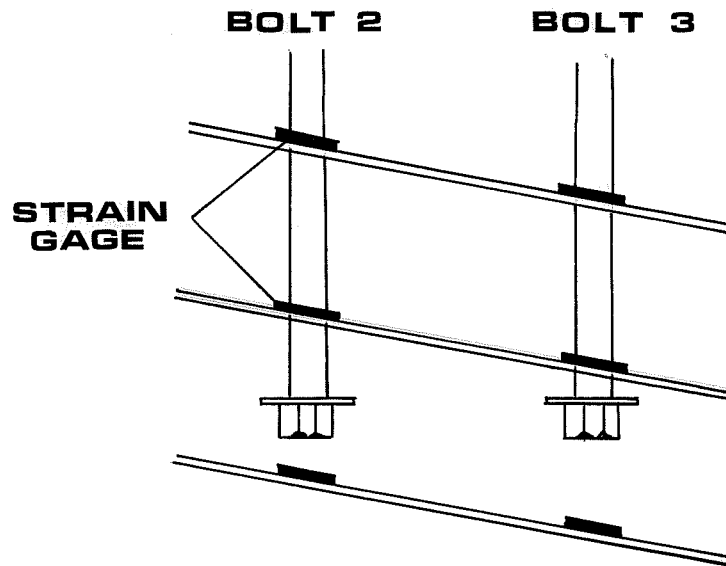
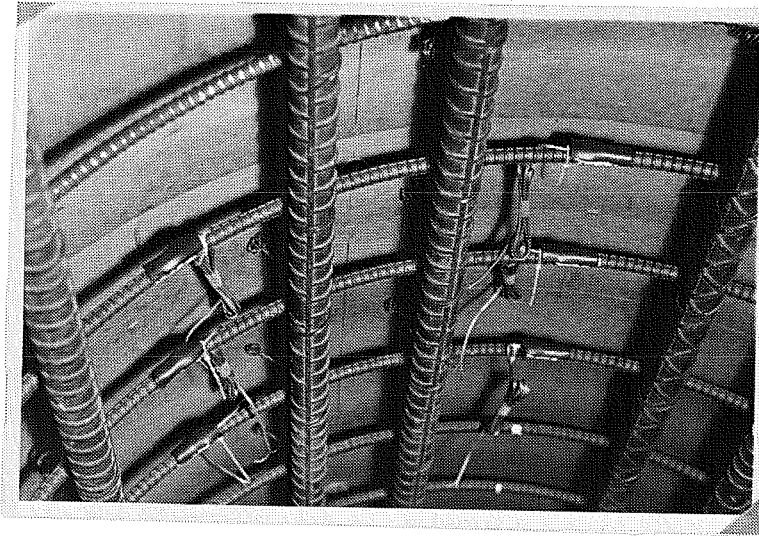


Fig. 2.14 Strain gages mounted on spiral bars at the anchorage end of the top bolts

end. After losing several gages due to abrasion against the concrete as the bolt slipped, the two lead gages were moved out of the concrete, and in the last six tests replaced by four gages, 90° apart, on the protruding bolt.

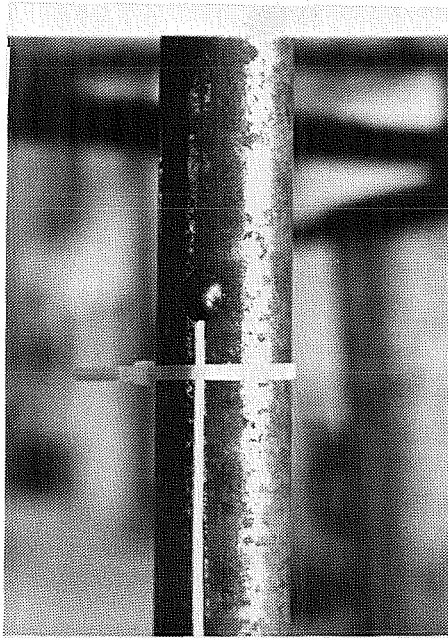
Significant bending on a bolt may accompany the pullout force as the bolt is loaded. To cancel the effect of bending stresses in a bolt, at least two gages, 180° apart, need to be averaged when calculating the bolt force.

Spirals in tests NOW through STG2 were typically instrumented as shown in Fig. 2.14. The two hoops at the front of the anchorage device and one hoop behind it were gaged at the location of the upper-level bolts.

Slip Wires. Anchor bolt movement relative to the concrete was measured by means of slip wires. A 0.059 in. diameter piano wire was attached to the anchor bolt at selected locations. A short 90° bend at the end of the wire was inserted into a hole of equal diameter drilled in the bolt. Plastic tubing was placed over the entire length of the wire to allow free movement and to prevent bonding. The plastic tube was sealed at the bolt end to prevent cement from interfering with the wire movement. Fig. 2.15 shows details of lead and tail wires attached to a bolt. Note that the tail slip wire passed through a small hole drilled in the washers. The wire was oriented parallel to the bolt axis in the direction of slip. Typically, slip was measured at lead and tail ends of the bolt as shown in Fig. 2.13.

A linear potentiometer was used to measure movement of the slip

(a)



(b)



Fig. 2.15 (a) Lead slip wire; (b) tail slip wire and strain gage at the anchorage end.

wire (Fig. 2.16). The wire movement relative to the concrete surface was measured by setting the potentiometer rod in compression against a small aluminum plate fastened to the wire end. A spring tensioned the wire to reduce wobble within the plastic tube.

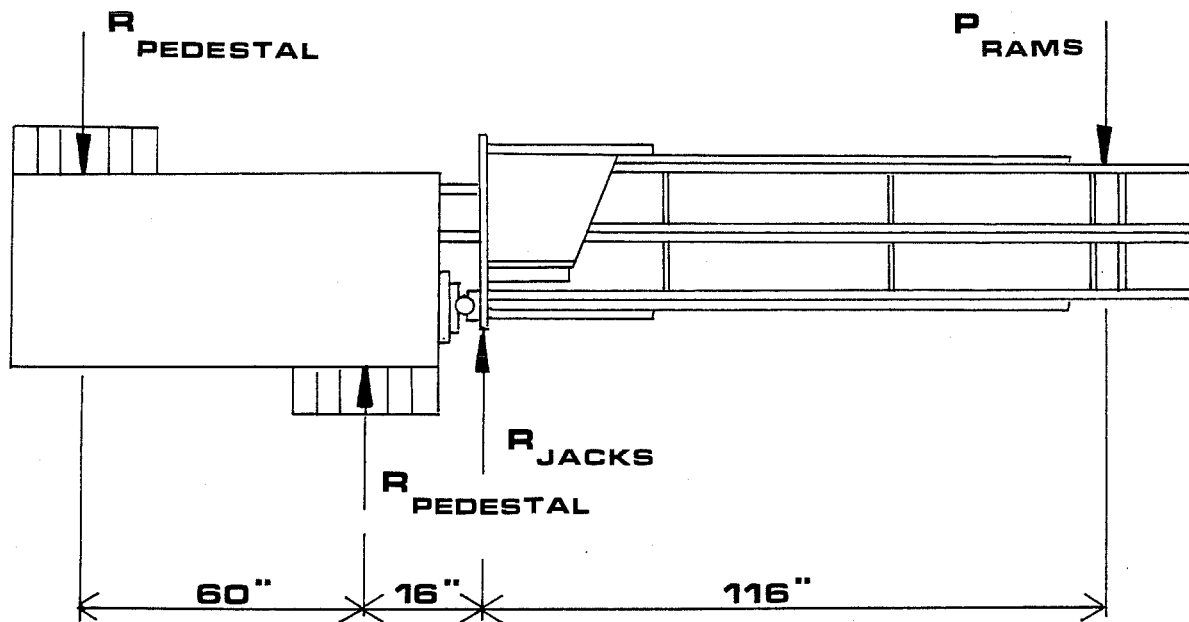
### 2.3 Loading System

The loading system models the pullout force on a bolt group connection for typical drilled shaft footings. By fixing a heavy member with a concentrated load at the end, a moment is applied on the connection which realistically simulates the loading pattern in the field. All the reaction conditions are not duplicated, however. The shear reaction which is transferred to the bolts in the prototype structure is not imposed on the test bolts; the bolts are tested in pure tension.

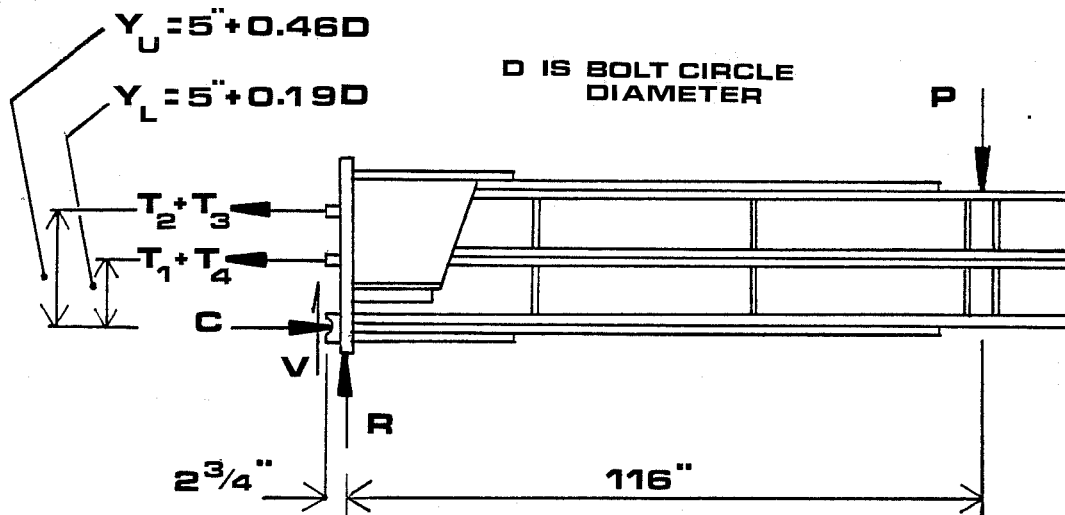
A general free body diagram of the specimen and loading beam set-up is shown in Fig. 2.17. Note in Fig. 2.17b that the bending moment is resisted by a couple consisting of the tension in the bolt group, and a compressive force acting on a bearing plate.

2.3.1 Test Frame. The assembly of the test frame requires (1) positioning the specimen; (2) aligning and supporting the loading beam by means of jacks; (3) mounting, extending and securing rams to the test floor; and finally, (4) fixing the beam to the anchor bolts at the face of the specimen.

Figures 2.18 to 2.20 are schematic drawings and views of the test frame. Three reinforced concrete collars were set on a thin layer of grout to hold the specimen in place. The rear of the specimen was



(b) Loading beam



(a) Specimen and loading beam

Fig. 2.17 Free body diagrams of test set-up



# TEST FRAME

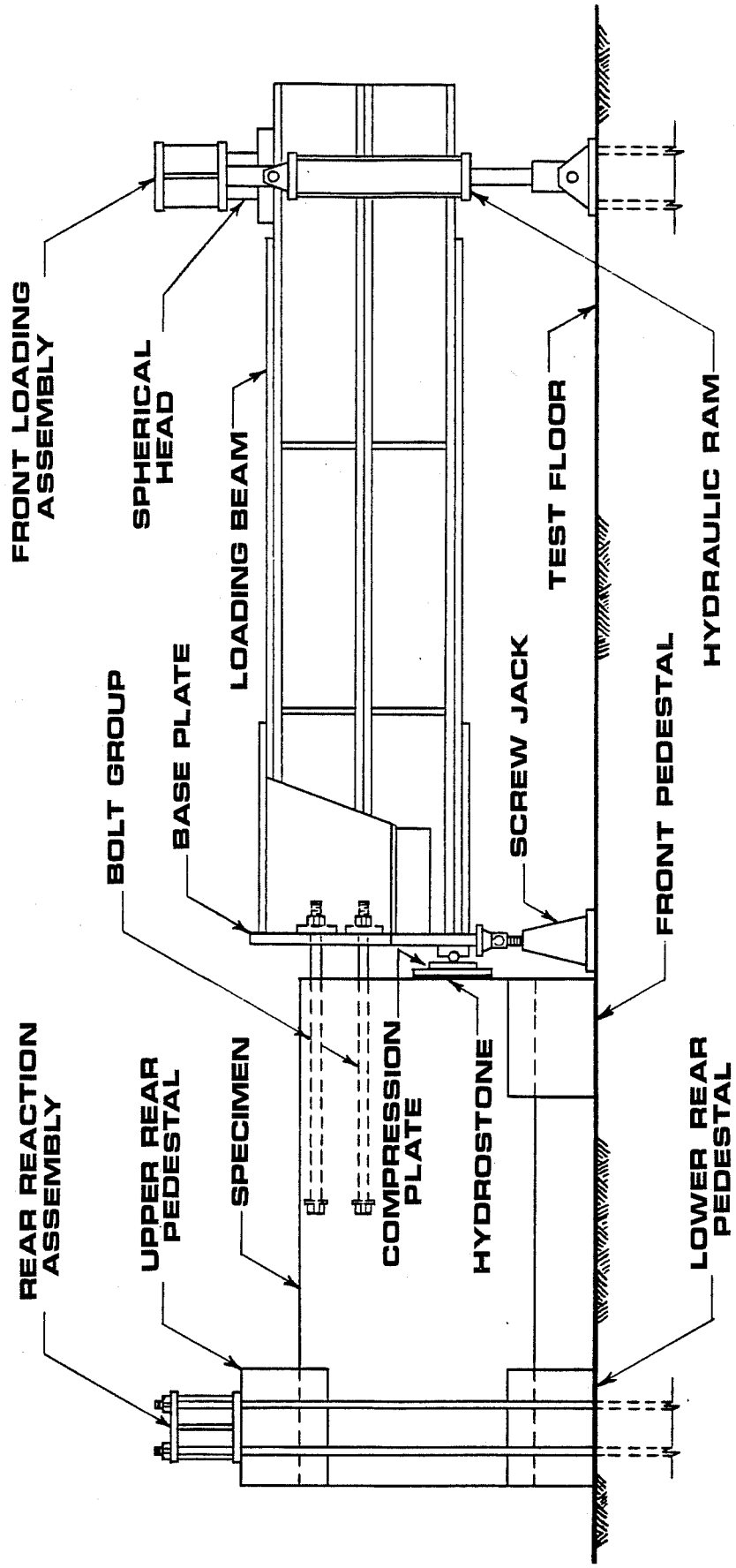


Fig. 2.18 Test frame - elevation

# TEST FRAME

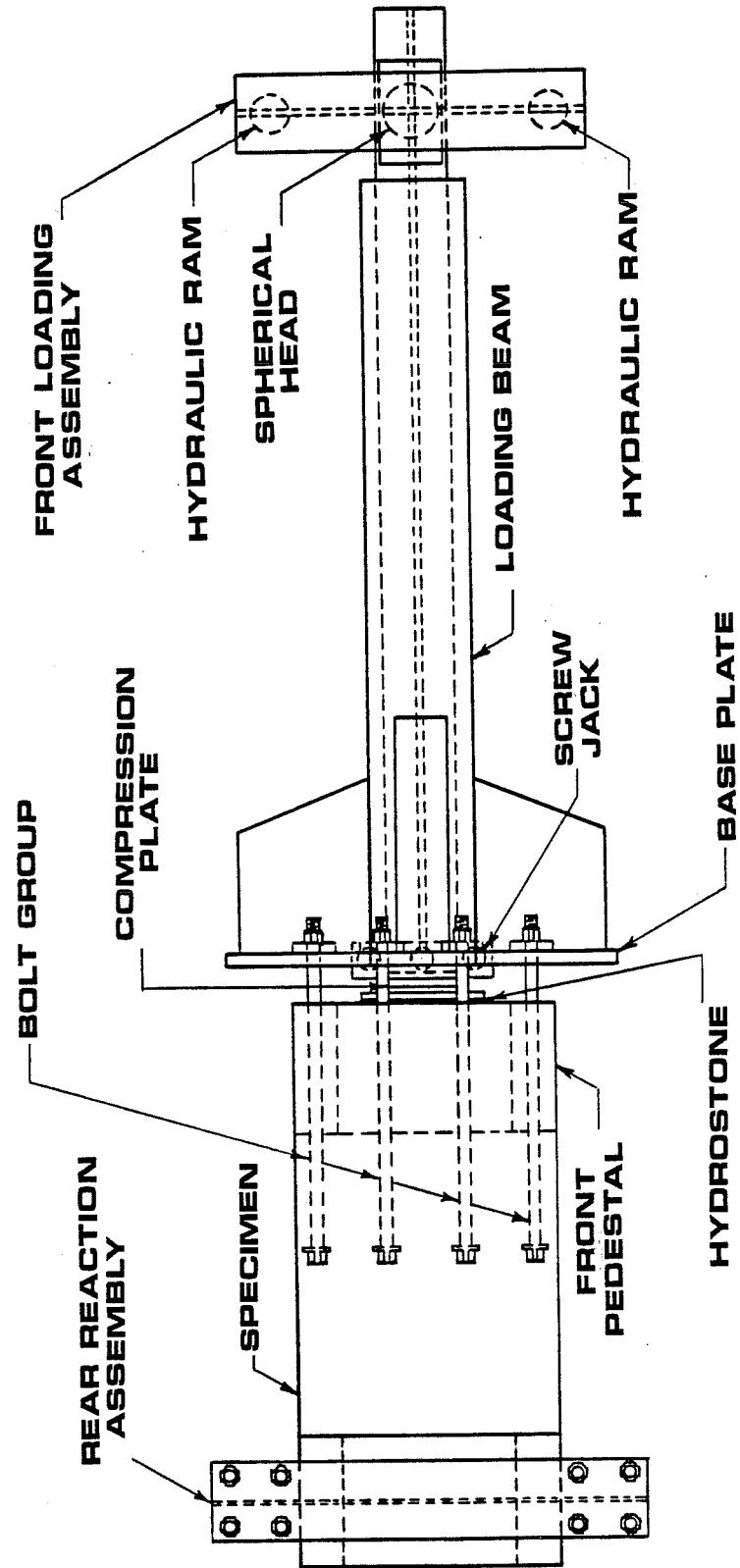


Fig. 2.19 Test frame - plan view

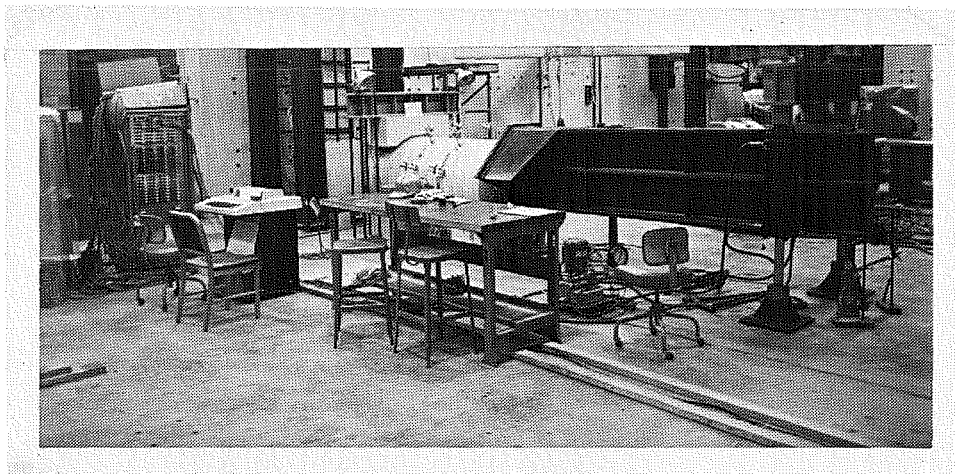
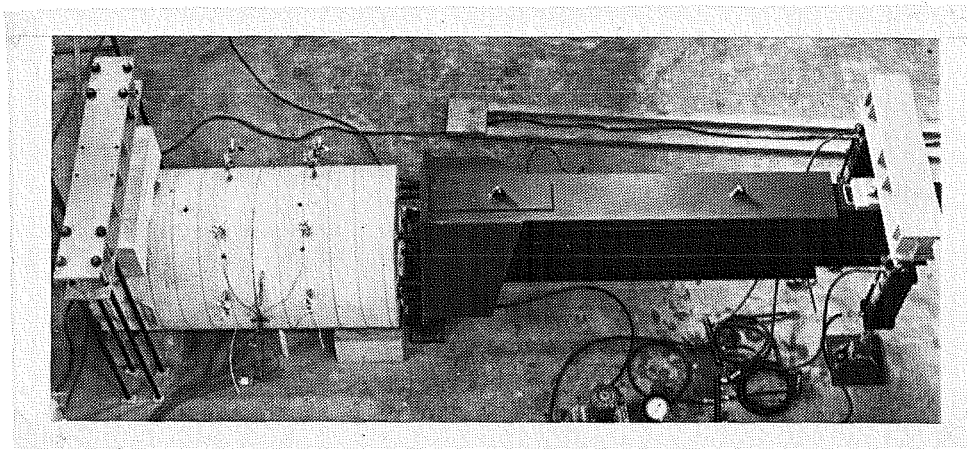


Fig. 2.20 Test set-up prior to testing

tied down to the test floor with eight high-strength rods and collars, as shown in Fig. 2.21. The lower pedestals aligned and supported the specimen before the test.

The loading beam was fabricated from two W14x53 wide-flange sections and reinforced with 1 x 8 in. cover plates to a design capacity of 1400 kip-ft. A 1-1/2 in. thick, slotted base plate and a number of stiffeners were welded at the connection end. The 9 x 2 in. slots, which were oriented at 45 degrees in the base plate, allowed flexibility to test a large number of bolt groups with no additional adjustment to the set-up. The stiffeners assisted the base plate in rotating as a rigid plane to ensure symmetry in the pullout forces. Nuts and washer plates were used to fix the anchor bolts to the loading beam (Fig. 2.23).

As shown in Fig. 2.22, the front-loading assembly applied a concentrated load to the end of the beam by means of two 70-ton hydraulic rams reacting against bolts secured to the test floor. A cross-beam and spherical head transferred the load from the rams to the loading beam. The use of the spherical head compensated for small misalignments of the loading beam.

At the interface (Fig. 2.24), a bearing plate on a 1/2 in. thick hydrostone layer transferred the compression force to the specimen. Swiveling jacks were placed under the beam to channel the applied (shear) force directly to the test floor.

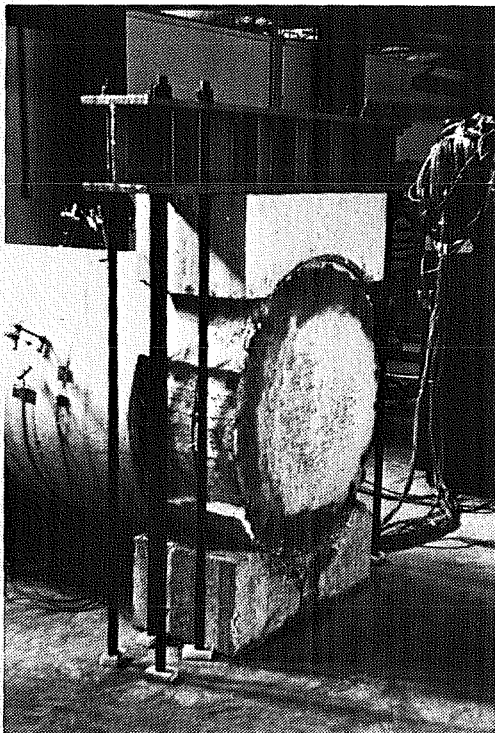
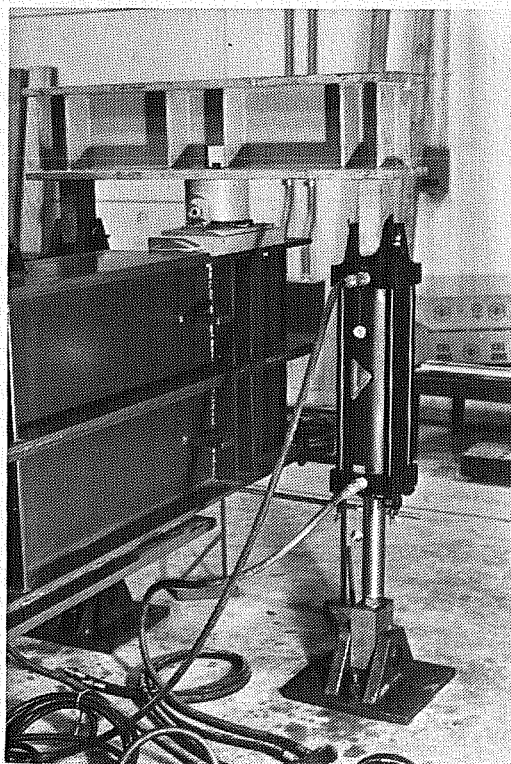


Fig. 2.21 Rear reaction assembly of test frame

Fig. 2.22 Front loading assembly of test frame



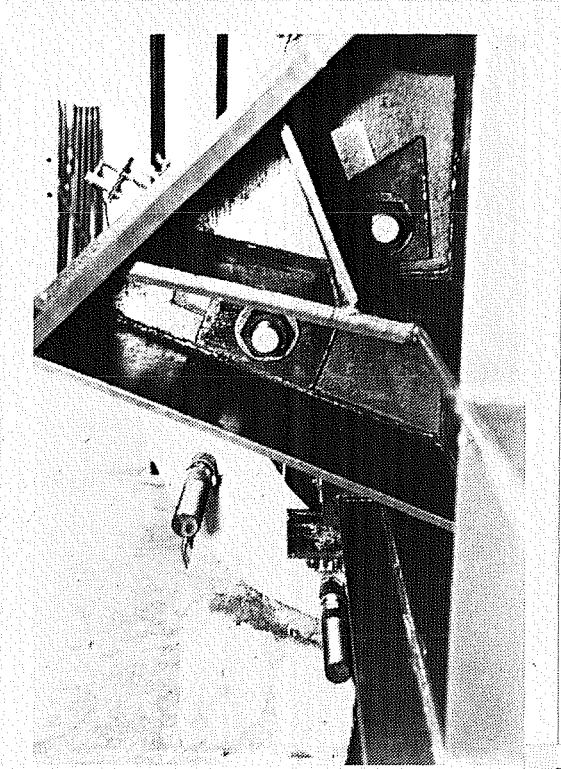


Fig. 2.23 Anchor bolts fixed to loading beam

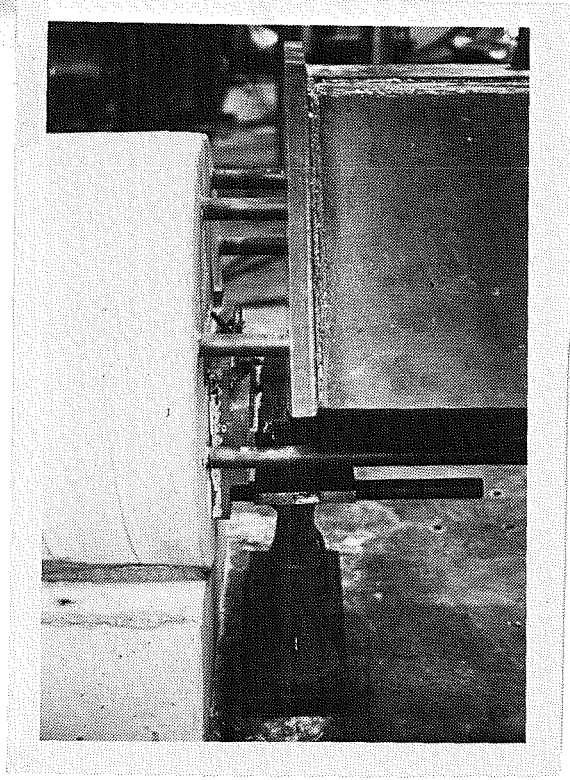


Fig. 2.24 Specimen — loading beam interface

## 2.4 Test Procedure

Two bolt groups were tested in each specimen. First, the weaker bolt pattern was loaded to failure. Afterward, the specimen was rotated into place for testing the other group.

Prior to testing, the loading beam was secured to the bolt group by means of nuts, which were hand-tightened to a snug fit. A reference line indicating the location of the washers was drawn on the surface of the specimen. All data channels were read before any load was applied to the beam.

The tensile pullout force on the anchor bolt group was applied in small increments (load stages) until failure of the group occurred. Near failure, the surface of the specimen was examined and cracks were marked. The development of crack patterns and the failure surface were photographed. Top bolt force and slip measurements were monitored during the test to ensure that a symmetrical pullout was indeed achieved. The loading sequence and the bolt force and slip measurements at each load stage are detailed below.

2.4.1 Loading Sequence. Constant load increments were applied to the beam until it was no longer possible to increase the load. This stage was labeled "failure"; however, the upper level bolts usually failed one or two load stages earlier. At first, the load was applied in 5 kip increments, up to about one-half to two-thirds of the failure load. The increments were reduced to 2 or 3 kips at later stages. Beyond failure, the pullout proceeded by monitoring the deflection at the

beam end, as measured by dial gages. The post-failure load stages were not performed during the first test on each specimen to avoid unnecessary damage (cracks) to the second test on the opposite side of the same specimen. Typically, the applied load was sustained within 10 percent of its peak value for an additional beam deflection, up to two inches.

2.4.2 Load Stage Measurements. A load stage was completed by increasing the load on the beam to a set level and reading all channels which provided bolt slip and strain data. A typical load stage lasted from 3 to 5 minutes.

The beam was loaded with hydraulic rams. The pressure in the input line (the hose and manifold connecting the pump to the lower chamber in the rams) was measured with a 10,000 psi pressure transducer connected to a strain indicator (Fig. 2.25). A calibrated 10,000 psi pressure gage was also placed in the line to verify the transducer measurements.

The applied load and the data channels were read once in a load stage. Typically, the channels were scanned immediately after the load was read. A second load reading was taken, however, at the end of the scanning in tests STG1 and STG2. In general, the load was observed to remain constant during the scanning. At load stages past failure, the load dropped 5 to 10 percent during the time measurements were taken or cracks marked.

The VIDAR Digital Data Acquisition System scanned output signals from strain gages and linear potentiometers and converted the signals into digital voltages. The information for every channel was recorded



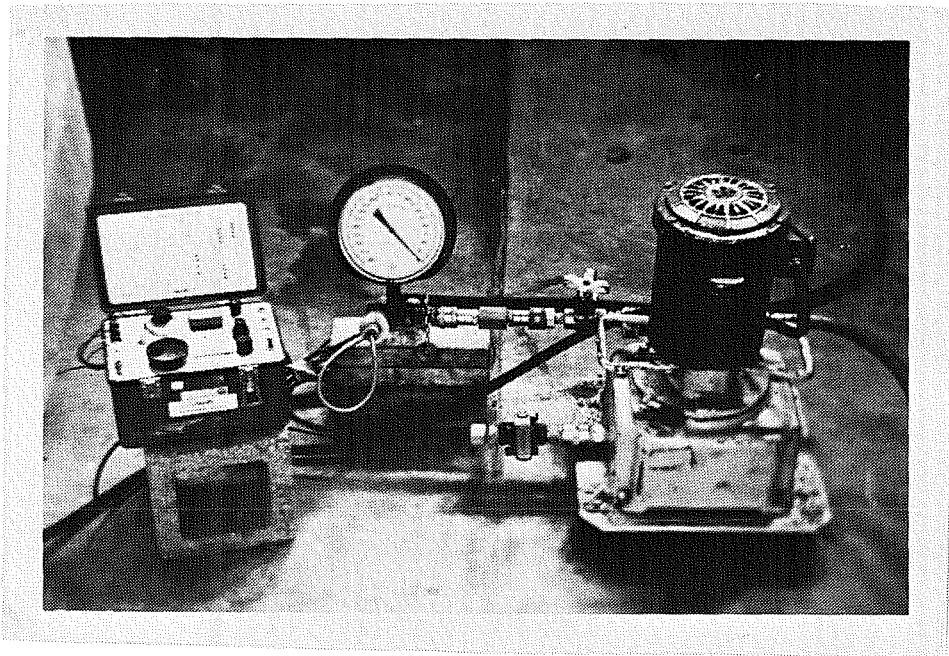


Fig. 2.25 Electric pump, pressure gage, and strain box used to control the load applied on the beam

on magnetic tape and printed on a hardcopy at the test site.

Initial voltage readings were subtracted from readings taken after each load increment, and their difference interpreted as slip and strain measurements. Ideally, to obtain the initial readings, the data channels were read just before the first load increment was applied. Frequent torquing and preloading stages in most tests, however, altered the initial readings.

It is important to explain how torquing and pre-loading stages were treated in presenting the test results. If asymmetrical loading of the top bolts resulted after the first few stages, two options were available to correct the situation. Some bolts could be tightened, while others were loosed with a torque wrench (torquing) to level off the bolt tensions. A second alternative was to unload the beam, check the alignment of the loading frame, and restart the test. When the bolts were torqued, the change in bolt tension due to the torquing was lumped with that resulting from the next (beam) load increment, and considered as a single load stage. If the beam were unloaded before applying the definite loading sequence, the pre-loading stages were deleted from the results. The above procedure is a general approach, while a detailed test-by-test explanation is presented later with the results.

## CHAPTER 3

### TEST RESULTS

#### 3.1 Introduction

In this chapter, experimental test results from six anchor bolt groups are presented. The loading and response of the bolts are described in terms of bolt tension versus slip curves. A model of the wedge-splitting failure mode is derived from surface cracking observed on the test specimens. Finally, the effect of nominal transverse reinforcement in the form of a spiral cage is evaluated.

The nomenclature describing the anchor bolt group installation was presented in Fig. 2.5. Other terms that will be used in the discussion are defined as follows:

- (1) Applied load - load applied by the rams on the loading beam.
- (2) Bolt tension - load on a bolt as determined from strain gages at the lead end of a bolt.
- (3) Lead slip - recorded movement ( $\pm 0.0001$  in.) of a slip wire mounted on the bolt at the face of the specimen (Fig. 2.13). Slip includes the bolt elongations and the relative displacement between the anchor bolt and the concrete.
- (4) Tail slip - bolt displacement measured at the anchorage end (Fig. 2.13).
- (5) Nominal load ( $P_n$ ) - approximate load on the beam used to label load stages and identify cracks during a test.

- (6) Spiral stress - stress measured from a strain gage on first spiral bar crossing the bolt ahead of bearing face;  
 $f_y = 40$  ksi assumed.
- (7) Peak load ( $T_{\max}$ ) - tensile capacity of a test bolt in a group.

Basic Calculations. Bolt tensions were calculated from direct strain measurements on each bolt. Equilibrium considerations were used only as a check on the direct measurements as explained in Appendix A.

The tensile force on a bolt was calculated as follows:

$$\text{bolt force} = \left( \begin{array}{c} \text{measured} \\ \text{strain} \end{array} \right) \left( \begin{array}{c} \text{modulus of} \\ \text{elasticity} \end{array} \right) \left( \begin{array}{c} \text{bolt} \\ \text{area} \end{array} \right)$$

The strain measurement was taken as the average of four (or two) gages on the protruding bolt length as shown in Fig. 2.13. At least two gages, 180 degrees apart, were averaged to cancel bending stresses induced on the bolts. No stress-strain curve was obtained for the bolt material; instead, a modulus of elasticity,  $E_s = 30,000$  ksi, and a nominal yield stress,  $f_y = 105$  ksi, were assumed in calculating stresses. Since bolt yielding did not occur in any test, defining the yield stress level was not a critical factor. The bolt area,  $A$ , was  $2.40 \text{ in.}^2$  for the 1-3/4 in. bolts. A reduced value,  $0.80A = 1.92 \text{ in.}^2$ , was used in tests STG1 and STG2 with lead gages mounted on the threaded length of the bolts. Notice in Fig. 3.1 that to place gages on the threaded length, it was necessary to grind down all the thread at the cross-section.

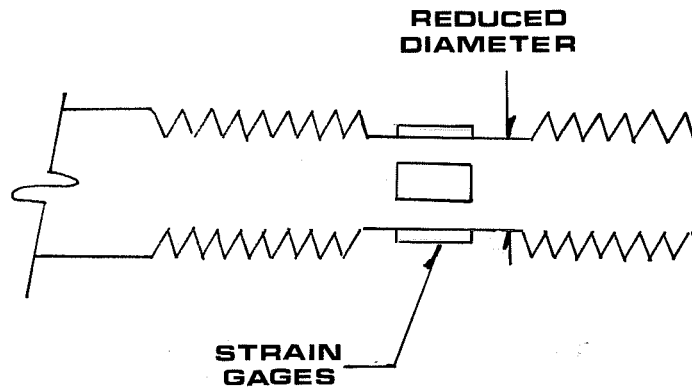


Fig. 3.1 Lead strain gages mounted on threaded length

Pre-loading and Torquing. A preloading sequence in tests NOW and SC6 was conducted to correct apparent asymmetrical loading of the bolt group. This incidental loading sequence was distinguished and deleted from the actual loading sequences presented in this chapter.

In test NOW, bolts 2 and 3 were stressed to  $0.80T_{\max}$  and  $0.57T_{\max}$  respectively; they were then unloaded, before the test loading was applied. No detrimental effect on the bolt group resulted from this loading. During the actual loading sequence, bolt 2 was tightened with a torque wrench when the applied load on the beam was 10 kips. The effect of torquing bolt 2, other than early load slip and an unusually steep increment in bolt tension (evidenced in Fig. 3.2), were negligible on the performance and ultimate capacity of the bolt.

In preloading stages in test SC6, the top bolts were stressed to  $0.33T_{\max}$ . The only apparent effect of such a loading was additional lead slip at early stages of the load sequence, as shown in Fig. 3.3.

### 3.2 Load-Slip Relationships

The results of six tests on anchor bolt groups described in the previous chapter (Table 2.2) are presented in Figs. 3.2 through 3.7. On those figures, the tensile forces on the bolts in a group were plotted at left as a function of the load applied on the beam. The right side shows the response of the bolts in terms of lead slip-bolt tension curves. Brought together, the two plots record lead slip and tensile force increments for the individual bolts as the beam was loaded. The response of the top bolts is extended in Section 3.4 to include tail slip measurements and bolt forces after failure.

The response of the anchor bolts correlated with the orientation of the bolt group and the method of loading. In general, the upper-level bolts resisted most of the moment until they reached their capacity and failed. Then the bolts at the lower level gained load at a faster rate as the upper-level bolts were unable to carry increased load or to hold the load applied. In terms of average values, the load on the lower-level bolts was 1/4 to 1/2 of the top bolt load at 2/3 of the group capacity, and 1/2 to 2/3 of the top bolt load when the group reached its capacity. Bolt 1 in tests NOW (Fig. 3.2) and STG1 (Fig. 3.6), however, did not take any significant load until after the top bolts had failed.

Relatively small lead slip of bolts 1 and 4 had occurred when bolts 2 and 3 reached their capacity. In addition, tail slip data (not shown) for bolts 1 and 4 indicated very little tail slip in tests SC6 (0.01 in.) and SC8 (0.03 in.), and no tail slip in the other four tests

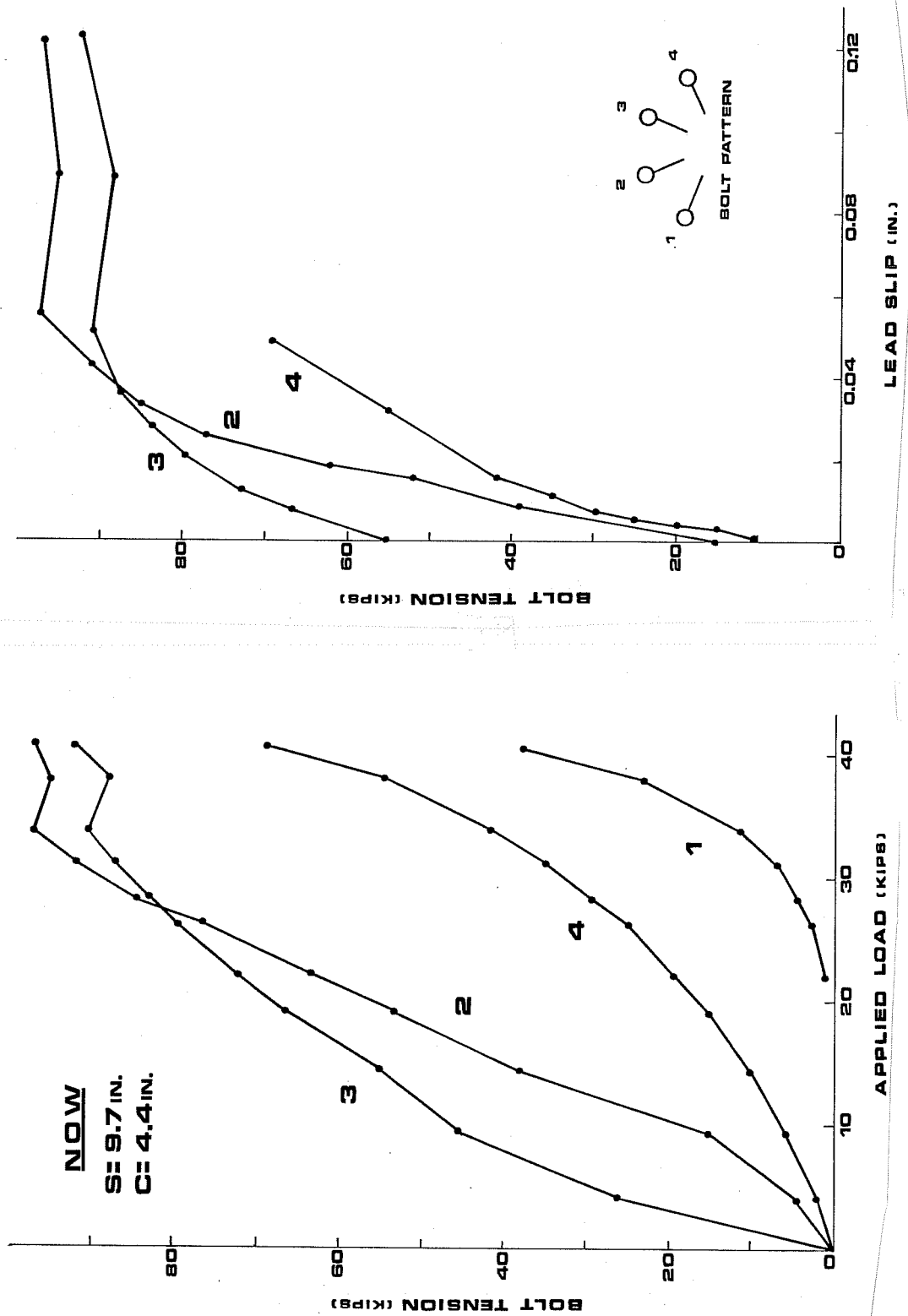


Fig. 3.2 Loading and load-slip curves of anchor bolts in test NOW

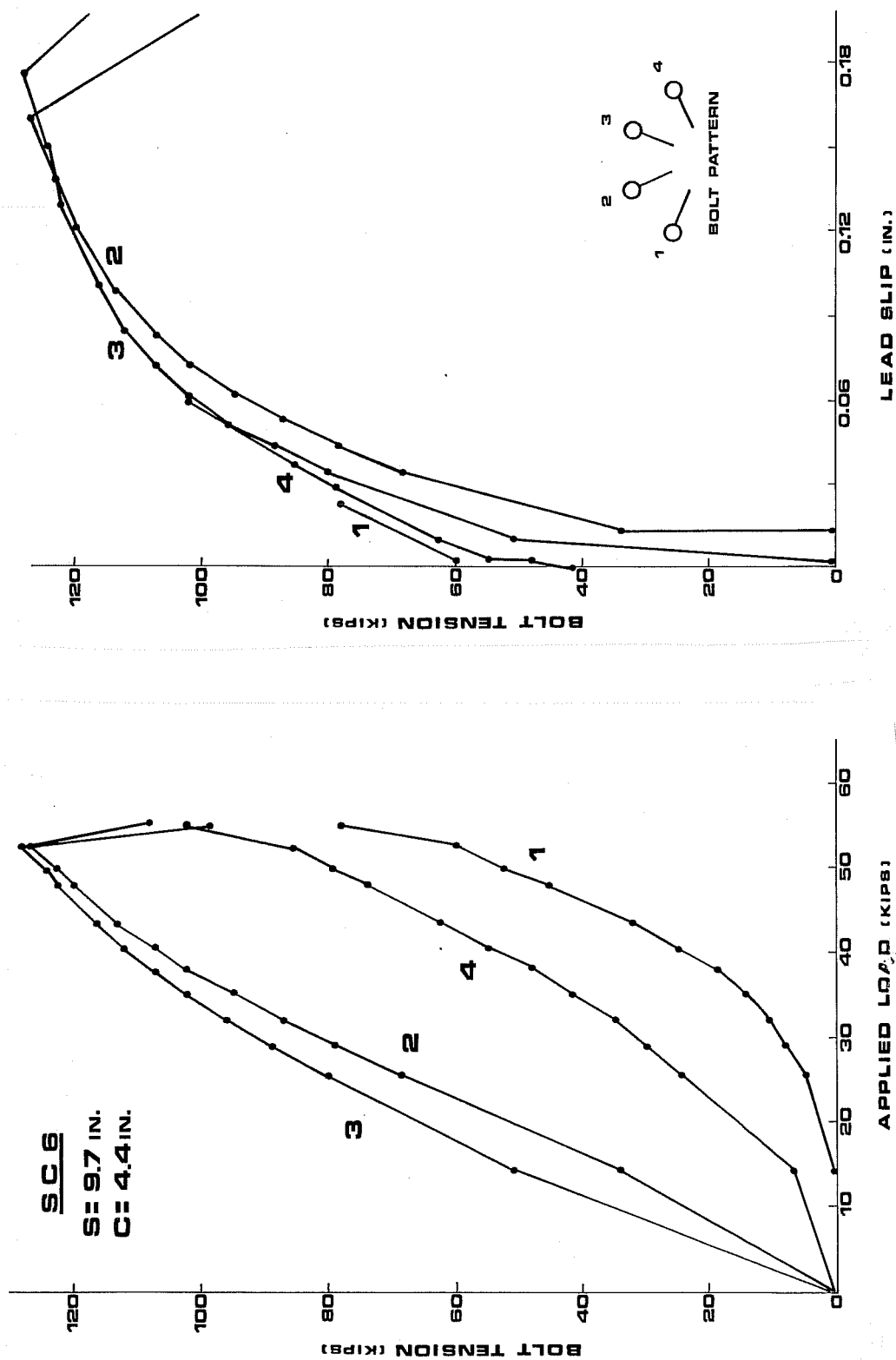


Fig. 3.3 Loading and load-slip curves of anchor bolts in test SC6



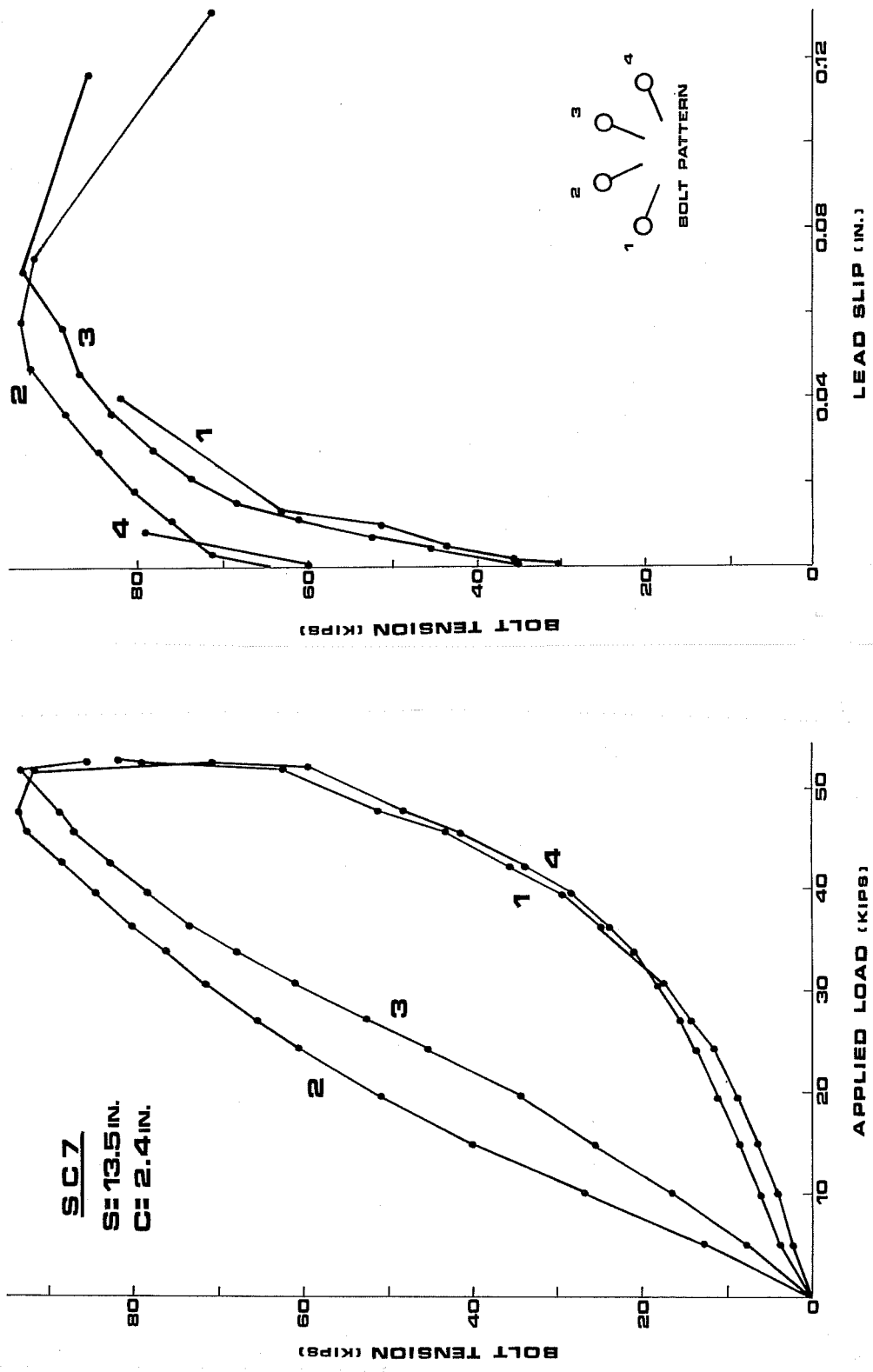


Fig. 3.4 Loading and load-slip curves of anchor bolts in test SC7

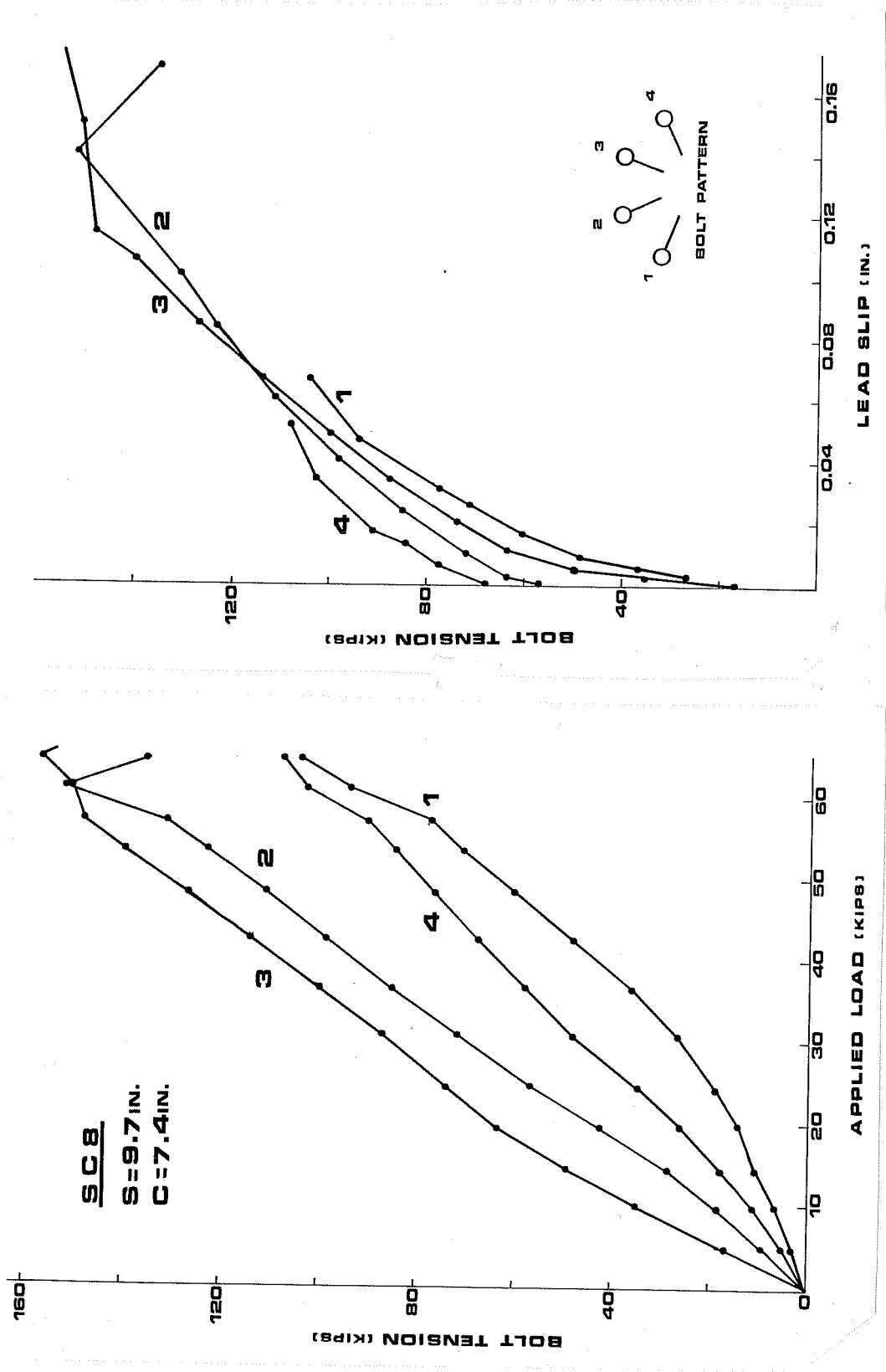


Fig. 3.5 Loading and load-slip curves of anchor bolts in test SC8

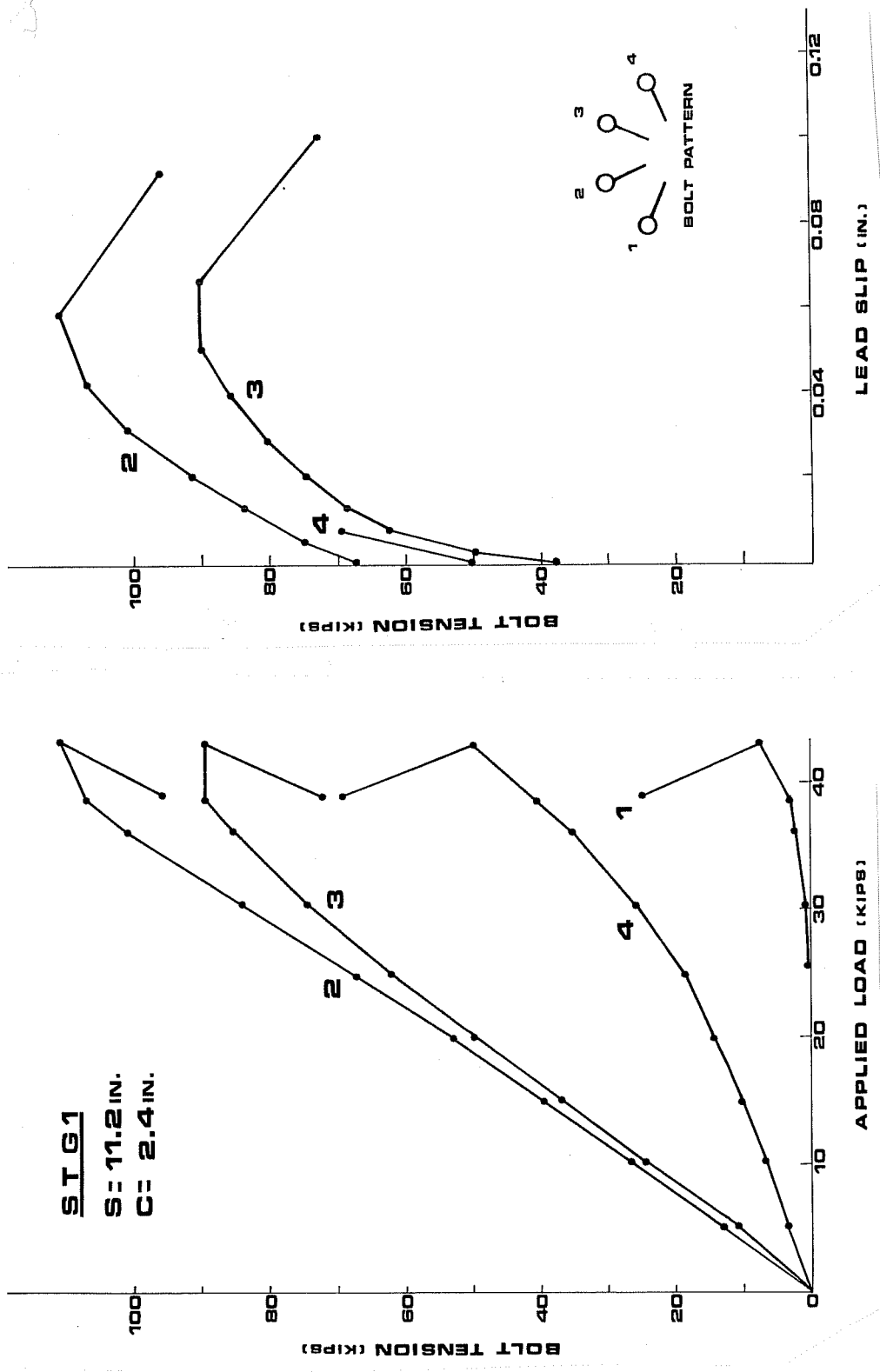


Fig. 3.6 Loading and load-slip curves of anchor bolts in test STG1

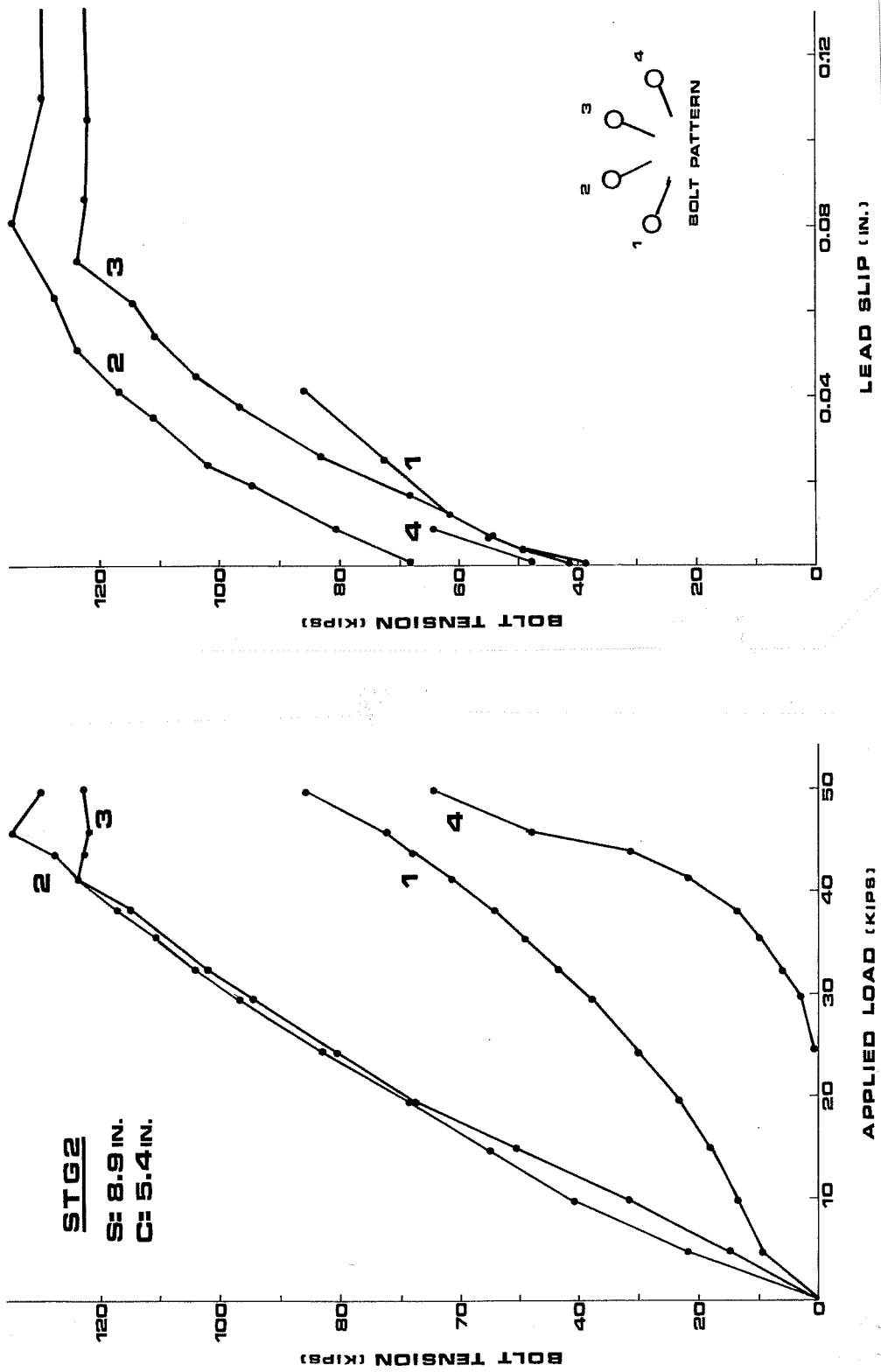


Fig. 3.7 Loading and load-slip curves of anchor bolts in test STG2

when the top bolts failed. These observations suggest that the cone of compacted concrete in front of the anchorage was not fully developed on the lower level bolts at failure, and, consequently, the interaction of splitting forces between the upper and lower level bolts was minor.

The top bolts responded fairly symmetrically to the loading. As a test proceeded, the tensile force and slip on the bolts leveled off. The difference between bolt forces noted in early stages was no longer as pronounced. The difference between top bolts capacities was less than 8 percent in all tests, except test STG1, where the effect of staggering, rather than asymmetrical loading, resulted in a 19 percent difference. Bolts 2 and 3 were observed to fail simultaneously, or at adjacent load stages.

Two major observations on the method of loading and response of the anchor bolt groups are:

(1) Although 4-bolt groups were tested, actually, only the top two bolts failed with minor interaction from the lower-level bolts. The test results can be compared in terms of top bolt performance with similar tests conducted on 2-bolt groups.

(2) The close agreement observed in the response of bolts 2 and 3 permits the use of average values as a valid representation of the group behavior and capacity.

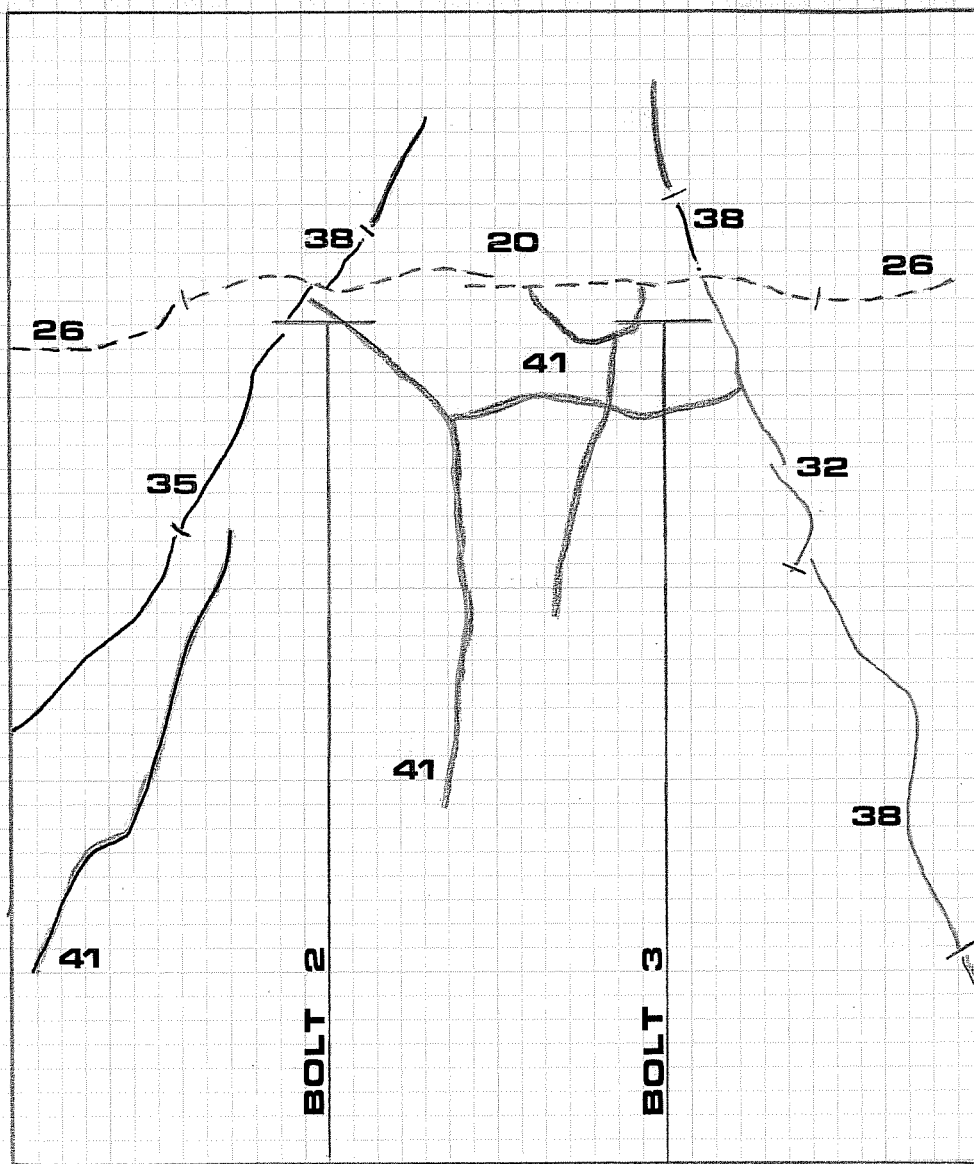
### 3.3 Crack Patterns

Surface cracking observed in the tests is presented by means of photographs and diagrams to scale in Figs. 3.8 through 3.18. Top bolt data at critical load stages are tabulated with the figures for easy reference to the bolts' condition near failure. Nominal load values ( $P_n$ ), written on the specimen surface, identify the tabulated data with the development of particular cracks.

The diagrams represent a 40 in. x 48 in. area on the curved surface of the specimens as if it were "unfolded" on a straight plane. The axes for bolts 2 and 3, radially projected on the specimen surface, are drawn in the diagrams and photographs.

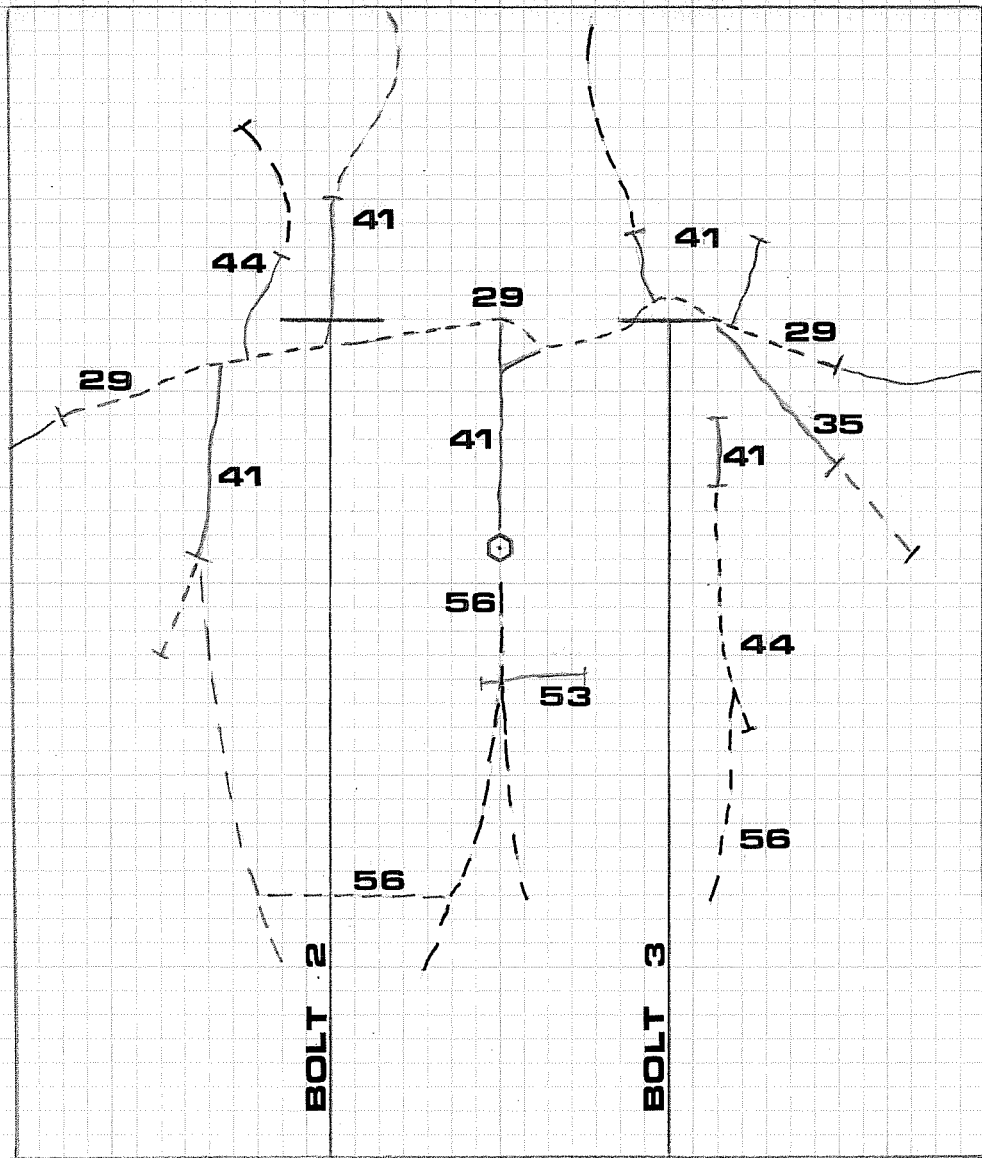
As a general observation on all tests, cracking prior to failure was almost uniquely associated with bolts 2 and 3; only limited (initial) cracking across bolts 1 and 4 above the nut and washers was observed in several tests. It seems reasonable to assume that crack interaction did not occur between top and bottom bolts.

The top bolts were observed to fail in a wedge-splitting mode as previously described for single bolts.<sup>4</sup> Initially, a crack appeared across the bolts on top of the washers. Close to, or at, the group capacity, major cracks emerged near the anchorage end and extended forward along the sides and top of the anchor bolts completing failure surfaces from the bolt to the exterior of the specimen. The failure surfaces intersected at the zone between the two top bolts. The concrete cover on top of the bolts was observed to split and uplift as the bolts failed.



Nominal load $P_n$ (k)	Bolt tension (k)	Tail slip (in.)	Lead slip (in.)	Bolt tension (k)	Tail Slip (in.)	Lead Slip (in.)
20	53.5	.000	.015	66.6	.000	.007
32	92.1	.009	.042	87.2	.017	.035
35	97.5	.016	.054	90.7	.027	.050
38	95.2	.050	.091	88.3	.070	.088
41	96.9	.079	.121	92.5	.093	.123

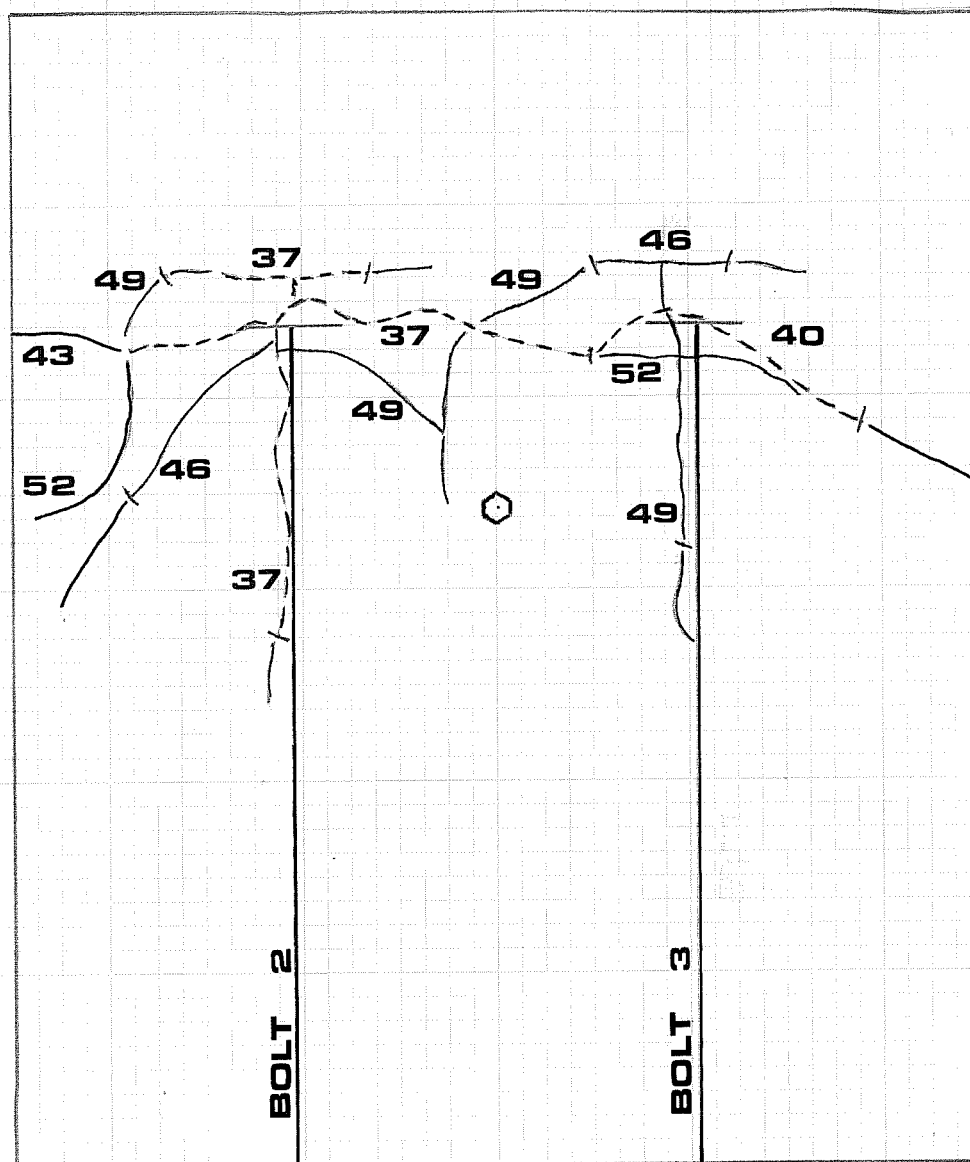
Fig. 3.8 Development of crack patterns of top bolts in test NOW



Nominal load $P_n$ (k)	Bolt tension (k)	Tail slip (in.)	Lead slip (in.)	Bolt tension (k)	Tail slip (in.)	Lead slip (in.)
29	78.8	.011	.044	88.8	.011	.043
41	107	.041	.083	112	.040	.084
44	113	.054	.098	116	.052	.100
53	127	.121	.159	128	.111	.176
56	102	.160	.198	98.6	.150	.215

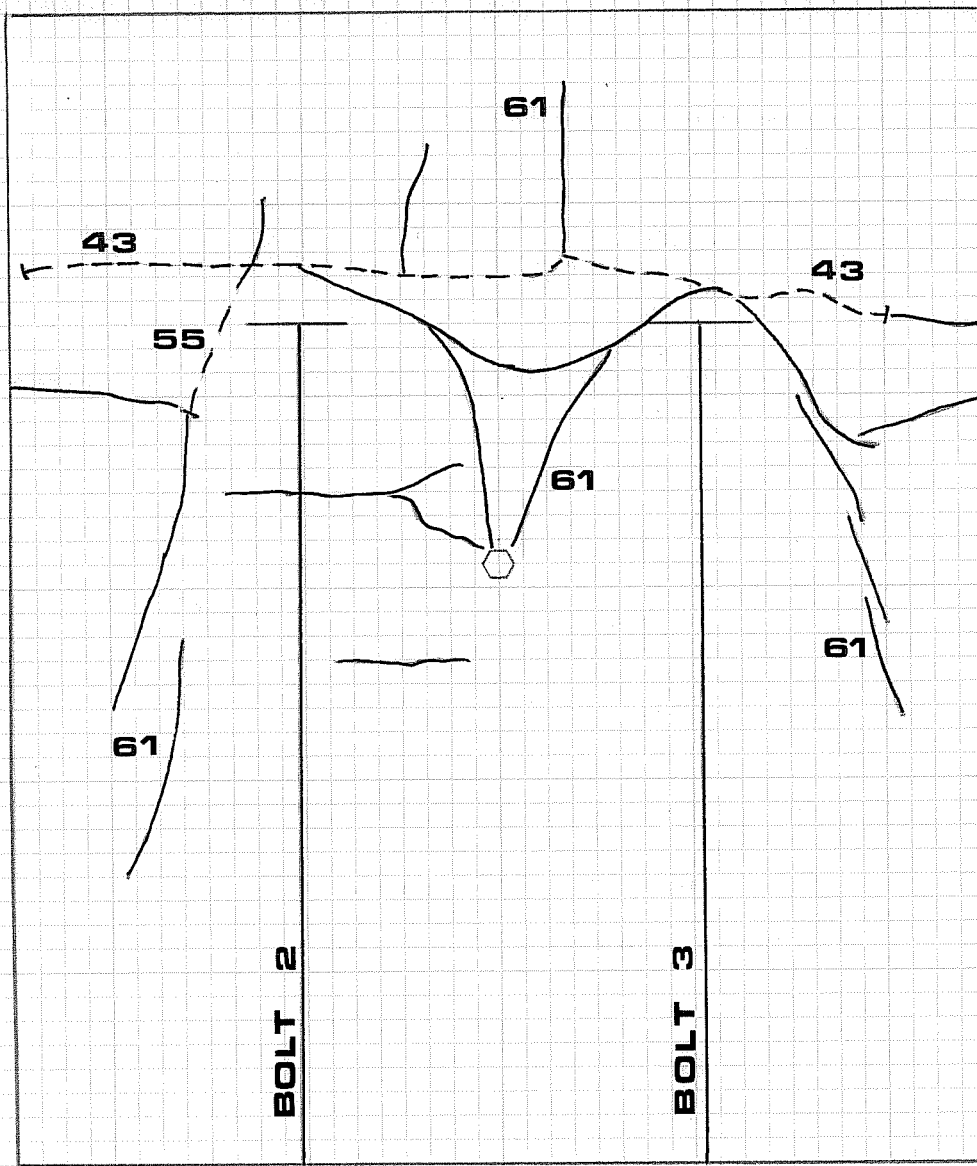
Fig. 3.9 Development of crack patterns of top bolts in test SC6





Nominal load $P_n$ (k)	Bolt tension (k)	Tail slip (in.)	Lead slip (in.)	Bolt tension (k)	Tail slip (in.)	Lead slip (in.)
37	80.1	.015	.018	73.4	.000	.021
40	84.3	.020	.027	77.9	.000	.028
46	92.6	.035	.047	86.7	.005	.046
49	93.6	.048	.058	88.4	.014	.057
52	92.1	.067	.073	93.4	.023	.070

Fig. 3.11 Development of crack patterns of top bolts in test SC7



Nominal load $P_n$ (k)	Bolt tension (k)	Tail slip (in.)	Lead slip (in.)	Bolt tension (k)	Tail slip (in.)	Lead slip (in.)
43	99	.013	.041	114	.010	.067
55	123	.039	.084	140	.037	.106
61	152	.082	.142	151	.082	.151

Fig. 3.13 Development of crack patterns of top bolts in test SC8

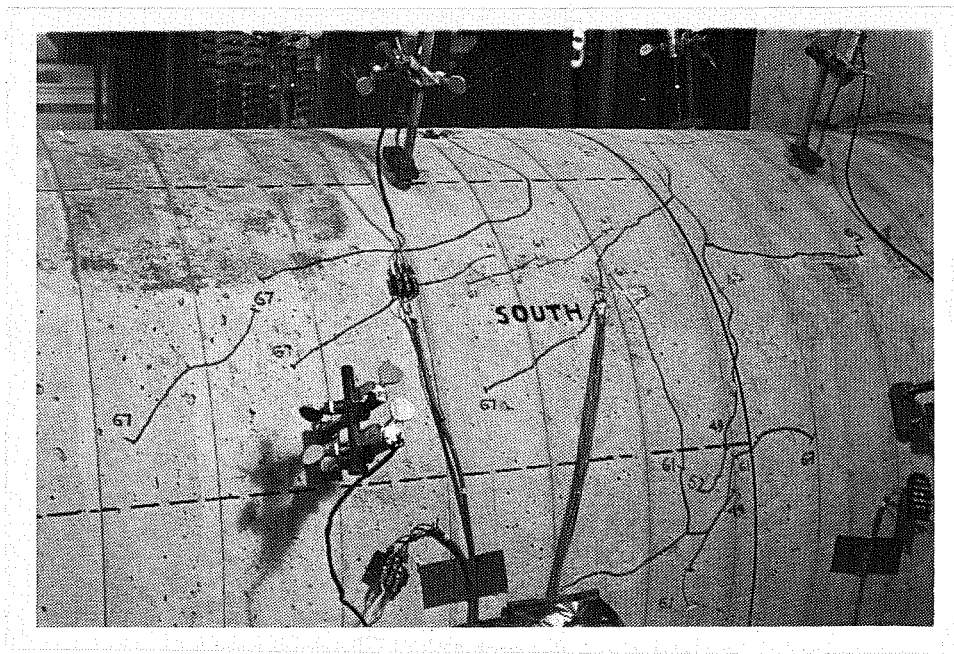
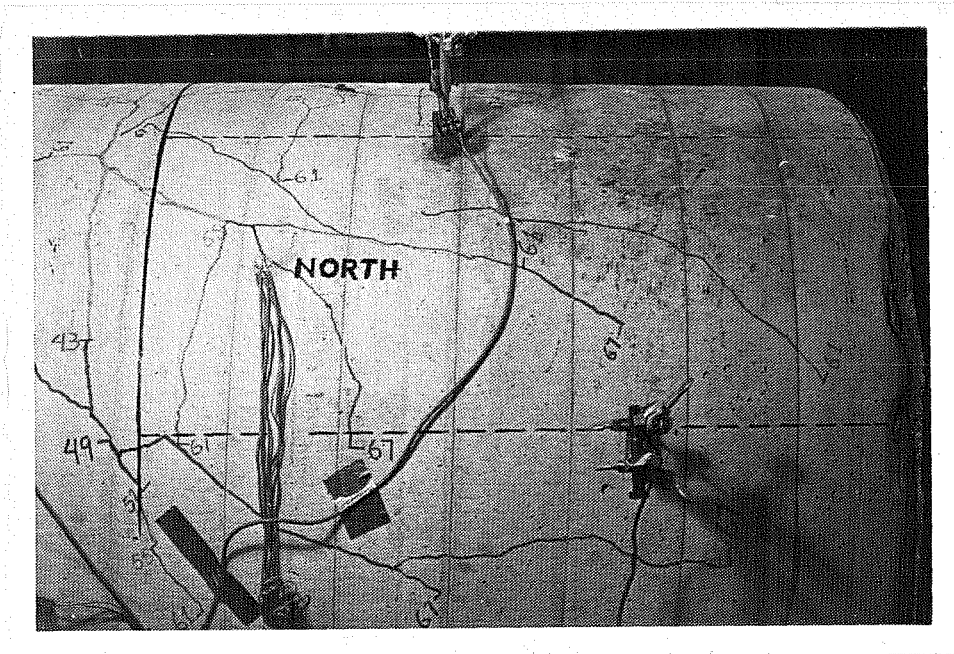
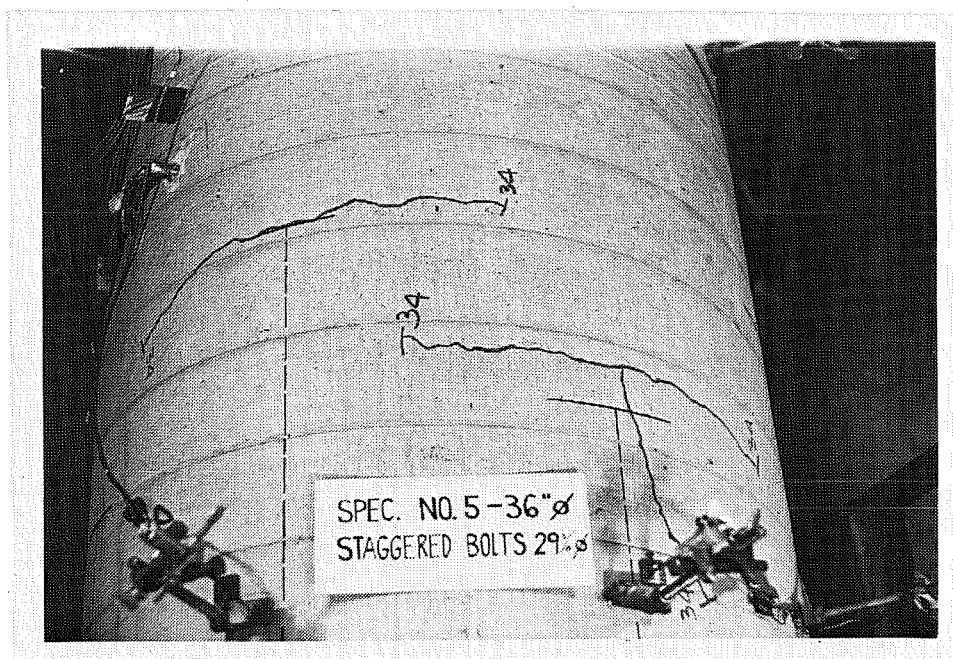
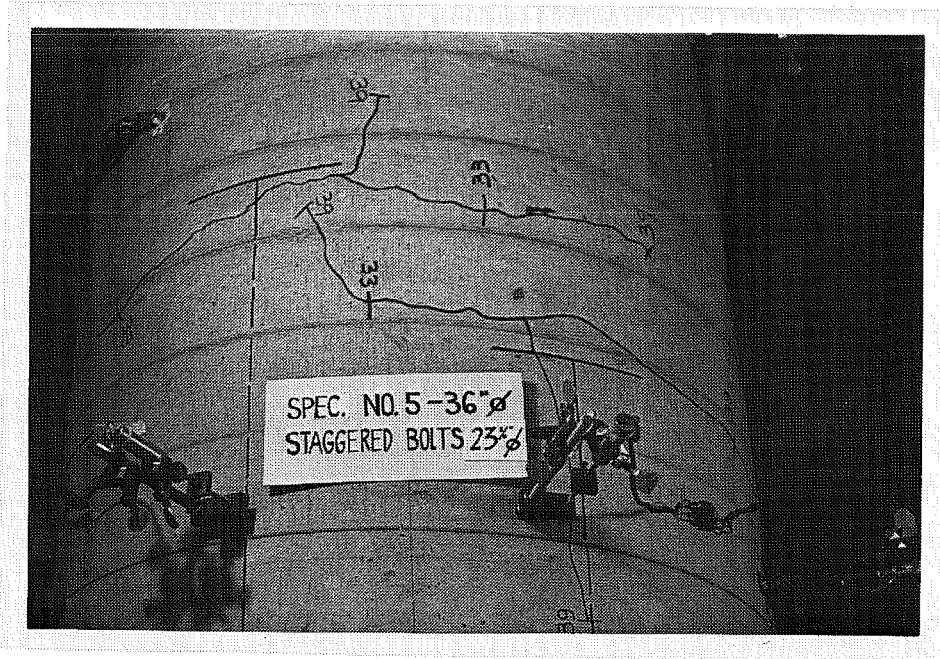


Fig. 3.14 Specimen surface at failure: test SC8



Nominal load $P_n$ (k)	Bolt tension (k)	Tail slip (in.)	Lead slip (in.)	Bolt tension (k)	Tail slip (in.)	Lead slip (in.)
34	92	.000	.021	80	.000	.029
37	101	.003	.032	86	.001	.040
43	111	.028	.059	90	.031	.067
46F	96	.071	.093	72	.088	.101

Fig. 3.15 Initial cracks and bolt data near failure in test STG1



Nominal load $P_n$ (k)	Bolt tension (k)	Tail slip (in.)	Lead slip (in.)	Bolt tension (k)	Tail slip (in.)	Lead slip (in.)
33	102	.003	.025	104	.014	.045
39	117	.013	.041	115	.023	.062
42	124	.021	.051	124	.034	.072
45	128	.031	.063	123	.046	.086
48	135	.046	.081	122	.062	.105
51	130	.073	.110	123	.086	.131

Fig. 3.17 Initial cracks and bolt data near failure in test STG2

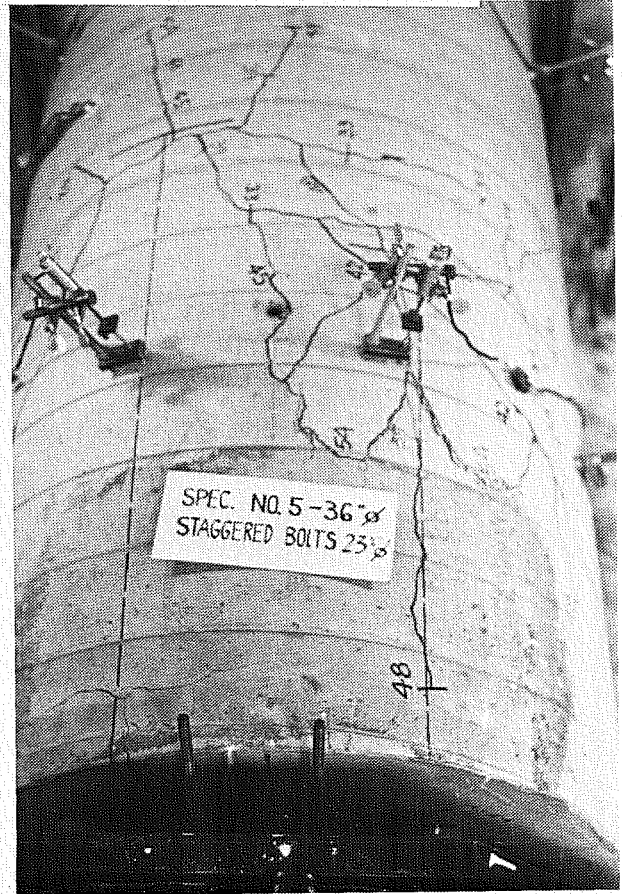
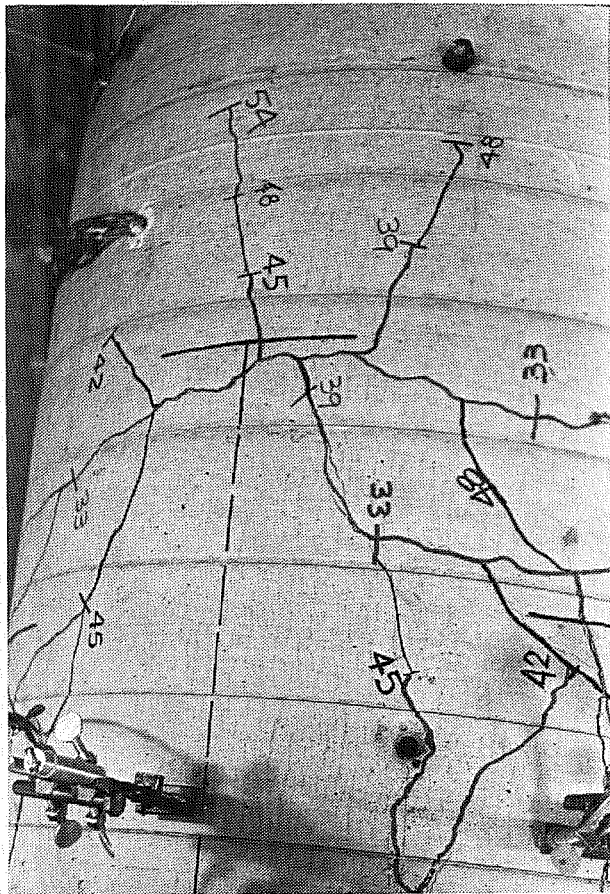
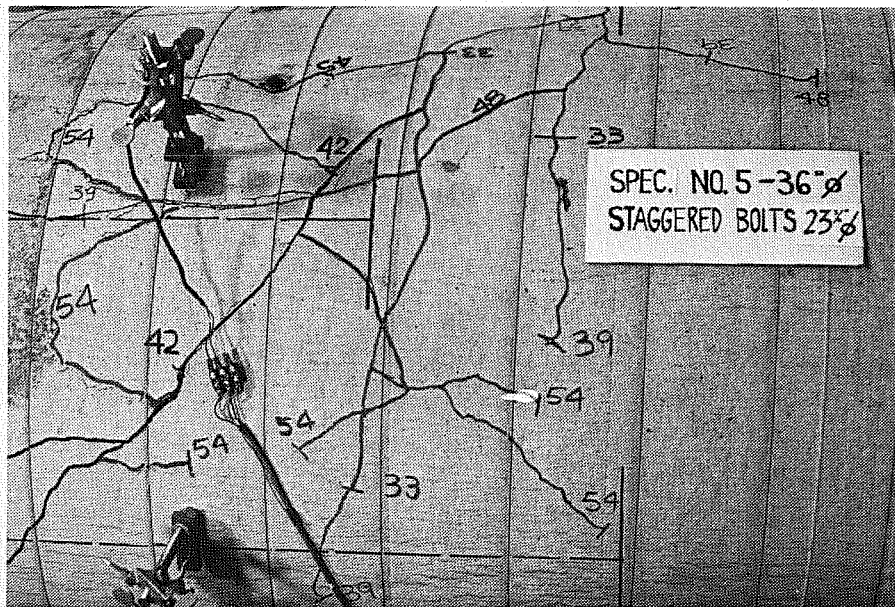


Fig. 3.18 Crack patterns of top bolts: test STG2

The amount of concrete cover on top of the bolts influenced the characteristics of the concrete spalling in the test specimens. For large cover, a tendency to split and uplift the concrete in two blocks, one on top of each bolt, extending far ahead of the anchorage device was observed (Figs. 3.10 and 3.13). All the major cracks surfaced together, at the stage, or immediately after the top bolts reached their capacity. In test SC7 and STG1 (Figs. 3.12 and 3.16) with small cover, the spalling was relatively localized, with abundance of cracks above the washers and a distinctive longitudinal splitting straight above the bolts.

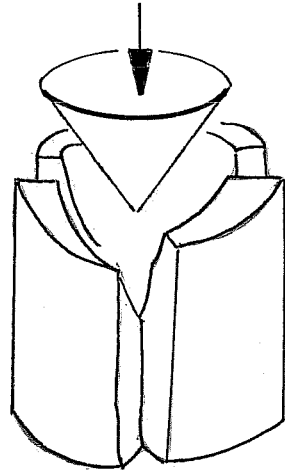
The cone of crushed and compacted concrete ahead of the bearing area was observed to form, at least for the top bolts, in all tests. It seems reasonable to assume that the cone developed shortly after the bolts had started to slip at the anchorage end. As reported in previous research<sup>1,2,4</sup> and corroborated here from strain gage readings at mid length and the anchorage end (Fig. 2.13), the load on a bolt near failure is resisted mostly by bearing mechanism with little steel to concrete bond transferring load along the bolt length. A 50 percent value could be taken as a conservative estimate of the load transferred at the end anchorage. When significant tail slip (greater than 0.003 in.) was first recorded on the top bolts, the bearing stresses at the washer (test NOW excluded) were calculated assuming that 50 percent of the bolt tension was resisted by the bearing mechanism. Calculated stresses of 0.9 to 1.2 times the concrete compressive strength confirm that the concrete had crushed when the bolts started to slip at the anchorage end. Figure 3.19 shows the cone of compacted concrete after removal of the concrete cover.

Modelling Wedge Splitting Failure. The formation of a truncated cone of compacted concrete in front of the bearing surface at the anchorage end shows some similarity to the shear cone usually observed in 6 x 12 in. cylinders tested in compression (Fig. 3.20a). The shear cone in the cylinder pushes outwards and splits the unconfined concrete. Similarly, compression forces, radiating from the surface of the truncated cone (as suggested in Fig. 3.20b) split and eventually uplift the surrounding concrete at the anchorage zone.

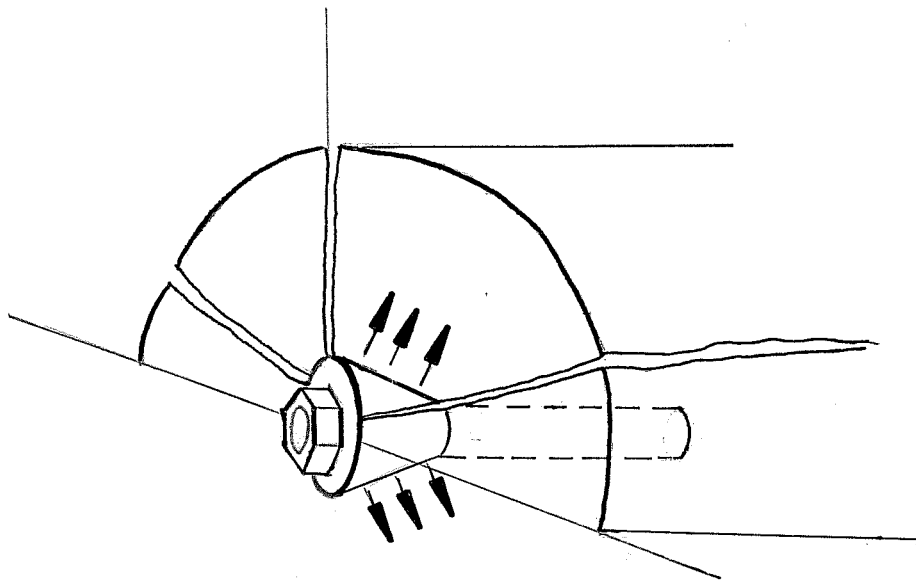
A conceptual drawing of the wedge-splitting failure for bolts 2 and 3 in the test specimens is shown in Fig. 3.21. The model agrees well with crack patterns observed on the surface of the test specimens and reflects the nature of the splitting forces. Segments AA' through EE' represent longitudinal cracks on the surface along the sides and on top of the bolts. A typical failure surface (i.e. plane 2AA'2) extends from the washer and the root of the cone towards these segments (i.e. AA'). Failure surfaces from bolts 2 and 3 intercept along segment FF' in the interior and emerge along plane FCC'F. Initial cracking, which was observed perpendicular to the bolts above the washer line, occurs in plane 2A'E'32. The uplifted concrete cover on bolt 2 is represented in Fig. 3.21b.

As suggested in Fig 3.21c (front view), the splitting in plane 2BB'2 and 3DD'3 is most likely restrained by the spiral bars placed in the test specimens (Fig. 2.10). A large cover also diminishes the likelihood of these planes extending completely to the exterior of the specimen.



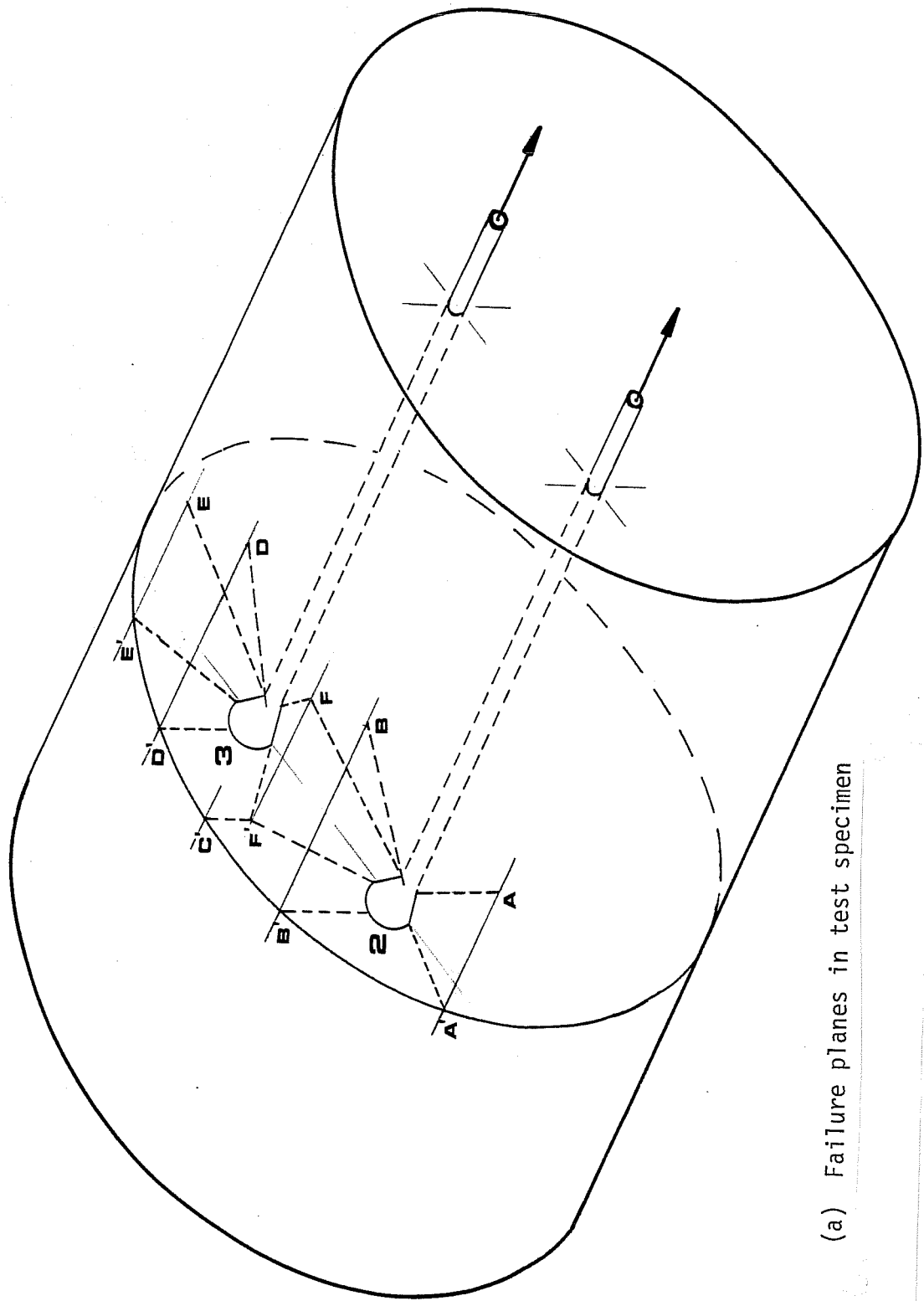


(a) Shear cone splitting concrete cylinder



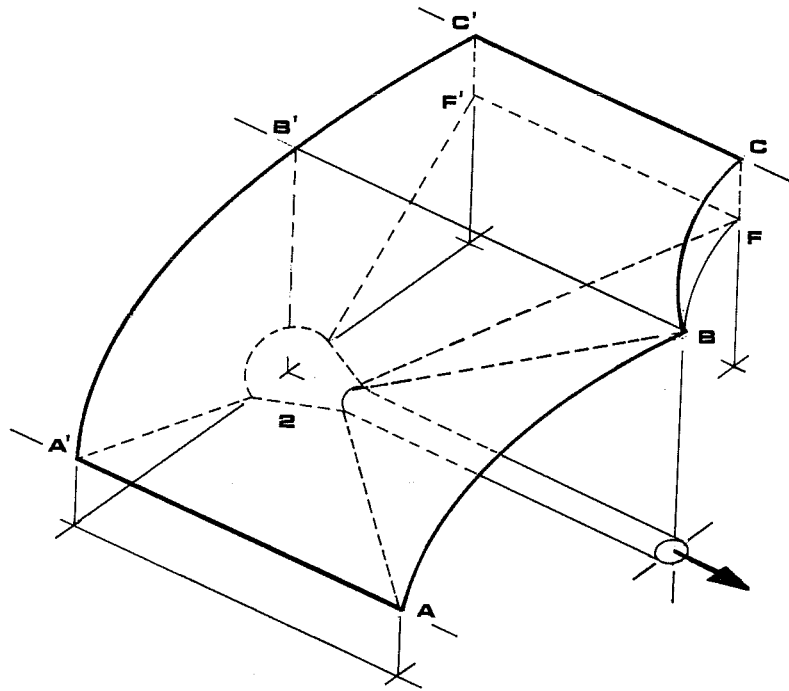
(b) Compressive stresses splitting concrete at the anchorage end of anchor bolt

Fig. 3.20 Splitting force radiated out of concrete cone

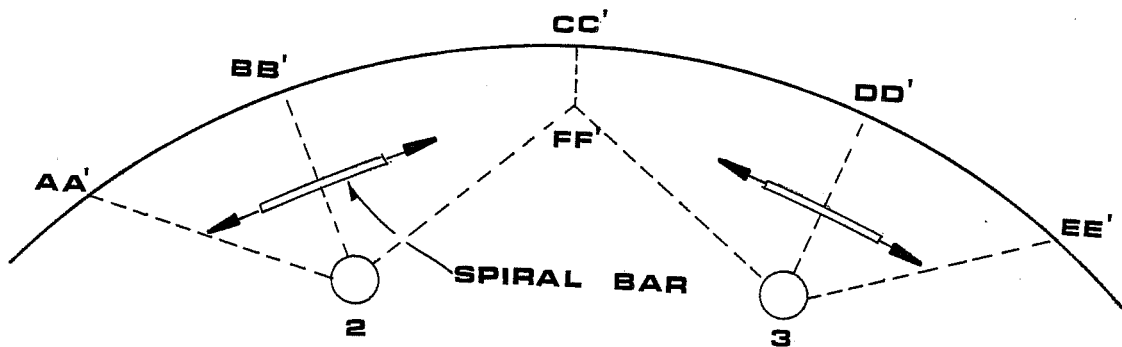


(a) Failure planes in test specimen

Fig. 3.21 Model of wedge-splitting failure of top bolts



(b) Concrete uplift - bolt 2



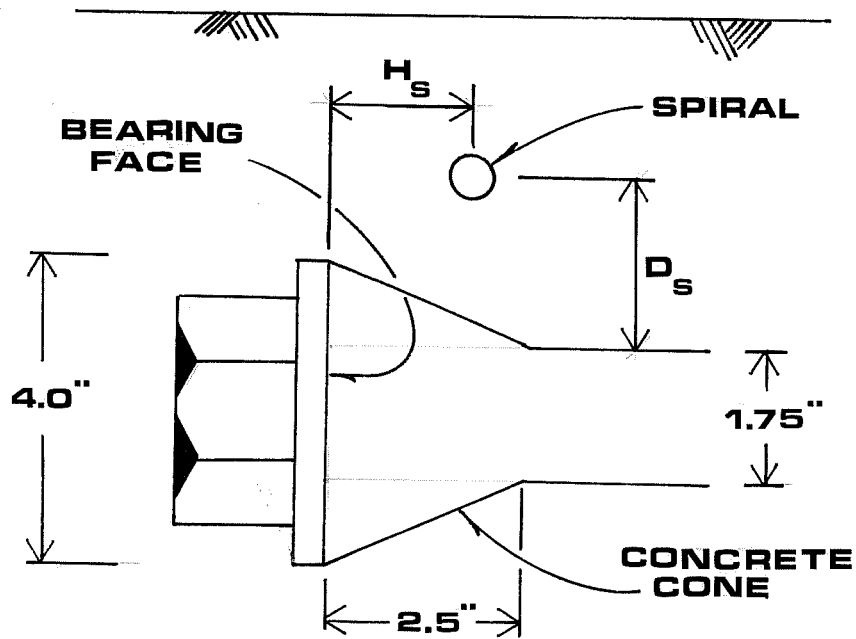
(c) Front view at the anchorage end

### 3.4 Transverse Reinforcement

The effect of transverse reinforcement at the anchorage end, in the form of a spiral cage as described in Sec. 2.2.1, is discussed here. The exact location of the bars crossing ahead of the bearing surface for the top bolts varied in every test, as shown in Fig. 3.22. Since the spiral pitch was held constant (6 in.) in all tests, the position of the first bar ahead of the washer was the only variable affecting restraint to splitting by the spirals.

The spiral performance is evaluated in each test by: (1) a comparison of spiral stresses measured in the first bar ahead of the bearing surface versus the percentage of the peak load ( $\%T_{\max}$ ) on the corresponding bolt (Figs. 3.23 through 3.25); (2) the amount of tail slip prior to any significant drop in the load for the top bolts; and (3) the crack pattern observed on the specimen surface (Figs. 3.8 through 3.18).

NOW. Spiral bars, very far from the bearing face ( $h_s = 5.0$  in. and 5.5 in.), did not record any significant stress before the bolts reached their capacity (see Fig. 3.23). At 100 percent  $T_{\max}$ , few cracks were visible on the surface, and a small tail slip was measured for the top bolts ( $P_n = 35$  k in Fig. 3.8). Two stages later ( $P_n = 41$  k), tail slip quadrupled to an average 0.086 in. and extensive cracking was observed. The spirals yielded rapidly during these load stages, and the load on neither bolt dropped to less than 97 percent of their peak value.



Test	Bolt	$h_s$ (in.)	$d_s$ (in.)
NOW	2	5.0	2.0
	3	5.5	2.0
SC6	2	0.5	2.0
	3	1.0	2.0
SC7	2	1.0	0.0
	3	1.5	0.0
SC8	2	3.5	5.0
	3	4.0	5.0
STG1	2	5.0	0.0
	3	3.0	0.0
STG2	2	2.0	3.0
	3	0.0	3.0

Fig. 3.22 Position of spiral bars ahead of bearing face

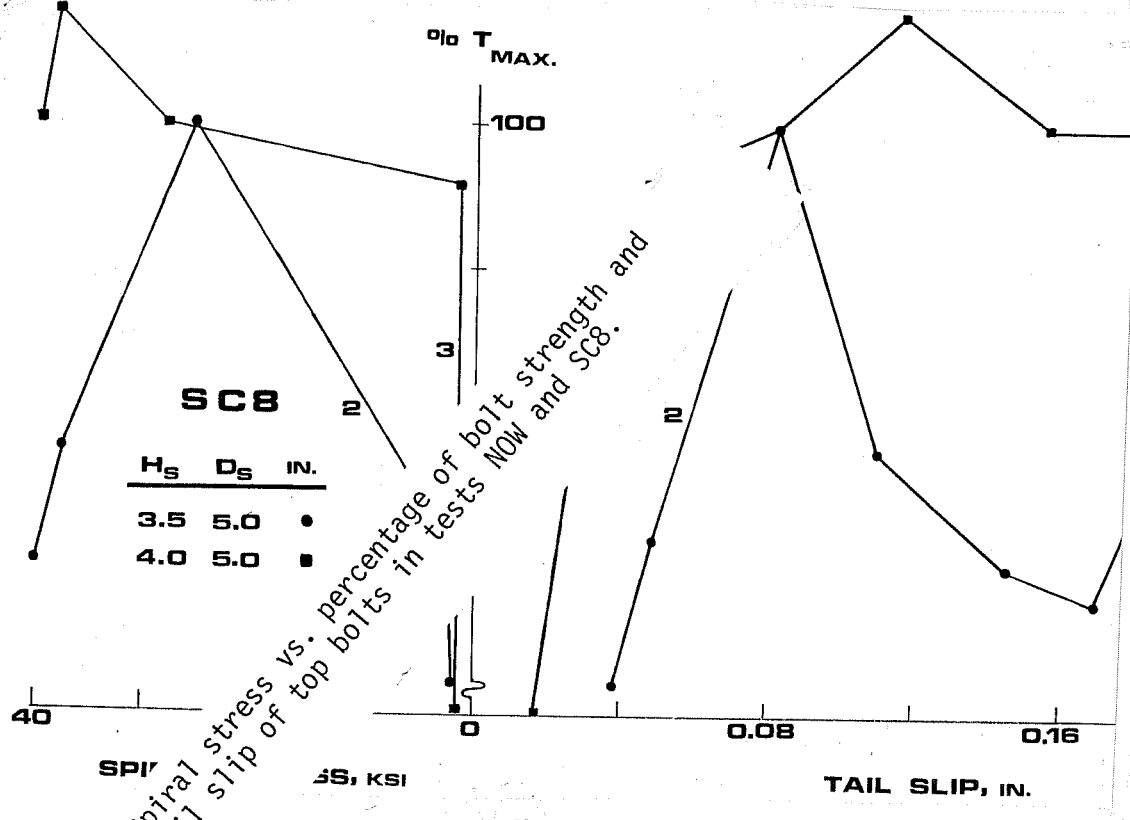
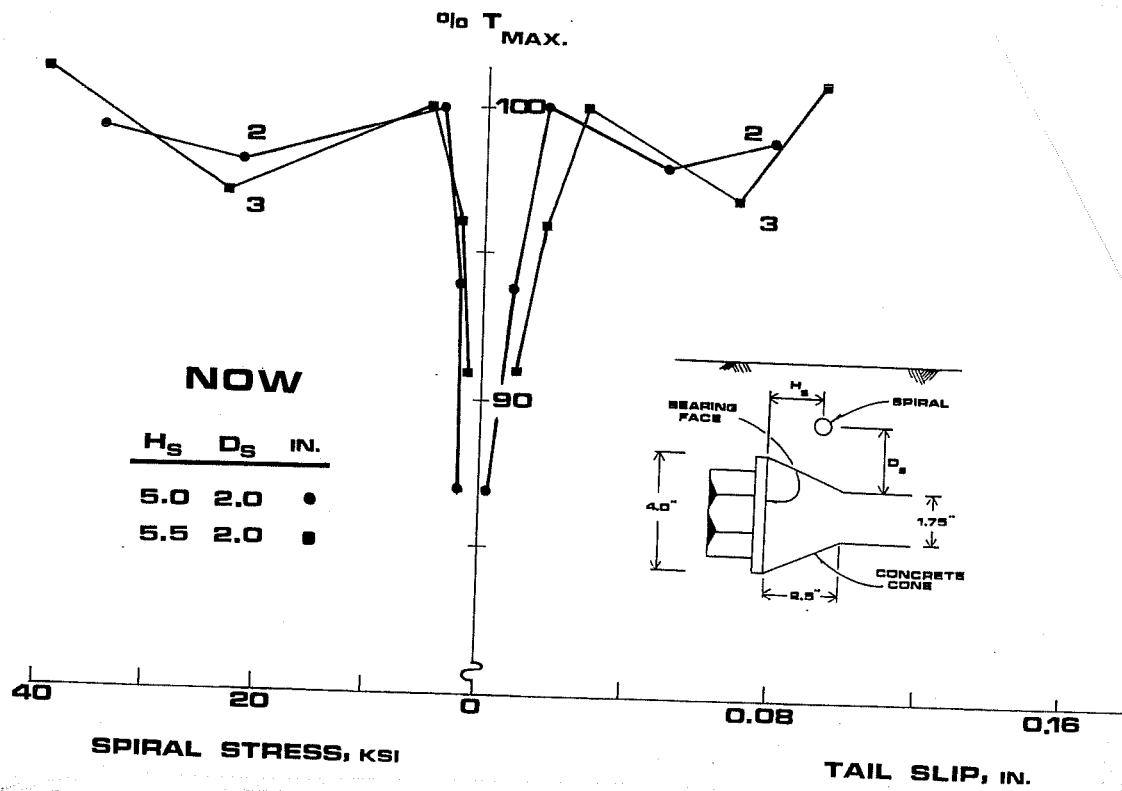


Fig. 3.23 Spiral stress vs. percentage of bolt strength and tail slip of top bolts in tests NOW and SC8.

SC8. In test SC8, with a large bolt-to-spiral clearance ( $d_s = 5.0$  in.) and deep cover, the spiral stresses were negligible (Fig. 3.23) for bolt loads up to 86 and 98 percent  $T_{max}$  and an average tail slip of 0.050 inch. Cracks were observed to surface suddenly at the time the top bolts reached their capacity ( $P_n = 61$  k). The spiral stress increased rapidly to about 27 ksi at failure and yielding of the bars occurred at the next load stage. Bolt 3 sustained 100 percent  $T_{max}$  for an additional tail slip of 0.120 in., but the load in bolt 2 dropped 16 percent before it started to increase again.

STG2. The spiral stresses for bolts 2 and 3 were significantly different in this test as shown in Fig. 3.24. The difference in the stresses prior to failure indicates that the hoop above bolt 2, 2 in. ahead of the washer, restrained the crack on top of the cone more efficiently than the one for bolt 3, placed just behind the cone ( $h_s = 0.0$  in.). The early presence of a longitudinal crack on top of bolt 3, as shown in Fig. 3.17 ( $P_n = 39$  k), supports this observation. Notice, however, that the stress in the bar above bolt 3 increased at a steep rate after failure, and that both bolts sustained their load very well.

It is concluded for these three tests that (1) the spiral was effective in restraining the splitting once the bolts reached their capacity, but (2) the positions of the bars relative to the bearing surface were inadequate to restrain the cracks earlier.

SC7. Top bolts resting against the spiral bars in shallow cover ( $C = 2.4$  in.), exhibited an abrupt failure as shown in Fig. 3.24. The spiral hoops, at 1.0 in. and 1.5 in. ahead of the washers, were posi-

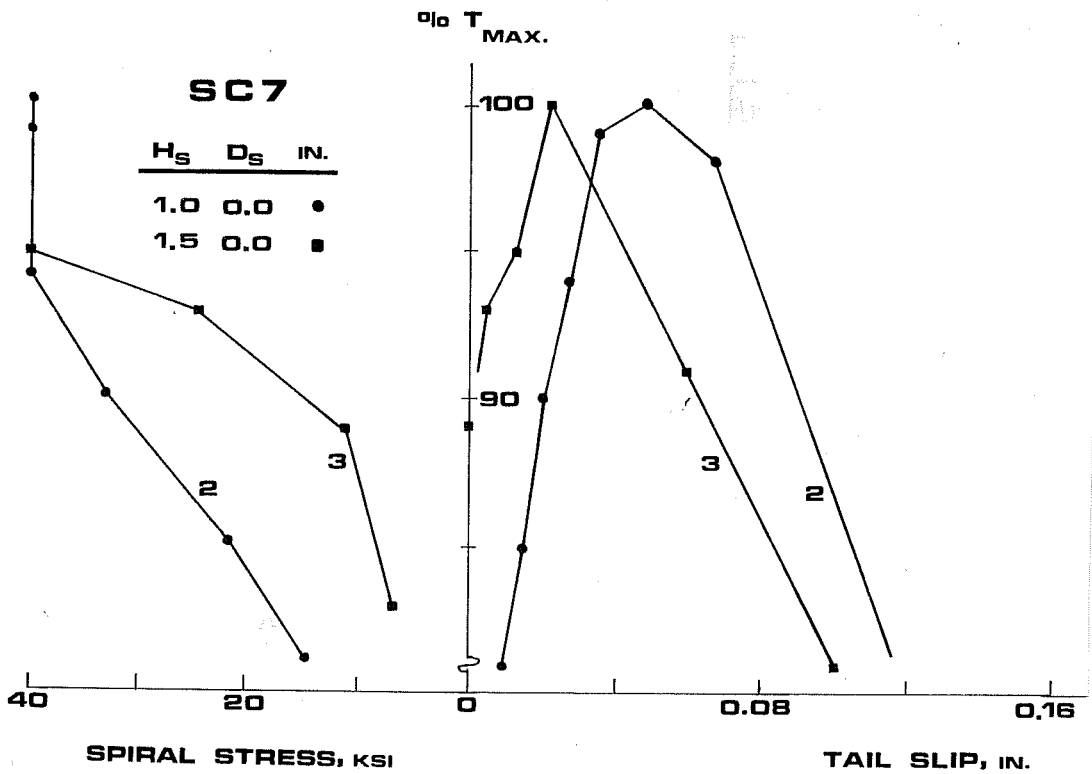
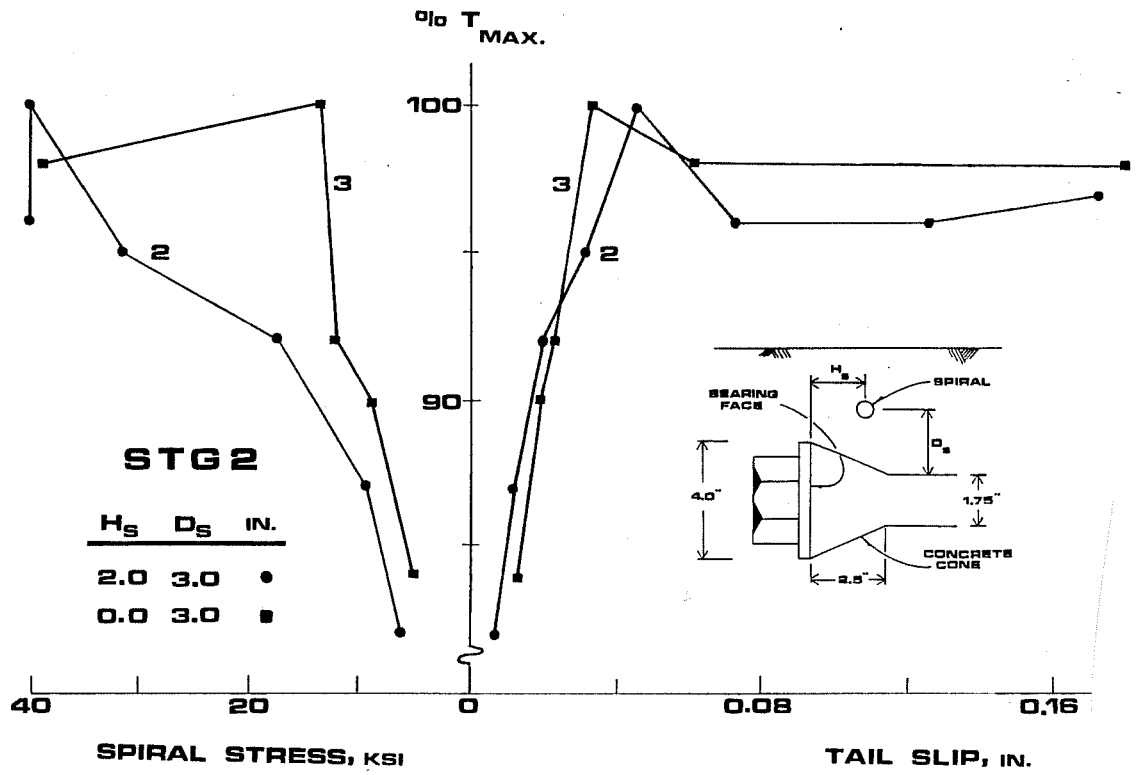


Fig. 3.24 Spiral stress vs. percentage of bolt strength and tail slip of top bolts in tests STG2 and SC7.



tioned within the assumed geometry for the cone of compacted concrete (see Fig. 3.22). The hoop on bolt 2 was stressed early (21 ksi at 85 percent  $T_{max}$ ) and both hoops yielded at 95 percent  $T_{max}$  with small (0.020 in. average) tail slip. The early stresses in the bars were most likely associated with the formation of the cone (in which the hoops were embedded) rather than to any restraining effect on cracks due in the surrounding concrete once the cone had developed. A longitudinal crack on top of the bolts was observed on the surface at 85 and 95 percent  $T_{max}$  for bolts 2 and 3, respectively (see Fig. 3.12,  $P_n = 37$  k and 49 k).

STG1. In test STG1, the bolts rested against the spirals, which crossed far ahead ( $h_s = 5.0$  in. and 3.0 in.) of the bearing surface. The top bolts reached their peak load before any significant spiral stress (less than 13 ksi in Fig. 3.25) were measured and failed abruptly afterward. Longitudinal cracks right above bolts 2 and 3 were observed as shown in Fig. 3.16.

For tests SC7 and STG1, with bolts resting against the spiral bars in shallow cover, it is concluded that the transverse reinforcement did not restrain effectively the splitting above the bolts at the anchorage end.

SC6. Adequate placement of the transverse reinforcement in test SC6 was observed to increase the strength of the anchor bolt installation. The spiral hoops were positioned very close to the washer, on top of the expected concrete cone, as illustrated in Fig. 3.22. The first hoop in front of the bearing face yielded near 90 percent  $T_{max}$  for bolts

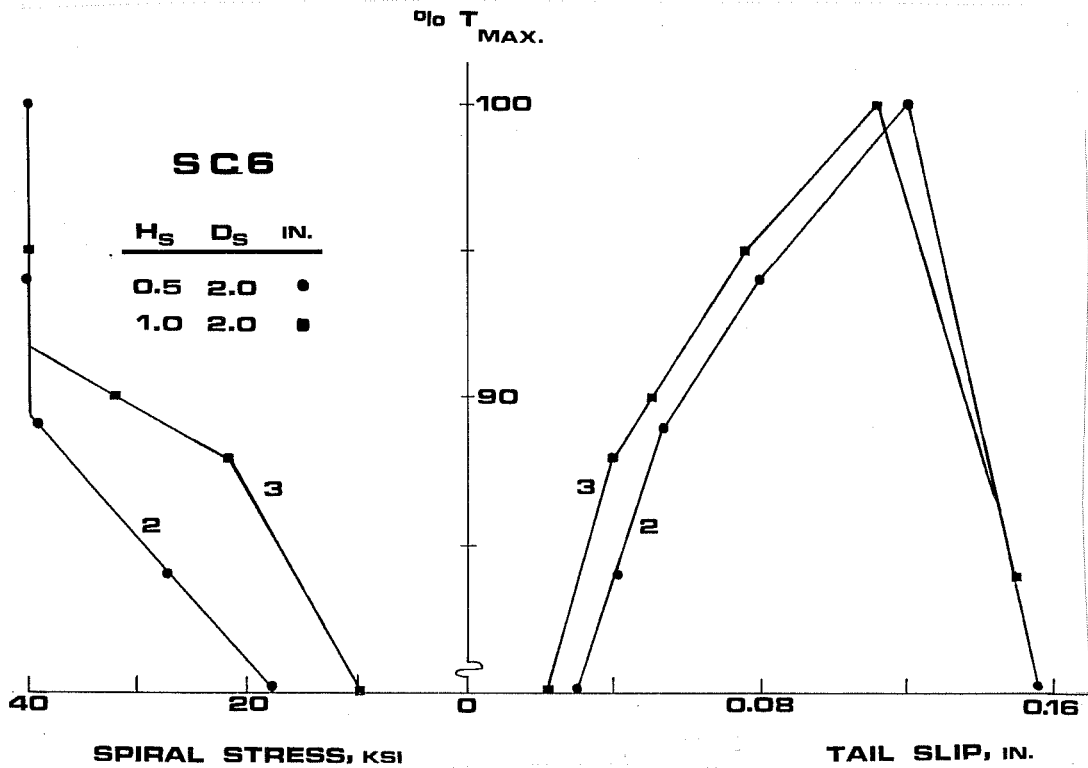
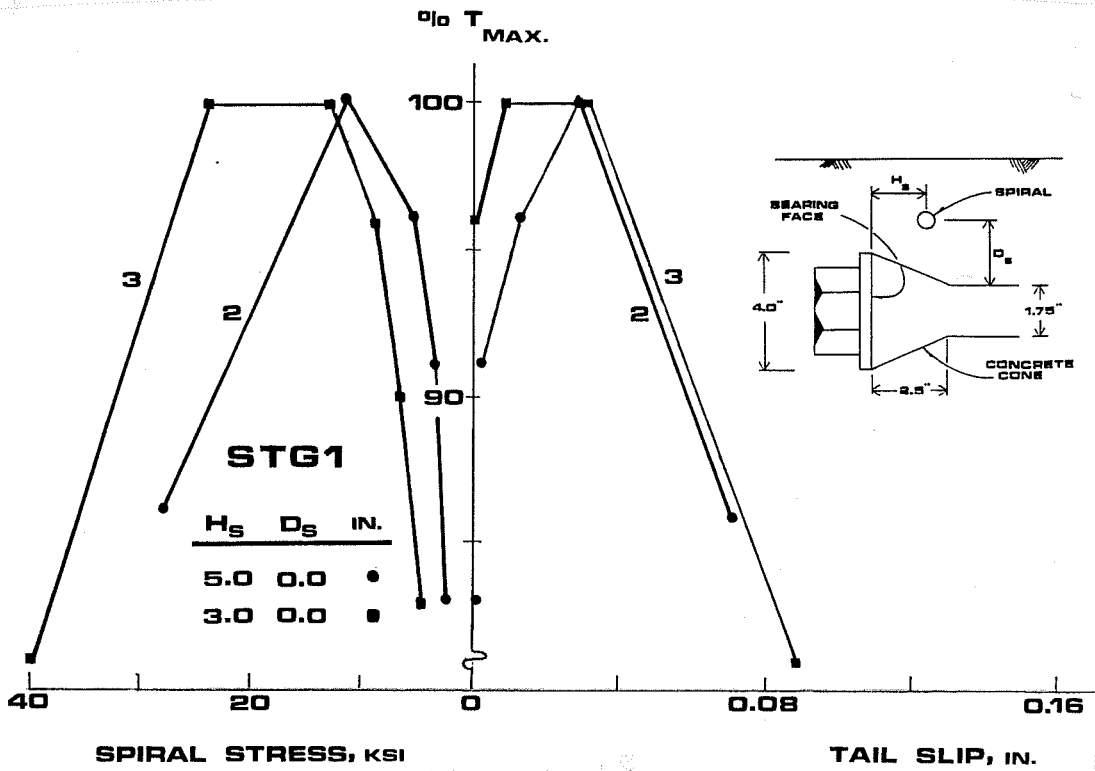


Fig. 3.25 Spiral stress vs. percentage of bolt strength and tail slip of top bolts in tests STG1 and SC6.

## CHAPTER 4

### TEST COMPARISONS

#### 4.1 Introduction

The results from nine anchor bolt groups tested, including three tests reported by Cichy<sup>1</sup> and six tests presented in Chapter 3, are compared in this chapter. The comparisons demonstrate the effect of (1) bolt spacing, (2) clear cover, (3) bolts with variable lengths, and (4) reduced bearing area on the tensile capacity of anchor bolt groups.

The response of the top bolts in a group are compared in terms of normalized bolt tension ( $T/\sqrt{f'_c}$ ) versus lead slip curves. As discussed in the previous chapter, only the response of the top two anchor bolts in the 4-bolt pattern was significant in determining the group capacity. Normalizing the tensile force with respect to  $\sqrt{f'_c}$  to cancel out the effect of variable concrete strength on the bolt capacity is consistent with previous research; Hasselwander et al.<sup>4</sup> expressed the bolt capacity in terms of this factor (Eq. 4.1). The variation in concrete strength was shown to be small (Table 2.2).

The reduction in strength for each bolt in a group is measured in terms of "relative" capacity ( $T_{max}/T_n$ ). The measured peak load on the bolts tested ( $T_{max}$ ) is compared with the nominal tensile capacity (single bolt capacity,  $T_n$ ) of a bolt with similar geometry loaded individually.  $T_n$  is calculated using Eq. 4.1. Since all anchor bolts failed in a wedge splitting mode, the nominal capacity  $T_n$  provides a

2 and 3 (Fig. 3.25). A second hoop, 6 in. ahead of the first, also yielded just before the top bolts reached their capacity. The average tail slip at failure was 0.115 inches, the most of any test, some with larger concrete cover (SC8). Concrete was lifted in two sharply defined blocks, one on top of each bolt, which extended about 25 inches in front of the washers (Fig. 3.10). The few cracks observed at the anchorage zone prior to failure extended sideways or diagonally to the bolt, but none occurred straight on top of the bolt along its axis. The cracks were successfully restrained by the spiral near the anchorage zone and forced to travel farther ahead before they could surface and develop a failure plane.

Perhaps a rough estimate of the strength gain which resulted from the spiral confinement in test SC6 could be drawn by comparing this test with test STG2, where the spirals showed relatively minor effect on strength under a similar clear cover condition ( $C = 5.4$  in. versus 4.4 in. in test SC6). The average tail slip at ultimate was 0.04 in. for the top bolts in test STG2. Assuming a tail slip at ultimate between 0.04 and 0.06 inches as typical for test SC6, had the spirals not been effective, the bolts capacity could be estimated from Fig. 3.25 as 85 to 90 percent of the actual value. Note that at 90 percent  $T_{max}$  the spiral was providing full restraint (yielded) at the anchorage zone.

valid reference for comparison.

The manner in which bolt loads were determined from measurements of strain and load on the test apparatus is explained in Appendix A.

#### 4.2 Single Bolt Capacity

The expression for the tensile capacity of an isolated anchor bolt failing in a wedge-splitting mode is presented below:

$$T_n = 0.140A_b \sqrt{f'_c} \left[ 0.7 + \ln \left( \frac{2C}{D_w - D} \right) \right] \quad \text{Eq. 4.1}$$

The equation for the single bolt capacity contains the following parameters:

- (1) bearing area at the anchorage end ( $A_b$ )
- (2) concrete compressive strength ( $\sqrt{f'_c}$ )
- (3) clear cover ( $C$ )
- (4) washer and bolt diameter ( $D_w - D$ )

Except for a reduced bearing area in test NOW, clear cover and concrete strength were the only parameters in Eq. 4.1 varied in the test program. The clear cover, bearing area, and bolt diameter were typically within the range used in developing the equation (Table 2.2). The embedded length was held constant (35 in.) in all tests, except STG1 and STG2 with variable lengths (30 in. and 40 in.). The embedded length was greater than  $12(D_w - D)$  as suggested in the development of Eq. 4.1. Table 4.1 lists the single bolt capacity for the nine anchor bolt groups comprising the test program.

Table 4.1 SINGLE BOLT CAPACITY (1)

Test	C(in.)	$f'_c$ (psi)	$T_n$ (kips)
SC1	2.4	3500	123
SC2	5.4	3600	194
SC4	5.4	4200	209
NOW(2)	4.4	3900	102
SC6	4.4	3900	183
SC7	2.4	3600	124
SC8	7.4	3600	220
STG1	2.4	3800	128
STG2	5.4	3900	202

(1)  $A_b = 10.16 \text{ in.}^2$   $L = 35 \text{ in.}$   $D = 1.75 \text{ in.}$   $D_w - D = 2.25 \text{ in.}$

(2)  $A_b = 4.29 \text{ in.}^2$   $D_w - D = 1.17 \text{ in.}$

#### 4.3 Effect of Bolt Spacing

The performance of anchor bolt groups embedded at different spacings is compared here. In Fig. 4.1 the response of bolts 2 and 3 in tests SC1 and SC7 is shown, while in Fig. 4.2 the average response for the top bolts in tests SC2 and SC4 is illustrated. The effect of bolt spacing has been isolated from clear cover and concrete compressive strength, which also affect the capacity of an anchor bolt installation, by comparing tests with the same clear cover, and normalizing the bolt tension with respect to  $\sqrt{f'_c}$ .

As shown in Fig. 4.1, an increase in bolt spacing from 11.2 in. to 13.5 in., with a 2.4 in. clear cover, did not effect significantly the average bolt capacity. The average of the bolts' loads in each group is about the same. On the other hand, the same 2.3 in. increase

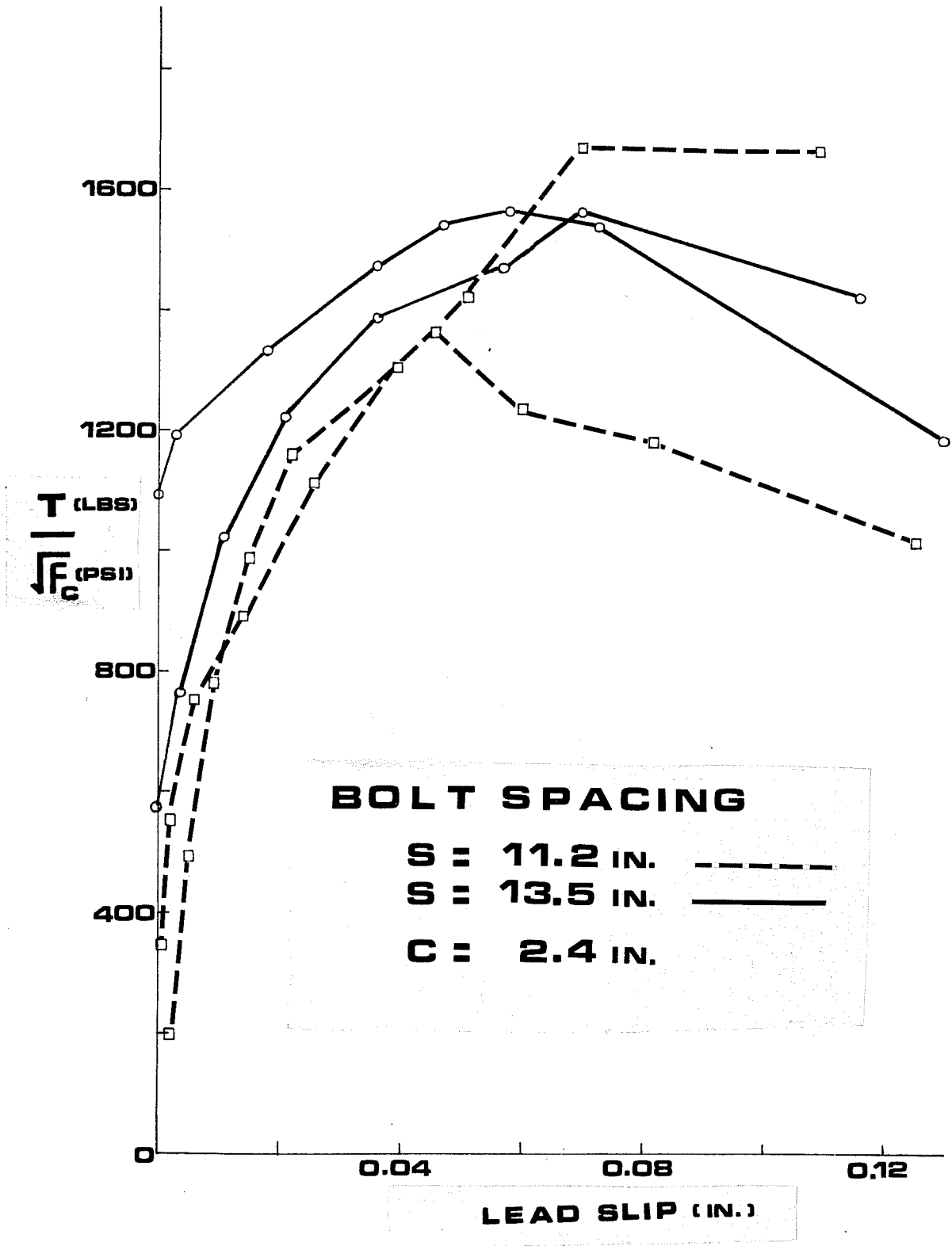


Fig. 4.1 Effect of bolt spacing: tests SC1 and SC7

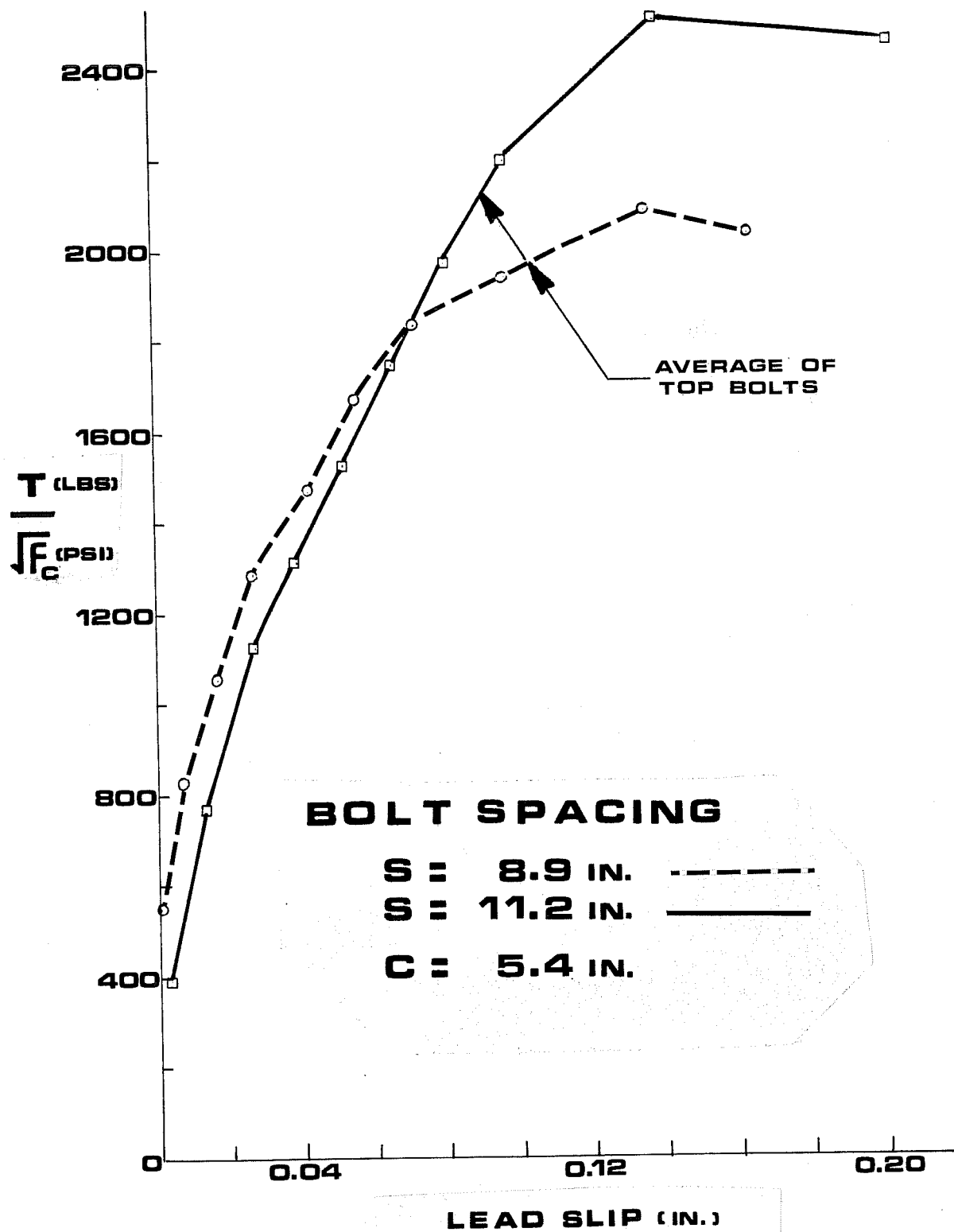


Fig. 4.2 Effect of bolt spacing: tests SC2 and SC4



Table 4.2 EFFECT OF BOLT SPACING

Test	Bolt Spacing (in.)	Clear Cover (in.)	Bolt	$\frac{T_{max}}{\sqrt{f'_c}}$	% Increase	$\frac{T_{max}}{T_n}$	% Reduction for Bolt Group
SC1	11.2	2.4	2	1670		0.80	27
			3	1360		0.65	
			avg.	1515		0.73	
SC7	13.5	2.4	2	1540		0.75	25
			3	1560	2	0.75	
			avg.	1550		0.75	
SC2	8.9	5.4	2	*		*	36
			3	*		*	
			avg.	2080		0.64	
SC4	11.2	5.4	2	*		*	23
			3	*		*	
			avg.	2500	20	0.77	
SC6	9.7	4.4	2	2030		0.69	31
			3	2040		0.70	
			avg.	2030		0.69	

\* Individual bolt values unavailable.

in bolt spacing from 8.9 in. to 11.2 in., with a 5.4 in. clear cover (Fig. 4.2), resulted in a 20 percent increase in the average bolt capacity. As bolts are embedded at closer distances, their capacity becomes more sensitive to spacing.

The change in capacity with spacing is summarized in Table 4.2, which lists normalized bolt capacity ( $T_{\max}/\sqrt{f'_c}$ ) and relative capacity ( $T_{\max}/T_n$ ) for five anchor bolt groups. The bolt interaction, as measured by the  $T_{\max}/T_n$  ratio, accounted for a 25 percent reduction in the average capacity for groups with 11.2 and 13.5 in. spacings (tests SC1, SC4 and SC7), while for a 9.7 in. spacing (in test SC6) it reduced the bolt capacity by 31 percent. The bolt group at the closest spacing tested, 8.9 in. (SC2), exhibited the largest reduction, 36 percent.

#### 4.4 Effect of Clear Cover

The effect of clear cover on the strength of anchor bolts has been examined in previous research, as explained in Secs. 2.2 and 4.2. The results are used here to evaluate whether different cover conditions at a given spacing further affect the interaction of bolts in a group.

In Figs. 4.3 and 4.4, bolt groups with different clear covers and constant spacing are compared. In Table 4.3, normalized bolt strength and relative capacity for the top bolts in the groups are listed. Increasing clear cover from 4.4 in. to 7.4 in., with a 9.7 in. spacing, resulted in a 24 percent increment in the average bolt capacity, as shown in Table 4.3 for tests SC6 and SC8. The increment in capacity predicted for an isolated bolt under similar clear cover conditions was 20 percent (220/183 from Table 4.1).

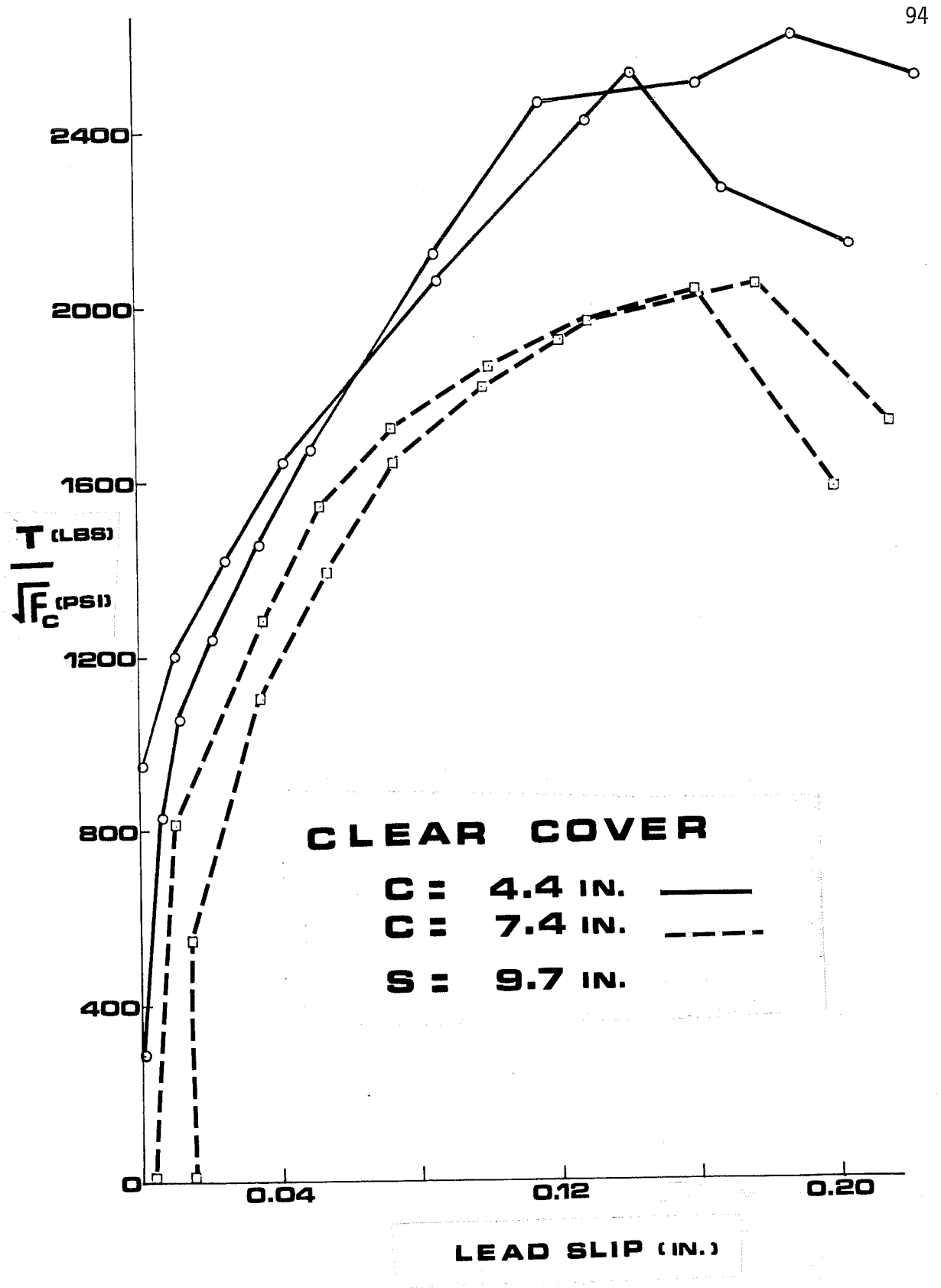


Fig. 4.3 Effect of clear cover: tests SC6 and SC8

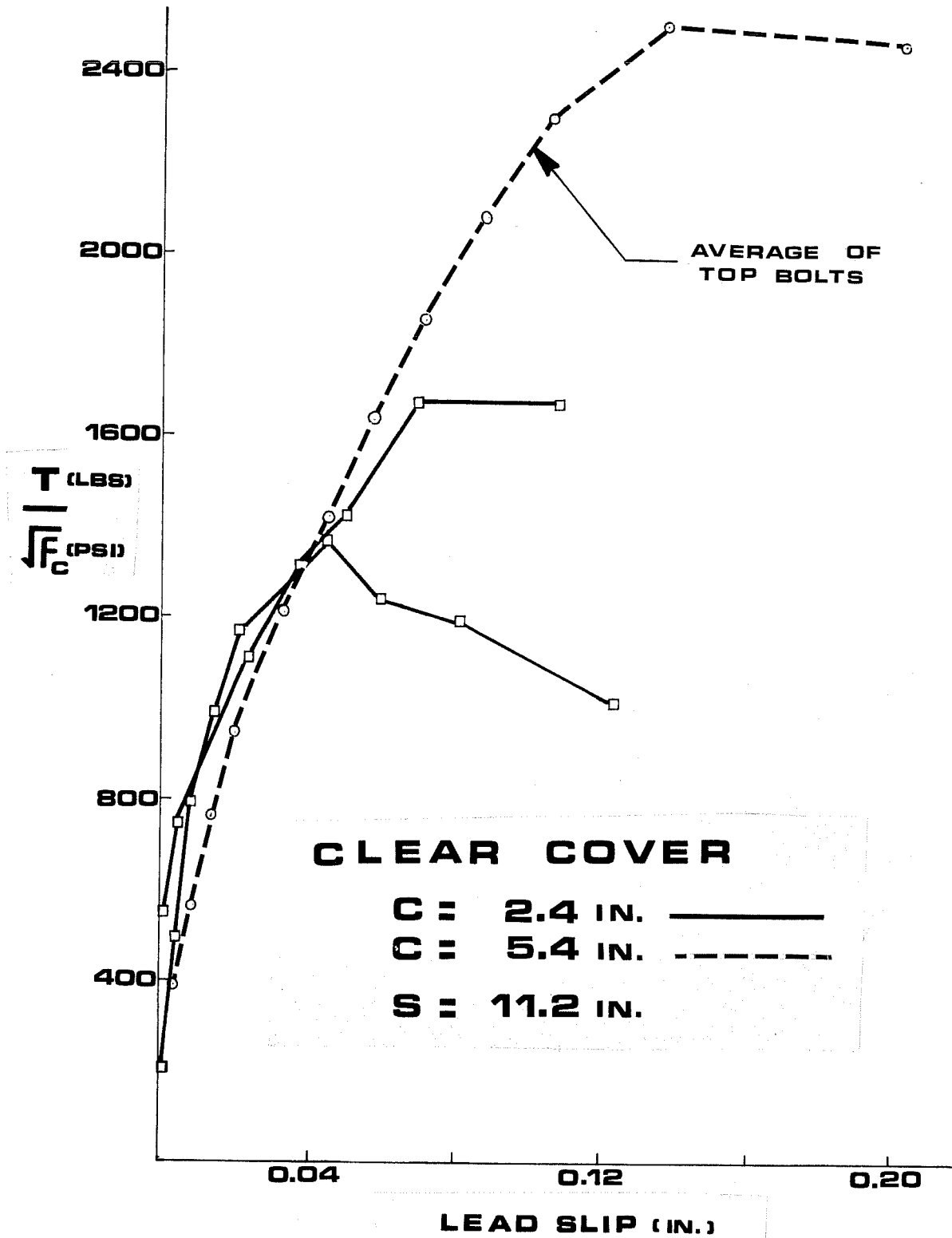


Fig. 4.4 Effect of clear cover: tests SC1 and SC4

Table 4.3 EFFECT OF CLEAR COVER

Test	Bolt Spacing (in.)	Clear Cover (in.)	Bolt	$\frac{T_{max}}{\sqrt{f'_c}}$	% Increase	$\frac{T_{max}}{T_n}$	% Reduction for Bolt Group
SC6	9.7	4.4	2	2030		0.69	
			3	2040		0.70	
			avg.	2030		0.69	31
SC8	9.7	7.4	2	2530		0.69	
			3	2470		0.67	
			avg.	2510	24	0.68	32
SC1	11.2	2.4	2	1670		0.80	
			3	1360		0.65	
			avg.	1515		0.73	27
SC4	11.2	5.4	2	*		*	
			3	*		*	
			avg.	2500	65	0.77	23

\* Individual bolt values unavailable.

The average capacity increased 65 percent when clear cover increased from 2.4 in. to 5.4 in. with a 11.2 in. spacing (tests SC1 and SC4, Table 4.3 and Fig. 4.4). A 70 percent (209/123 from Table 4.1) rise in capacity was predicted for a single bolt with similar geometry to those compared.

The observations corroborate that the expression for the tensile strength of an isolated bolt (Eq. 4.1) correctly predicts the effect of clear cover on the capacity of bolts in a group.

The bolt interaction ( $T_{\max}/T_n$  ratio) at a given spacing was not significantly affected by a variation in clear cover. As seen for tests SC1 and SC4 in Table 4.3, the difference in relative capacity was only five percent (0.77/0.73) when cover varied from 2.4 to 5.4 inches. For tests SC6 and SC8, increasing cover from 4.4 in. to 7.4 in. did not change the  $T_{\max}/T_n$  ratio.

#### 4.5 Effect of Bolt Staggering

Two tests (STG1 and STG2) were conducted on anchor bolts embedded with variable lengths in a group, as explained in Sec. 2.2.1. The "staggered" bolt groups, as referred to here, are compared with bolt groups (SC1 and SC2) having uniform embedment length and identical clear cover and spacing conditions in Figs. 4.5 and 4.6. Normalized bolt strength and relative capacity for the four tests are presented in Table 4.4.

Staggered bolts in test STG1 with a 2.4 in. clear cover and 11.2 in. spacing showed a slight increase (8 percent) in the average bolt capacity over a bolt group (SC1) with similar geometry and uniform embedded

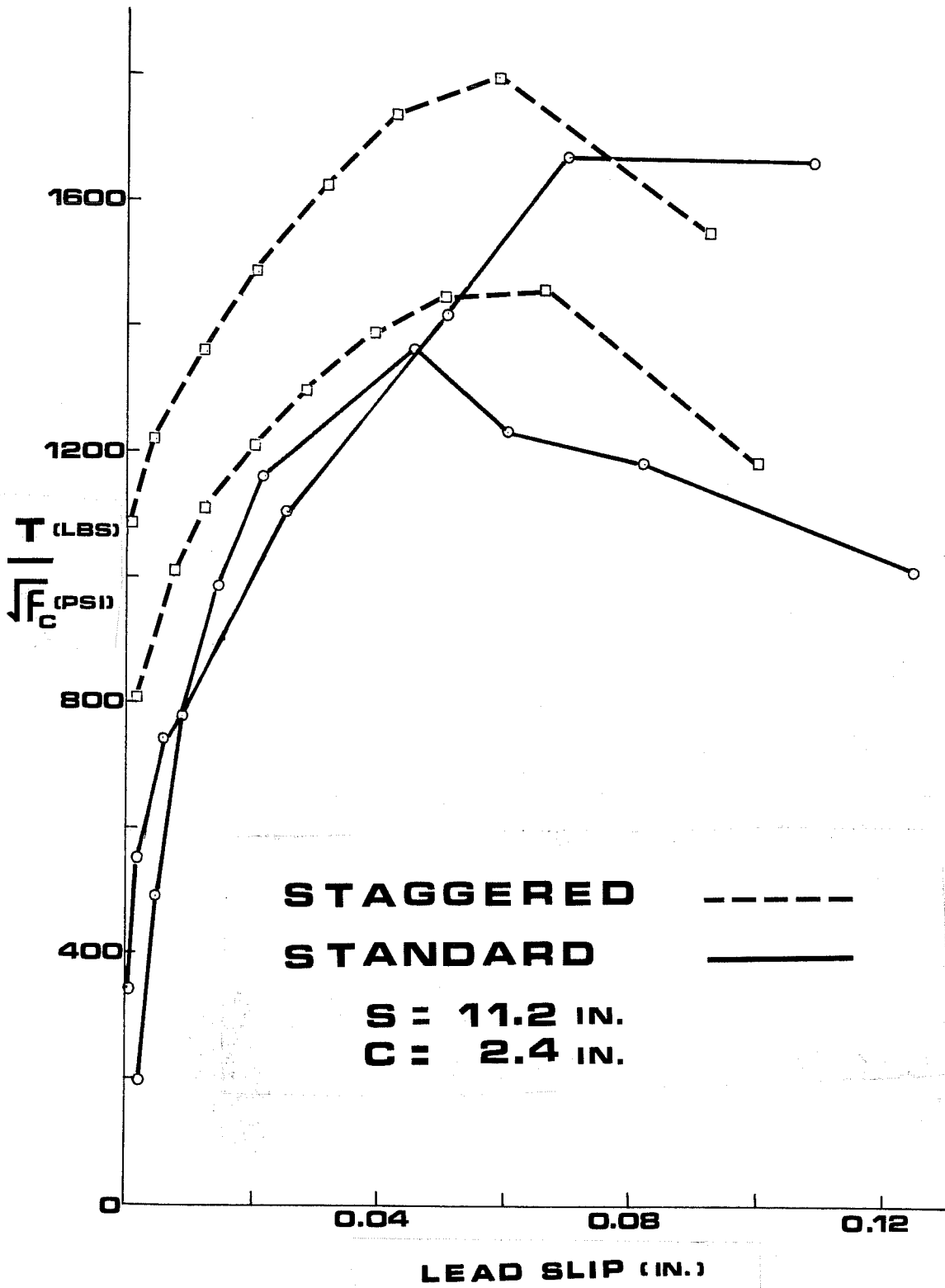


Fig. 4.5 Effect of bolt staggering: tests SC1 and STG1

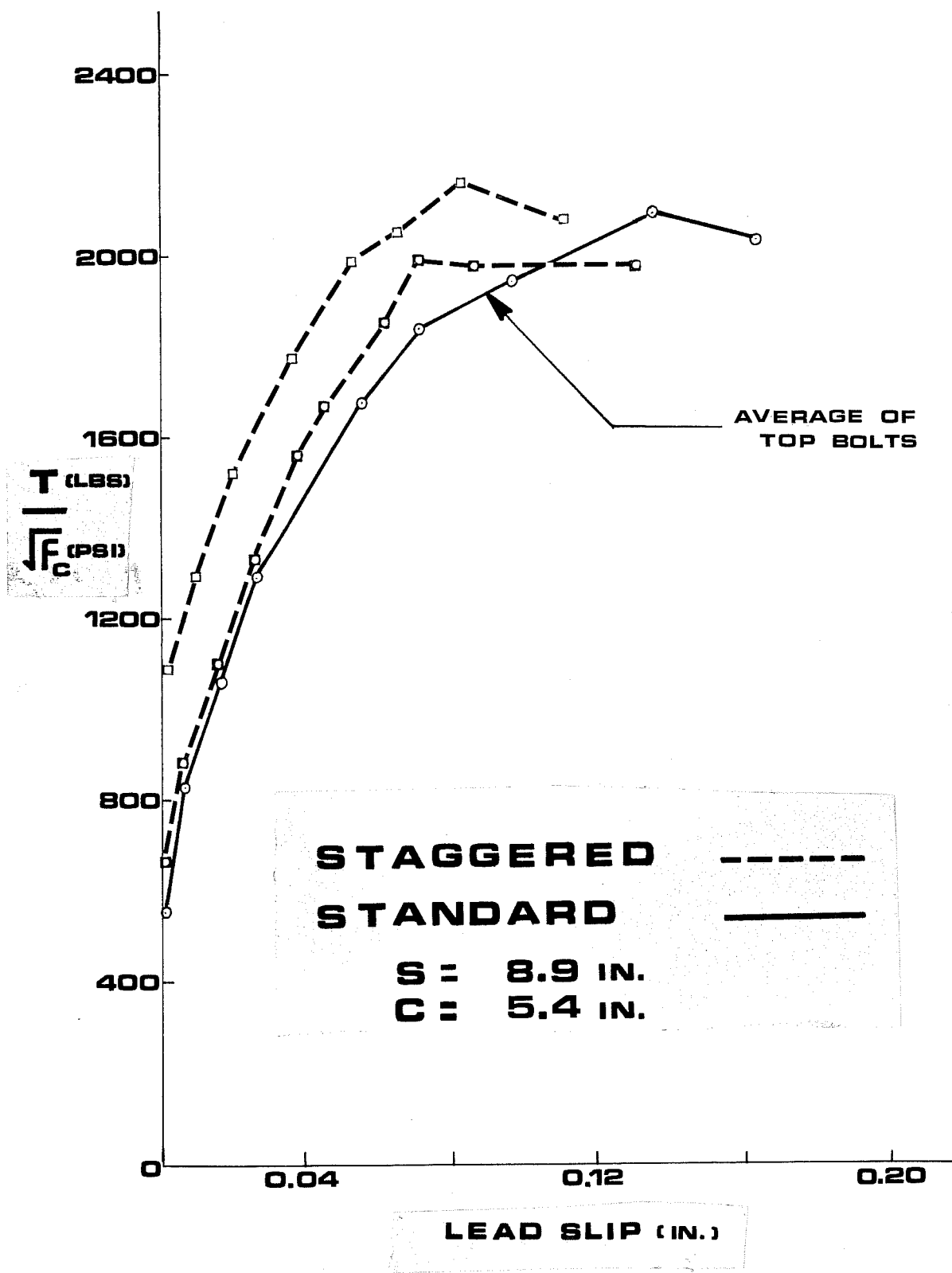


Fig. 4.6 Effect of bolt staggering: tests SC2 and STG2



Table 4.4 EFFECT OF BOLT STAGGERING

Test	Bolt Spacing (in.)	Clear Cover (in.)	Bolt	$\frac{T_{max}}{\sqrt{f'_c}}$	% Increase	$\frac{T_{max}}{T_n}$	% Reduction for Bolt Group
SC1	11.2	2.4	2	1670		0.80	
			3	1360		0.65	
			avg.	1515		0.73	27
STG1	11.2	2.4	2	1800		0.87	
			3	1450		0.70	
			avg.	1630	8	0.79	21
SC2	8.9	5.4	2	*		*	
			3	*		*	
			avg.	2080		0.64	36
STG2	8.9	5.4	2	2160		0.67	
			3	1990		0.62	
			avg.	2075	0	0.64	36

\* Individual bolt values unavailable.

length. Bolt 2, with longer embedment, failed almost as an isolated bolt ( $T_{\max}/T_n = 0.87$ ), while bolt 3 showed a lower capacity, comparable to the average capacity in test SC1. It is not clear whether the lower strength and notably more spalling (Fig. 3.16) near the anchorage end for bolt 3 resulted from a local weakness (aggravated by a shallow cover condition), or from splitting forces which had originated at bolt 2 and moved toward the anchorage zone of bolt 3. On the surface though, very little crack interaction was visible at the stage bolt 3 failed (Fig. 3.16,  $P_n = 43$  k). The short embedded length (30 in.) for bolt 3 had no effect on the bolt capacity. No cracks extended to the front face of the specimen.

In test STG2 with a 5.4 in. clear cover and 8.9 in. spacing, staggering did not increase the average bolt capacity (Fig. 4.6). Bolts 2 and 3 failed at comparable load levels with considerable interaction as observed from cracks on the surface (Fig. 3.18), and from  $T_{\max}/T_n$  ratios in Table 4.4.

Perhaps a distinction could be made between the staggered group embedded in shallow cover and large spacing versus the group with deep cover and small spacing. The former group with relatively smaller potential for bolt interaction (average  $T_{\max}/T_n = 0.73$  in test SC1) resulted in a very modest increase in average capacity, while the latter group with a greater tendency to interact (average  $T_{\max}/T_n = 0.64$  in test SC2) showed no improvement in capacity from staggering. The fact that cracking near the anchorage zone (prior to failure) is less extensive with shallow, rather than deep cover, explains why staggering was rela-

tively more successful in reducing the bolt interaction for the shallow cover condition.

The test results indicate that staggering is not a practical method to increase significantly the tensile capacity of an anchor bolt group. The emphasis is on practical considerations. Perhaps an offset of the anchor bolts considerably larger than used in the test program (10 in.) might prove successful in increasing the group capacity. The value of such an alternative in terms of additional bolt material and installation difficulty seems doubtful, however.

#### 4.6 Effect of Reduced Bearing Area

A nut without washers was placed at the embedded end of anchor bolts in test NOW. In Fig. 4.7 and Table 4.5, this bolt group is compared with another group (SC6) with standard anchorage device (as defined in Table 2.2). In both groups the clear cover and bolt spacing were the same.

The average bolt capacity was reduced by 26 percent when washers were not used at the anchorage end. However, a much greater decrease, 44 percent (102/183 in Table 4.1), equivalent to the reduction in the bearing area ( $A_b$ ) was predicted by the expression for the nominal bolt capacity (Eq. 4.1). The discrepancy above is clearly explained by noticing (Table 4.5) that the anchor bolts in test NOW failed with very little, if any, bolt interaction (average  $T_{max}/T_n = 0.92$ ), while for test SC6 the interaction was considerably greater ( $T_{max}/T_n = 0.69$ ). As illustrated in Fig. 3.8 for test NOW, the surfacing of two longitudinal

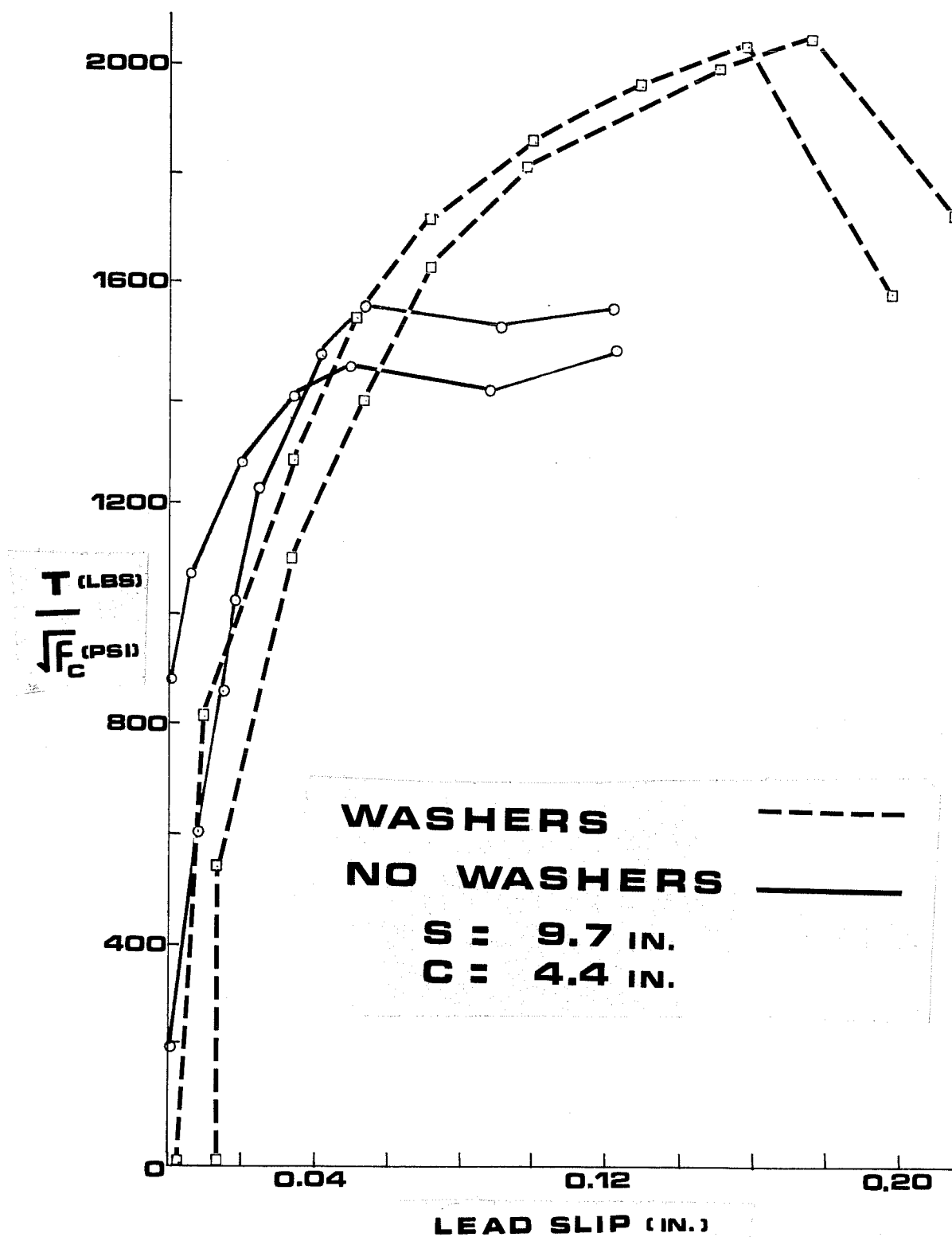


Fig. 4.7 Effect of reduced bearing area: tests SC6 and NOW

Table 4.5 EFFECT OF REDUCED BEARING AREA

Test	Bolt Spacing (in.)	Clear Cover (in.)	Bolt	$\frac{T_{max}}{\sqrt{f'_c}}$	% Increase	$\frac{T_{max}}{T_n}$	% Reduction for Bolt Group
SC6	9.7	4.4	2	2030		0.69	
			3	2040		0.70	
			avg.	2030		0.69	31
NOW	9.7	4.4	2	1560		0.96	
			3	1450		0.89	
			avg.	1500	-26	0.92	8

cracks (instead of one central crack as for test SC6) in the region between the top bolts, much after the top bolts reached their capacity ( $P_n = 35$  k) further indicates that splitting from bolts 2 and 3 did not extend sideways sufficiently to the adjacent bolts.

In conclusion, the anchor bolts with lower nominal capacity,  $T_n$  (due to the smaller bearing surface), exhibited significantly less reduction in strength than the group with a higher nominal capacity.

#### 4.7 Summary of Test Results

The average relative bolt capacity versus bolt spacing is summarized in Fig. 4.8 for the six standard (SC designation) anchor bolt groups in this study, and three tests reported by Hasselwander et al.<sup>4</sup>

4.7.1 Hasselwander's Tests. The tests on 2-bolt groups (H), as described in Table 4.6, were conducted with 1.0 in. diameter bolts, embedded in specimens with square 36 in. x 36 in. cross-section.

The anchor bolt group with a 10.0 in. spacing agrees very well with the results from the present study. In addition, the steep drop in relative capacity at 5.0 in. spacing confirms the trend observed in this study.

The relative capacity for the anchor bolt group with a 15 in. spacing is inconsistent with the trend exhibited in the other two tests, and with the results in the present study. The relatively smaller side cover (10.5 in.) which resulted when a larger spacing was used, provided less confinement to the bolts, and might explain the lower capacity for the group with 15 in. spacing.

Table 4.6 HASSELWANDER'S TWO-BOLT GROUP TESTS

Bolt Spacing (in.)	Clear Cover (in.)	$f'_c$ (psi)	$\frac{T_{max}}{T_n}$
5	2.5	2650	0.57
10	2.5	3900	0.72
15	2.5	2810	0.65

$$D = 1.0 \text{ in.} \quad L_d = 15D \quad D_w = 2.25 \text{ in.}$$

4.7.2 Capacity Reduction for Bolt Group. Six tests with spacing from 8.9 to 13.5 inches exhibited a reduction in nominal capacity of about 35 to 25 percent, as illustrated in Fig. 4.8. The test group (SC7) with 13.5 in. spacing, however, showed the same reduction as tests with 11.2 in. spacing. This result is inconsistent with the reduction trend demonstrated by the other tests between 8.9 and 11.2 in. spacings. Note that the extrapolation of the trend to the 13.5 in. spacing indicates about  $T_{max}/T_n = 0.85$ .

The capacity of the top bolts in test SC7 is suspected to be adversely affected by the position of a spiral bar in front of the washers. The bolts rested against the spiral cage. A hoop crossing just 1.0 to 1.5 in. ahead of the bearing face of bolts 2 and 3 (Figs. 2.10 and 3.22) appeared to interfere with the cone of compacted concrete.

The strength of a two-bolt group should exhibit a theoretical variation with spacing between 50 and 100 percent of the nominal capaci-

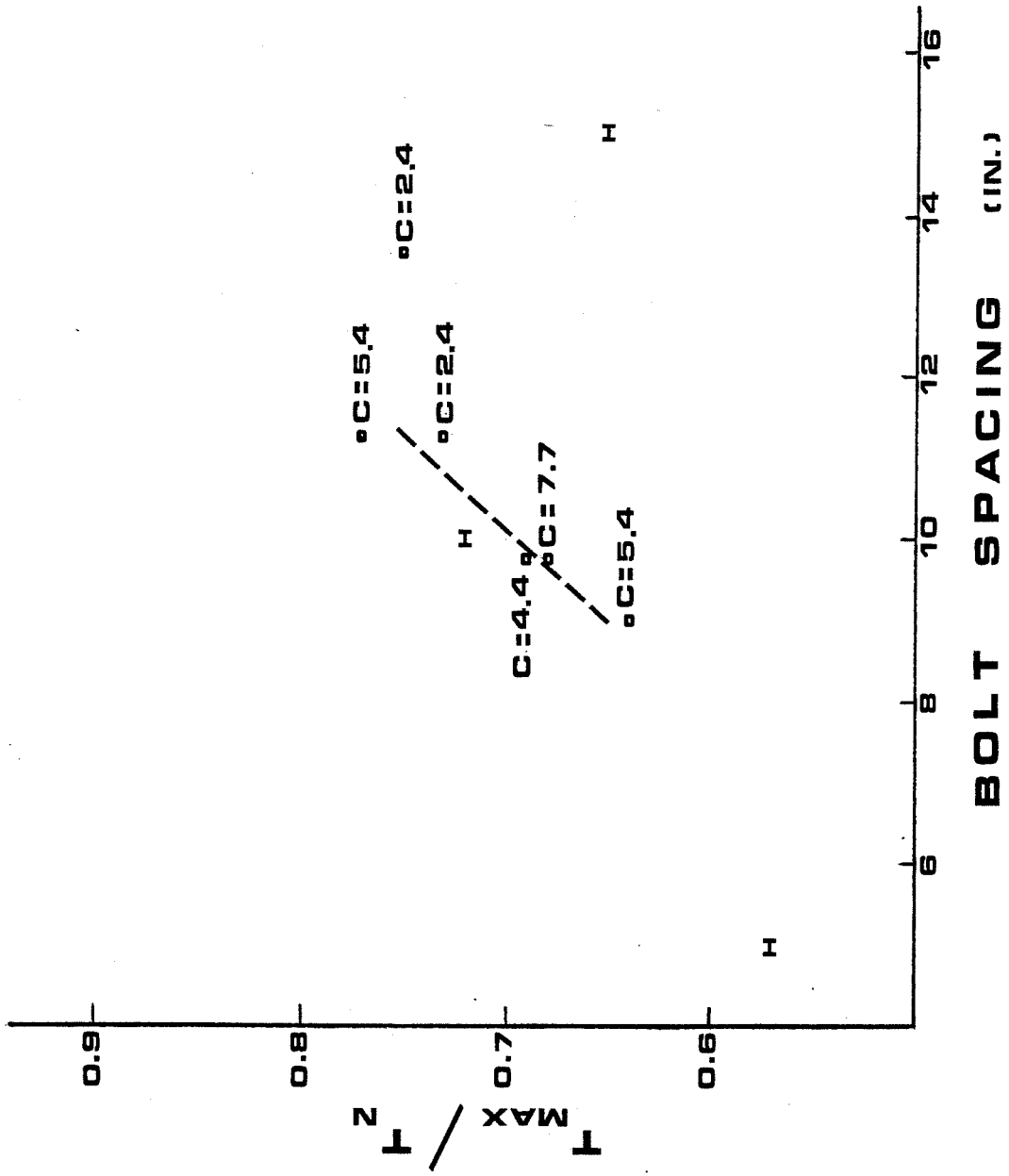


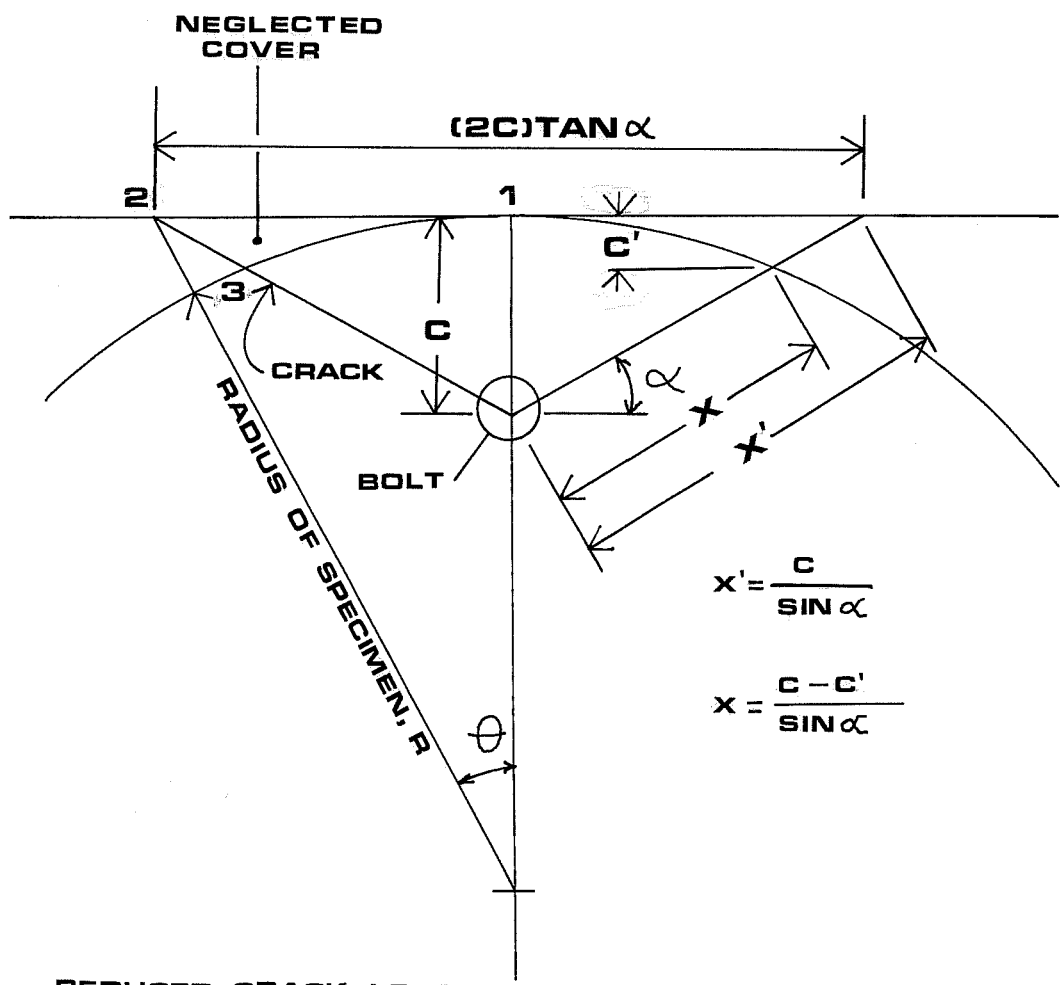
Fig. 4.8 Reduction in average capacity for bolts in a group with spacing



ty. The range in which spacing was varied in the test program does not show the bounds on the capacity for bolts in a group. If the trend observed here were to hold constant with a wider spacing variation, the group capacity is predicted to be near 50 percent of the nominal capacity at 6 in., and 100 percent at a spacing of 16 inches.

The lack of test data for very large (15 to 17 in.) and small (5 to 7 in.) spacings does not permit, however, a definite assessment of the effect of spacing on the group capacity, at present. Furthermore, two areas need to be investigated as considered below.

In comparing the measured bolt capacity with the nominal capacity, the effect of circular shape of the specimen was assumed to be negligible. A test result reported by Lee and Breen<sup>3</sup> indicated that the capacity for an isolated anchor bolt did not vary significantly when the bolt was embedded in a circular or rectangular specimen. In the test program the measured capacity for bolts embedded in a circular specimen was compared with the nominal capacity (Eq. 4.1) developed from test results on rectangular specimens. As shown in Fig. 4.9, the major splitting has to extend farther for a bolt embedded in a rectangular than in a circular specimen with the same clear cover. The restraint provided by the cover area  $123$  in the rectangular specimen is absent in the circular specimen. If the orientation of cracks were the same for any cover value, it appears (Fig. 4.9b) that the effect of circular shape should be more pronounced with larger cover. It is undefined, however, whether cracks might flatten (angle  $\alpha$  decrease) with small cover, which would also increase the effect of shape. These considerations suggest that an



$$X' = \frac{C}{\sin \alpha}$$

$$X = \frac{C - C'}{\sin \alpha}$$

REDUCED CRACK LENGTH:

$$\frac{X}{X'} = \frac{C - C'}{C}$$

$$\tan \theta = \frac{C}{R \tan \alpha}$$

$$C' = R - R \cos \theta$$

$$\frac{X}{X'} = 1 - \frac{1 - \cos \theta}{\tan \alpha \tan \theta}$$

Fig. 4.9 Effect of circular shape

anchor bolt group with large spacing in a circular specimen might show a reduction in nominal capacity associated with the specimen shape, not with bolt interaction. At close spacing, however, the interaction of splitting forces is the dominant factor reducing the bolt group capacity.

The comparison of two test groups with identical geometry, but one with reduced bearing areas for the anchor bolts (Sec. 4.6), demonstrated that the effect of bolt spacing on the group strength is dependent on the magnitude of the nominal capacity. The splitting from the bolts with smaller bearing surface (no washers) appeared relatively localized and less likely to interact at a given spacing. Therefore, it seems reasonable to correlate the reduction in capacity (at a given spacing) with a particular bearing area and bolt size ( $D_w - D$ ).

## CHAPTER 5

### SUMMARY AND CONCLUSIONS

#### 5.1 Summary of Study

In this study the behavior and tensile capacity of high-strength anchor bolt groups embedded in reinforced concrete piers was investigated.

Previous research had developed an expression for the tensile capacity of an isolated anchor bolt installation failing in a wedge-splitting mode. The objective of this study was to identify modifications to the single bolt capacity for the bolt group interaction in typical anchor bolt applications.

Bolt spacing and clear cover were the primary variables examined; in addition, the effect of (1) variable anchorage length in bolt group, (2) bearing area, and (3) transverse reinforcement were evaluated in a more limited fashion. The results from nine tests were compared.

The specimen was a model of a reinforced concrete drilled shaft footing with cast-in-place anchor bolts. Anchor bolts with 1-3/4 in. diameter and 105 ksi yield strength were arranged in a 4-bolt circular pattern, and embedded 35 in. into the concrete. A nut and washers provided anchorage at the embedded end. Two test groups were arranged with adjacent bolts embedded 5 in. above and below the standard anchorage length. Another test featured bolts without washers (only a nut) at the anchorage end. The concrete shafts, 36 and 42 in. diameters, were rein-

forced with sixteen #11 and #9 longitudinal rebars and #4 deformed spirals at 6 in. pitch. Two anchor bolt groups were cast in each specimen.

The bolt groups were tested in pure tension. By fixing a beam with a concentrated load at the end, a moment was applied to the anchor bolt connection which simulated the loading in the field. The beam applied a tensile force to the 4-bolt test group and compression was transmitted to a plate bearing on the end of the specimen. The transverse (shear) force (transferred directly to the test floor) was not imposed on the test bolts. The loading was applied in small increments until failure of the top bolts in the group occurred.

The response of the anchor bolt groups was measured from strain gages and slip wires attached to the bolts. Bolt strain and slip data were taken after each load increment. Instrumentation of the spiral bars at the anchorage end of the bolts provided additional information regarding the failure mechanism. The development of crack patterns and the failure surface were photographed.

## 5.2 Summary of Test Results

Consistent with the orientation of the loading on the four-bolt groups, only the two anchor bolts at the upper level failed with negligible interaction from the lower level bolts. The top bolts failed in a wedge-splitting mode as described for tests on isolated anchor bolts. Typically for all tests, the cone of crushed and compacted concrete developed ahead of the bearing face of the bolts to split and uplift the

concrete cover as the bolts failed. Crack interaction was visible at the specimen surface in the region between the top bolts. Concrete spalling near the anchorage end was relatively less extensive with smaller cover.

Adequate placement of the transverse reinforcement, in the form of spiral bars crossing the bolts ahead of the bearing face, was observed to restrain a major longitudinal crack straight above the anchor bolt. Spiral bars 1.0 in. in front of the bearing face and 2.0 in. above the top of the bolt appeared to restrain most efficiently the splitting; these bars yielded at 90 percent of the bolt strength. Bars placed farther ahead of the bearing area or at greater bolt-to-spiral clearances also yielded, after the bolts reached their capacity. Except for cases where bolts rested against the spirals and failed abruptly, the transverse reinforcement provided ductility to the anchor bolts installations.

Anchor bolt groups were compared in terms of normalized bolt tension ( $T/\sqrt{f'_c}$ ) versus slip curves for the top bolts. The bolt group interaction and strength reduction were evaluated by comparing the average test capacity with the nominal capacity for an isolated bolt with similar geometry ( $T_{max}/T_n$ ).

### 5.3 Conclusions

Based on the comparisons of test results, and observations of specimens tested, the following conclusions were drawn:

- (1) Bolt spacing from 11.0 to 13.5 in. reduced the tensile capacity of bolts in a group by 25 percent, while at closer spacing the capacity was further reduced, up to 36 percent with a 8.9 in. spacing.
- (2) The equation for the nominal capacity of an isolated anchor bolt correctly predicted the effect of clear cover on the group strength.
- (3) The reduction in strength at a given spacing was independent from clear cover.
- (4) Bolts with variable embedded lengths in a group (up to 10 in.) did not increase significantly the average group capacity.
- (5) The strength reduction at a given spacing diminished for bolts with a reduced bearing area (nominal capacity).

A P P E N D I X A



## A P P E N D I X A

### A.1 Equilibrium Check

The bolt loads calculated from strain gage readings were verified from static considerations on the free body diagram of the loading beam (Fig. 2.17b) as follows.

In Fig. 2.17b, the external moment ( $M_{ext}$ ) from the measured load  $P$  and the internal moment ( $M_{int}$ ) from the bolt loads were equated about the center of the socket:

$$M_{ext} = M_{int}$$
$$116P = (T_1 + T_4) Y_L + (T_2 + T_3) Y_U \quad \text{Eq A.1}$$

The  $M_{int}/M_{ext}$  ratio for the six tests reported in Chapter 3 are presented in Figs. A.1 through A.3. The darkened dot in the figures represents a load stage at which the top bolts reached their capacity.

The  $M_{int}/M_{ext}$  ratio is observed to stabilize at a value between 0.90 and 0.95 for all tests, about midway through the loading prior to failure. Following the stage at which the top bolts reached their capacity, the ratio drops due to the relaxation of the applied load while taking readings. For test STG2, reading the applied load during the data scanning (instead of prior to the scanning as explained in Sec. 2.4.2) resulted in a somewhat higher (0.98) ratio.

The equilibrium check, as expressed in Fig. 2.17b and Eq. A.1, was derived with several simplifications, which introduced inaccuracies

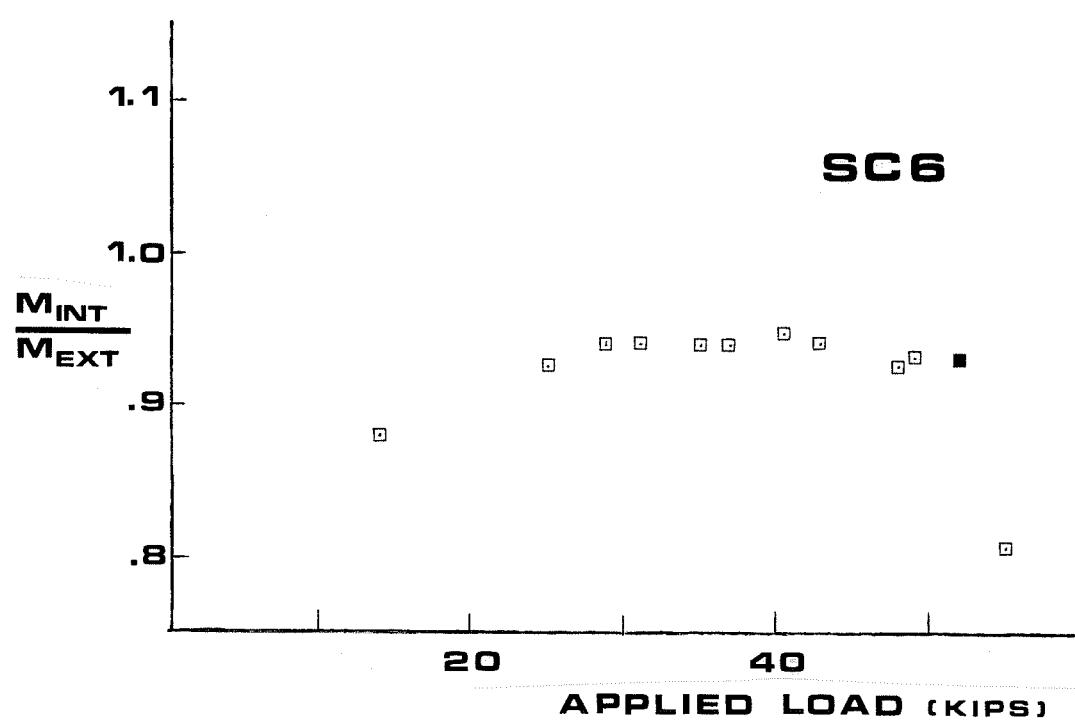
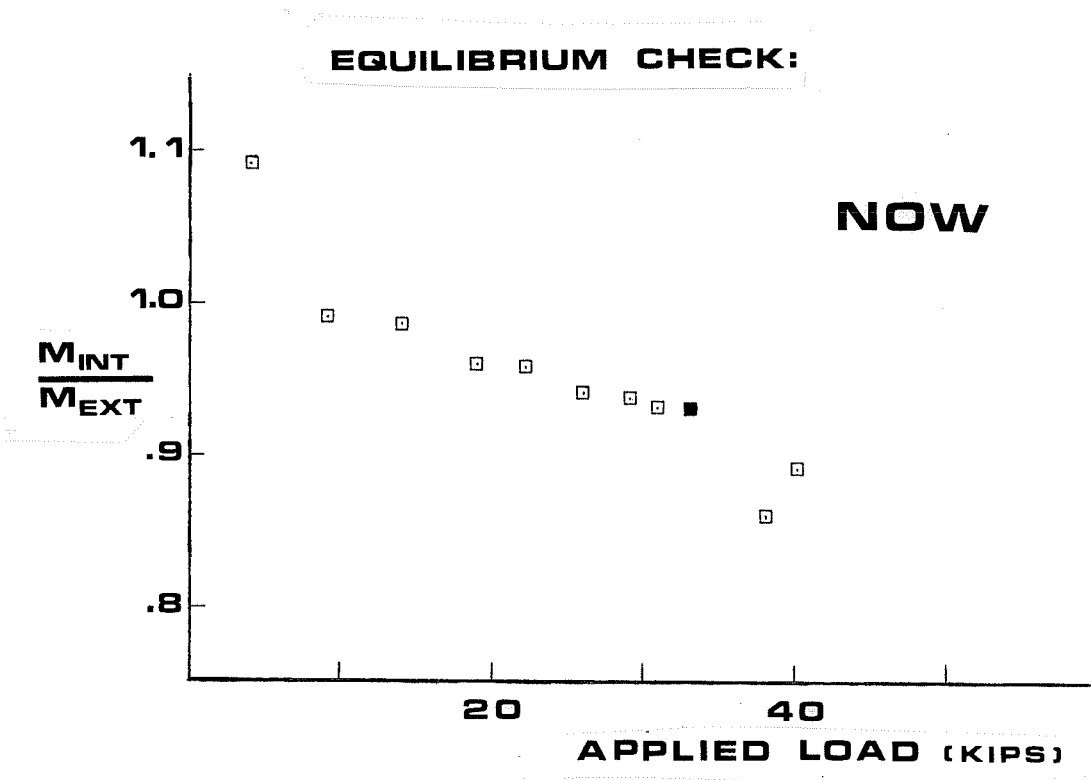


Fig. A.1 Equilibrium check in tests NOW and SC6

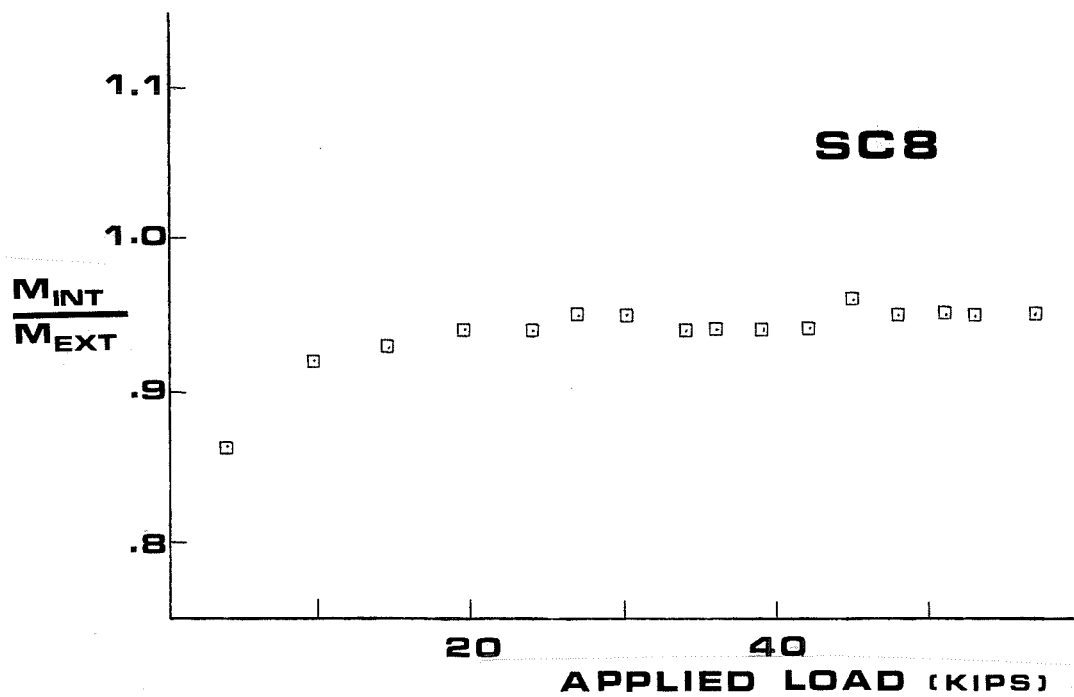
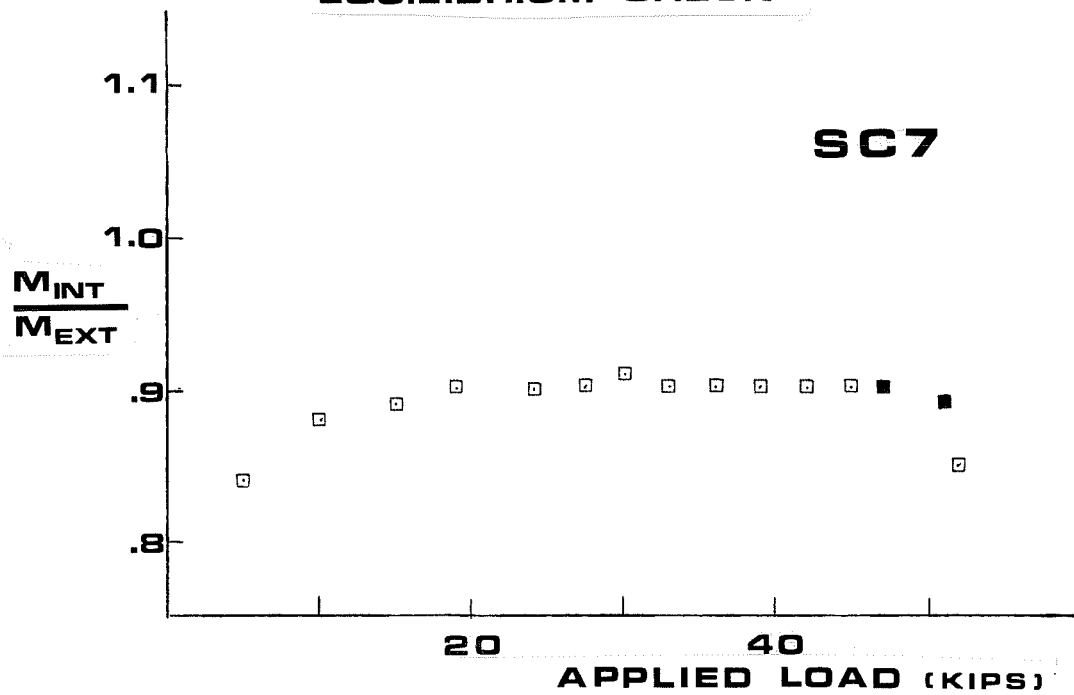
**EQUILIBRIUM CHECK:**

Fig. A.2 Equilibrium check in tests SC7 and SC8

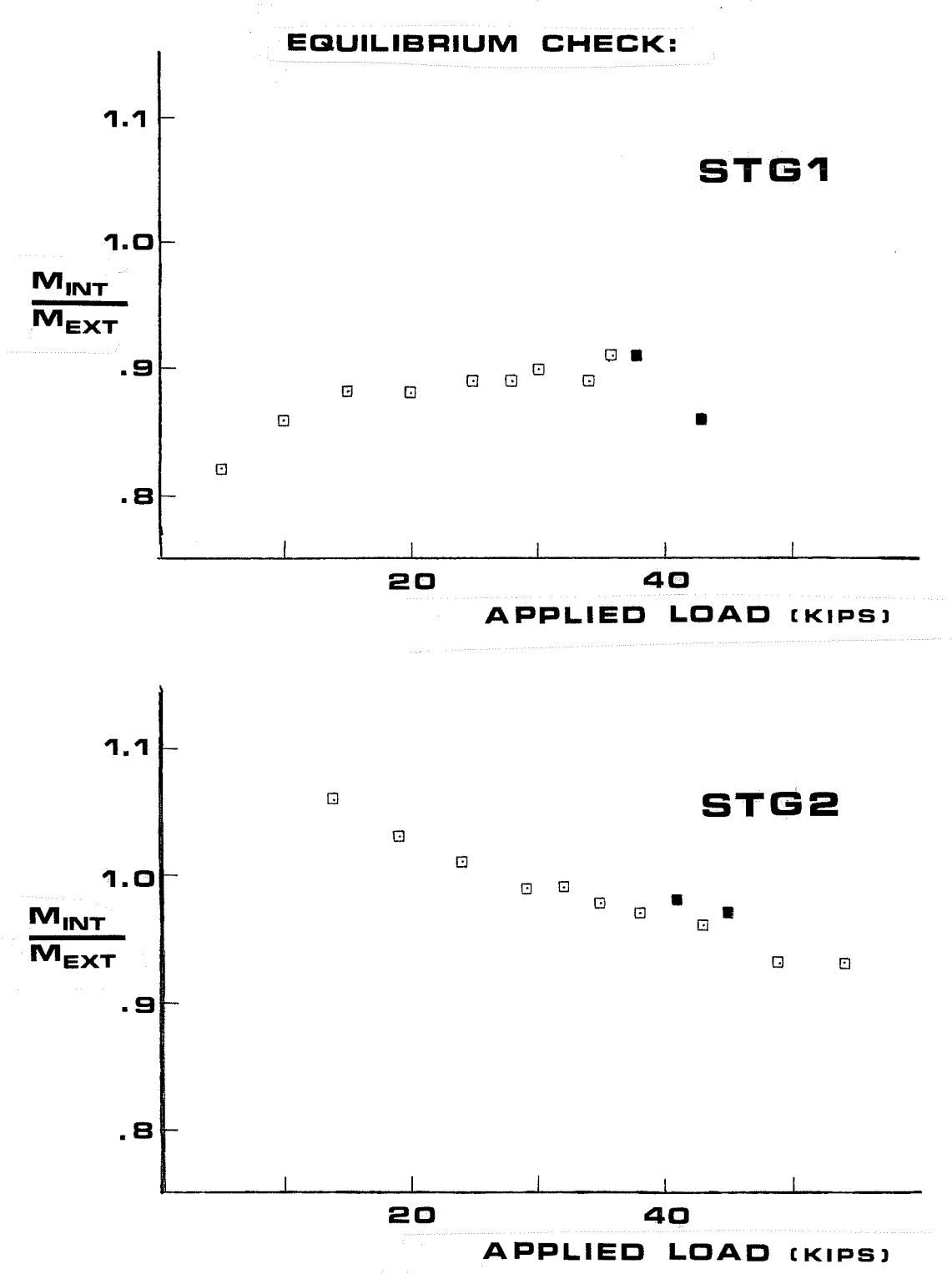


Fig. A.3 Equilibrium check in tests STG1 and STG2

in the procedure; two of those simplifications are discussed below.

As shown in Fig. A.4, the horizontal component of the jack reaction,  $H$  (neglected in Fig. 2.17b), is considered as follows:

$$\begin{aligned}\Sigma M_o &= 0 \quad \text{Assume } P = V \\ -H \cdot a - \Sigma(T \cdot Y) + 116P &= 0 \\ H \cdot a + T_R \cdot Y_R &= 116P \\ T_R \left( \frac{H}{T_R} \cdot a + Y_R \right) &= 116P\end{aligned}$$

The error from neglecting  $H$ :

$$e_1 = \frac{a(H/T_R)}{a(H/T_R) + Y_R} \quad \text{Eq. A.2}$$

where:

$$H = \mu V = \mu P$$

$$\mu = \text{friction coefficient } 0.4 \text{ to } 0.8 \\ \text{steel-to-steel}$$

$$a = 3.5 \text{ in.}$$

$$T_R = \text{resultant of the 4 tensile forces}$$

$$Y_R = \text{moment arm for } T_R, \text{ referred to point } 0 .$$

The error ( $e_1$ ) is evaluated for tests SC7 and SC8 at typical load stages as shown in Table A.1. For an assumed  $\mu = 0.6$ , neglecting the horizontal component of the jack reaction reduced the internal moment ( $M_{int}$ ) by two percent.

A most significant approximation in deriving Eq. A.1 was to assume the compressive force  $C$  acting horizontally through point  $0$  on the beam, as shown in Fig. A.5. Actually, the compression in the bottom

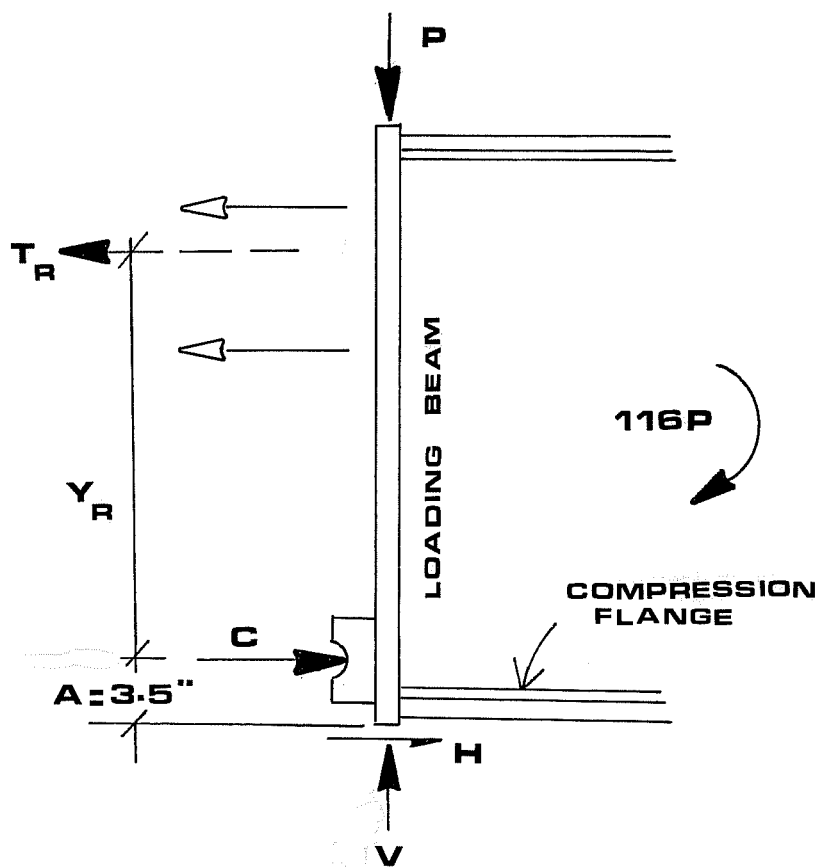


Fig. A.4 Reactions at the specimen - loading beam interface

FULL SCALE

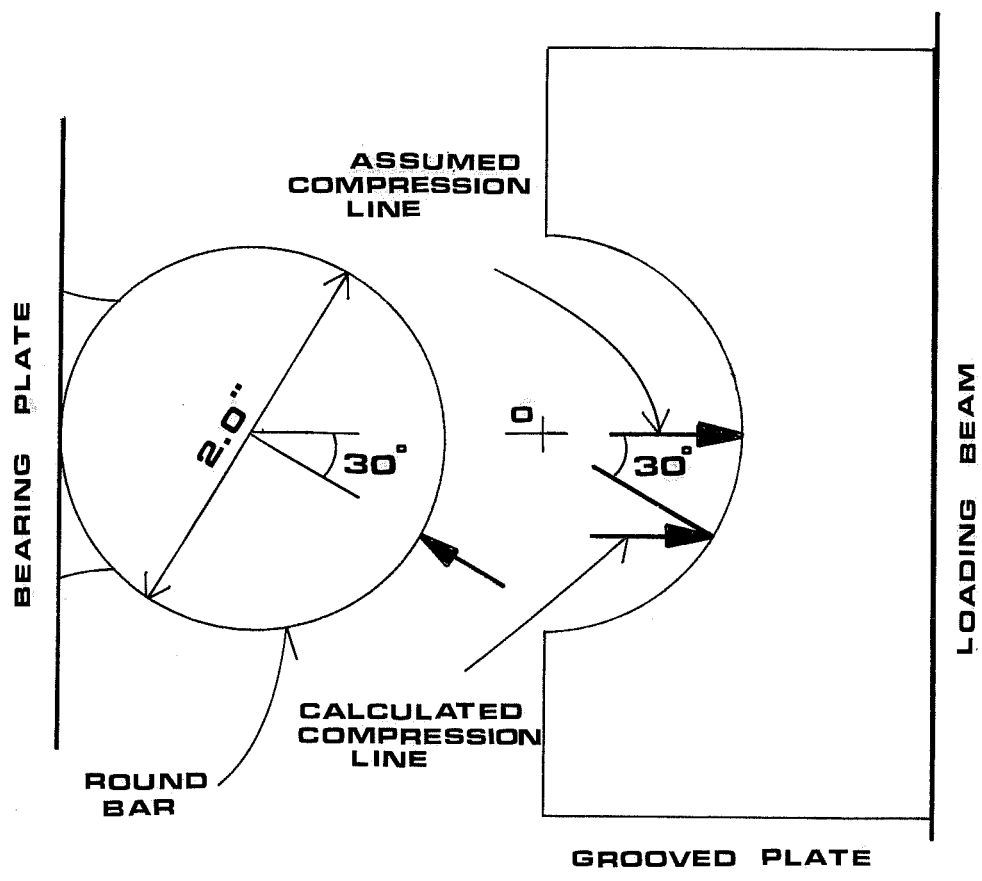


Fig. A.5 Grooved plate detail

Table A.1 ERROR DUE TO SIMPLIFYING ASSUMPTIONS

Test	P (k)	$1 - \frac{M_{int}}{M_{ext}}$	$T_R$ (k)	$Y_R$ (in.)	$\mu$	$e_1$	$e_2$
SC8	27.3	.049	207	14.56	0.6	.019	.033
	53.3	.046	418	14.14	0.6	.019	.034
SC7	30.6	.088	168	19.23	0.6	.019	.025
	45.6	.092	264	18.20	0.6	.020	.027



flange rises to the grooved plate and is transferred to the compression plate by bearing mostly against the lower quadrant of the round bar; that is, the resultant compression is inclined with the horizontal. Assuming a 30 degree inclination, the horizontal component of the compressive force acts on the beam along a line 0.5 inches below point O. The error from assuming a shorter lever arm for the internal couple is calculated as:

$$e_2 = \frac{0.5}{Y_R + 0.5} \quad \text{Eq. A.3}$$

The error ( $e_2$ ) tabulated in Table A.1 for tests SC7 and SC8 is shown to reduce the internal moment by about three percent.

The consistency in the  $M_{int}/M_{ext}$  ratio as well as the evaluation of the simplifying assumptions used in the equilibrium check gives confidence in the calculation of the top bolt forces within a 5 percent error for the six tests considered.

## A.2 Modification to Cichy's Results

The results from tests SC1, SC2 and SC4 were previously reported by Cichy.<sup>1</sup> There, the average load on the top bolts was determined from the tensile forces on the lower-level bolts, as calculated from two strain gages, and the simplified equilibrium expression, Eq. A.1. The equilibrium check for tests NOW through STG2 (conducted with the same set-up and procedure as used in the initial tests), and the simplifying assumptions as discussed above do justify, however, a modification to the equilibrium expression for a more accurate estimate of the bolt forces, as follows:

$$(T_1 + T_4) Y_L + (T_2 + T_3) Y_u = 116P (F) \quad \text{Eq. A.4}$$

As reported in the present study, the average load on the top bolts for tests SC2 and SC4 was calculated from strain gage readings for the lower-level bolts ( $T_1$  and  $T_4$ ), the measured load  $P$ , and Eq. A.4. A factor ( $F$ ) of 0.90 in test SC2 and 0.92 in test SC4 was used with the equation. The resulting average bolt capacity for tests SC2 and SC4 was ten percent lower than the value reported by Cichy.

For test SC1, the top bolt loads were individually determined from a mid gage reading ( $T_2$ ), and the average of two lead gages ( $T_3$ ). The bolt capacity exhibited for each bolt varied significantly ( $T_2 = 1.23T_3$ ) although the failure seemed fairly symmetrical from the crack pattern on the surface<sup>1</sup> and the slip data. It is not clear in this test whether a small clear cover condition or, using very few strain gages to estimate the tensile forces, resulted in the unusual scatter. The average capacity for the top bolts provides, nevertheless, an acceptable estimate of the group strength.

### A.3 Reliability in Measured Bolt Forces

Table A.2 summarizes the methods used to determine the tensile forces for all tests.

Note that for test SC3 at least one of the two lead gages on three bolts were lost during or prior to testing, making it highly unreliable, if not impossible, to calculate the forces on the top bolts. For that reason, test SC3 was excluded from this report.

In tests NOW and SC6, the lead gage readings for bolts 3 and 4

Table A.2 METHODS FOR CALCULATING BOLT FORCE

Test	Bolt 1	Bolt 2	Bolt 3	Bolt 4
SC1	A	C	C	A
SC2	A	D	D	A
SC3	E	A	E	E
SC4	A	D	D	A
NOW	A	A	B	B
SC6	A	A	B	B
SC7	A	A	A	A
SC8	A	A	A	A
STG1	A	A	A	A
STG2	A	A	A	A

## Method:

- A - Average of 2 or 4 lead gages.  
Most reliable.
- B - Adjusted lead gage readings.
- C - At least 1 out of 2 lead gages lost during the test. Mid gage reading used near failure.
- D - Estimate from external equilibrium and reliable gage readings of the force at bolts 1 and 4.
- E - Lead gages lost during test.  
Equilibrium not applicable.  
Unreliable.

were adjusted to account for a malfunction in several electronic data channels. The adjustment consisted of multiplying the average of two lead gage readings by a factor (1.14 in test NOW and 1.21 in test SC6 for bolt 3) which yielded a value representative of the mid gage reading near failure. As shown in Table A.3, the mid gage reading correlated very closely with the average reading at the lead gage near failure, typically. A very good agreement between the top bolt forces and  $M_{int}/M_{ext}$  ratios of about 0.93 for tests NOW and SC6 near failure, further justify the adjustment of the lead strain gage readings for bolt 3.

Force measurements with a "most reliable" rating (A) were calculated from two or four lead gages, 180 degrees apart, which showed a very consistent trend in cancelling the effect from bending stresses at the protruding length of a bolt.

A final reading, after the bolts were loosened at the end of a test, verified the accuracy of the lead strain gages by indicating bolt loads very close to zero. In a few cases, however, a discrepancy up to 4 kips occurred, which was neglected on the test results. This small difference was interpreted as the tensile force on a tightened bolt prior to the initial readings.

Table A.3 MID GAGE VS. LEAD GAGE AVERAGE READING  
AT BOLT CAPACITY ( $T_{max}$ )

Test	Bolt	$\frac{\text{Mid gage}}{\text{Lead gage average}}$
SC7	2	0.96
	3	1.06
SC8	2	0.66 <sup>1</sup>
	3	0.90
STG1	2	0.96
	3	0.98
STG2	2	0.89
	3	1.00

<sup>1</sup> Tail gage reading.

## B I B L I O G R A P H Y

1. Cichy, N.T., "Influence of Spacing and Concrete Edge Cover on the Strength of Anchor Bolt Groups," unpublished M.S. report, The University of Texas at Austin, May 1982.
2. Breen, J.E., "Development Length for Anchor Bolts," Research Report 55-1F, Center for Highway Research, The University of Texas at Austin, April 1964.
3. Lee, D.W., and Breen, J.E., "Factors Affecting Anchor Bolt Development," Research Report 29-2F, Center for Highway Research, The University of Texas at Austin, August 1966.
4. Hasselwander, G.B., Jirsa, J.O., Breen, J.E., and Lo, K., "Strength and Behavior of Anchor Bolts Embedded Near Edges of Concrete Piers," Research Report 29-2F, Center for Highway Research, The University of Texas at Austin, May 1977.
5. Hasselwander, G.B., "Behavior of High-Strength Anchor Bolts Embedded Near Edges of Concrete Piers with the Development of a Design Equation," unpublished Ph.D. dissertation, The University of Texas at Austin, August 1979.
6. Texas Highway Department, "Standard Specifications for Construction of Highways, Streets and Bridges," 1972 edition.
7. American Society for Testing Materials, "Alloy Steel and Stainless Steel Bolting Materials for High-Temperature Services," ASTM A193-74.

## V I T A

Marcos Rafael Calzadilla was born in Cienfuegos, Cuba, on January 20, 1958, the son of Idalia Garcia Lazo and Marcos Aurelio Calzadilla Fernández. After completing his high school work at Colegio San Ignacio de Loyola, San Juan, Puerto Rico, in 1975, he entered the University of Puerto Rico at the Recinto Universitario de Mayagüez. He received the degree of Bachelor of Science in Civil Engineering from the University of Puerto Rico in June 1980. In September, 1980, he entered The Graduate School of The University of Texas at Austin.

Permanent address: 36 Fresa, Milaville  
San Juan, Puerto Rico